McBain Associates
APPLIED RIVER SCIENCES
980 7th Street, Arcata, CA 95521 · PO Box 663, Arcata, CA 95518 · ph (707) 826-7794 · fax (707)826-7795

August 31, 2017

APPENDIX F: 2-DIMENSIONAL HYDRAULIC MODEL PREPARATION, CALIBRATION, VALIDATION, AND WUA CURVE FOR THE MAINSTEM SPROUL CREEK 2-D MODELING SITE - DRAFT

Prepared for: *California Trout*
c/o Darren Mierau
615 11th Street
Arcata, CA 95521

Prepared by: *McBain Associates*
980 7th Street
Arcata, CA 95519

1 INTRODUCTION

This memorandum is an appendix to the *Sproul Creek Site Specific Instream Flow Study* (main report) and describes the 2-dimensional (2-D) hydraulic model, SToRM (System for Transport and River Modeling [model]), used in estimating physical habitat for this instream flow study on the mainstem Sproul Creek, a tributary to the South Fork Eel River in Humboldt County, California (Figure F-1). Sproul Creek enters the South Fork Eel River 2.3 miles downstream from Benbow Dam, near Garberville, CA. The watershed has a mixed ownership. Boyle Forests LLP and Wagner Corporation, two large timber landowners, own more than 67% of the watershed. Medium-sized ranches and residential parcels comprise the remaining area. Sproul Creek has a history of timber harvest and impacts from the 1955 and 1964 floods. During the past several decades, sustainable forest management and a low rate of harvest have allowed the watershed to recover and sustain high quality salmonid habitat. The Sproul Creek watershed (24.0 mi^2) has approximately 21 linear miles of salmonid habitat, and supports stable runs of Chinook and Coho salmon, and steelhead. The CDFW Coastal Monitoring Program began conducting adult spawner surveys in Sproul Creek in 2011.

This appendix describes development of the model, including: (1) site selection; (2) data collection and topographic mesh preparation; (3) establishment of boundary and initial starting conditions, convergence and stability; and (4) model calibration and validation. In addition, this appendix describes methods used to estimate weighted usable area (WUA) for targeted biological species and life stages over a range of streamflows. WUA estimates are generated from post-processing of the depths and velocities predicted by the 2-D model, combined with cover and substrate data collected at the modeling site, and habitat suitability indices. The WUA curves generated from this modeling effort are used to estimate bypass flow criteria for target species for the mainstem Sproul Creek study reach.

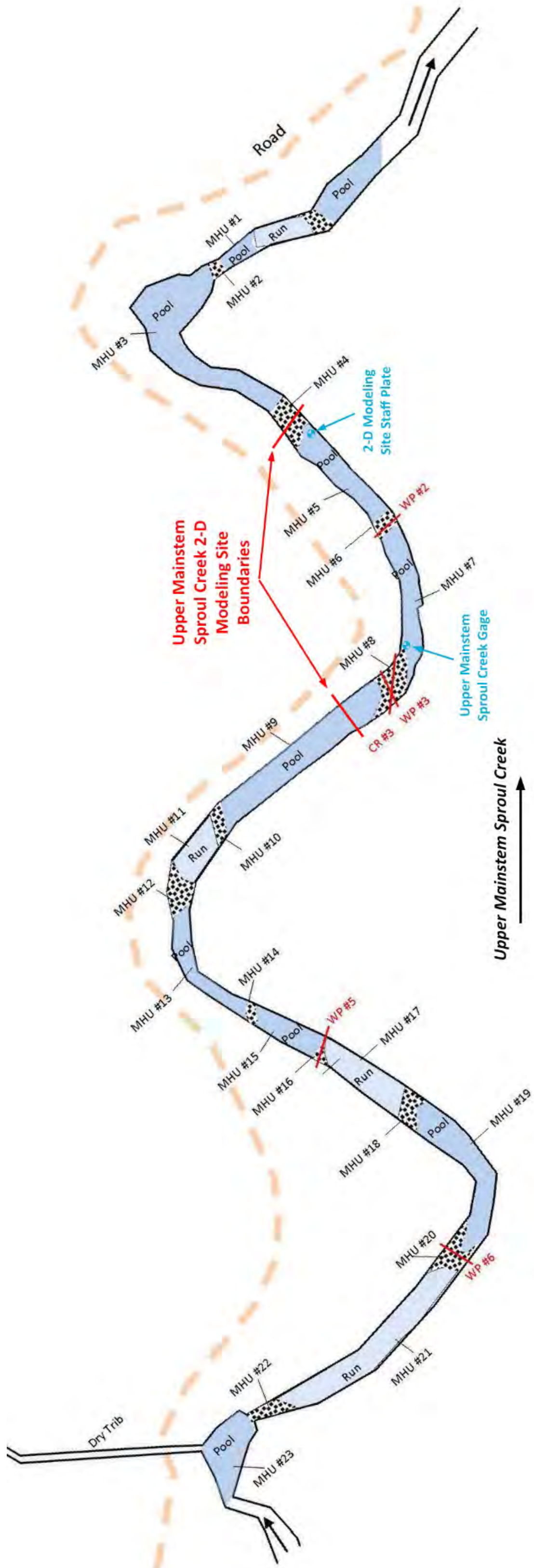

Figure F-1. Mainstem Sproul Creek mesohabitat map showing location of California Trout (CalTrout) stream gage, empirical hydraulic habitat assessment cross sections, and 2-D hydraulic modeling site.

2 MODEL BACKGROUND

SToRM is a numerical model that uses 2-D depth-averaged equations to predict flow within a natural channel. SToRM runs within the International River Interface Cooperative's (iRIC) graphical user interface software package. SToRM uses river flow, stage, detailed channel topography, and roughness estimates to compute force balances responsible for the distribution of depth, velocity, and boundary shear stress. The model computes water surface elevation, depth-averaged velocity, and boundary shear stress by solving conservation of mass and momentum equations (Simões 2013). Application of SToRM on Sproul Creek assumes that: (1) flow is steady, or at least does not vary appreciably over short time scales; (2) flow is hydrostatic (vertical accelerations are neglected); (3) turbulence can be treated adequately by the 2-D equations; and (4) shear stress vectors along the bottom are in the same direction as depth-averaged velocity and square of its magnitude. Development of the model equations, numerical techniques, and model structure are discussed in greater detail in Simões (2013).

iRIC is a software package developed through a partnership between Professor Yasuyuki Shimizu (Hokkaido University) and Dr. Jon Nelson (U.S. Geological Survey). This partnership integrated the Multidimensional Surface-Water Modeling System (MD_SWMS), developed by the USGS and RIC-Nays, developed by the Foundation of Hokkaido River Disaster Prevention Research Center. iRIC provides a cutting-edge platform that allows model developers and users an interface to set up, run, and output results from a variety of models (Figure F-2). The strength of the iRIC platform comes from the continued incorporation of suggestions and recommendations made by a growing number of model users and developers throughout the world.

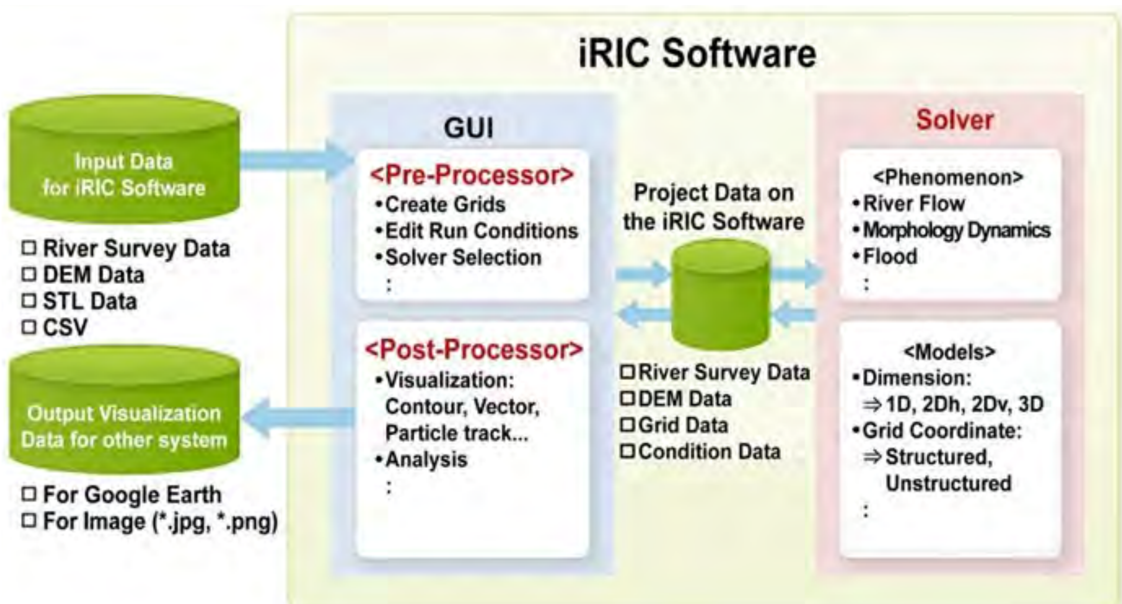

Figure F-2. Flow chart showing iRIC functions and features (iRIC 2014). iRIC allows users to input data through the graphical user interface (GUI) and run a variety of 1-D, 2-D, 2Dh (horizontal plane) and 2Dv (vertical plane), and 3-D hydraulic models.

3 DATA COLLECTION FOR MODEL INPUT

Understanding the project objectives, and targeted species and life stages, ultimately determines the level of effort necessary when collecting model input data. A 2-D model is prepared using topographic and bathymetric data generated from one of many survey methods (e.g., LiDAR, Total Station, Photogrammetry) and roughness data derived from a surface substrate and/or large wood and vegetation map. Ideally these data would be collected when topography, substrate, and cover do not change. In addition to these static data, water surface elevations that extend from the upstream modeling boundary to the downstream modeling boundary, observed velocities, and a well-defined stage–discharge rating curve (preferably generated from measured data) for a variety of flows are required for model calibration, validation, and upstream/downstream boundary and initial starting conditions. The following sections describe our collection of these data for the Upper Mainstem Sproul Creek 2-D modeling site.

3.1 Topography

CalTrout and McBain Associates (MA) staff mapped topography, substrate facies, and cover polygons between June 28 and 30, 2016, using a Nikon 521 DTM Total Station. Both the vertical and horizontal datum were arbitrarily set, with the vertical datum set to an elevation of 100.00 ft at the upstream Benchmark and the horizontal datum set to be an arbitrary 10000 easting and 10000 northing and field adjusted with a compass to a northern orientation (Figure F-1). Topographic breaks, such as top and/or toe of bank, as well as mass points between these breaklines, were surveyed to describe existing topography (Figure F-3). A total of 1,798 points were surveyed within the 23,050 ft^2 topographic boundary, with 1,785 of the surveyed points falling within the 23,030 ft^2 modeling boundary, including a section of channel 495 ft long. The point density within the modeling boundary averaged approximately 1 point per 12.9 ft^2. In most cases, this point density captured bed topography representative of each mapped facies, i.e., area with texturally distinct bed material. Additionally, point densities were increased to capture complex topography and features that would impact model hydraulics such as riffles, channel margins, boulders, bedrock outcrops, and large wood. (Figure F-3, Figure F-4).

Once the survey was complete, points were downloaded from the Total Station to AutoCAD Civil 3D. Breaklines along the tops and toes of banks and along the water's edge were drawn along with a boundary that encompasses all topographic and bathymetric points. A digital terrain model (DTM) was built from the surveyed points, breaklines, and boundary (Figure F-3). For input into the model, the DTM was resampled into a 0.5-ft point grid and exported to Microsoft Excel. Within Microsoft Excel, the point file containing eastings, northings, and elevations was exported as a space delineated *.tpo file and imported into iRIC for use with SToRM.

3.2 Surface Substrate and Roughness

Prior to collecting representative particle size information at the modeling site, delineation of facies within the topographic boundary was conducted. On June 28–29, 2016, fourteen facies boundaries were mapped using a Total Station to delineate areas with texturally distinct bed material (Figure F-3). Total Station mapped facies were downloaded into AutoCAD Civil 3D and later exported as a *.shp file for import into SToRM.

To quantify substrate within facies boundaries, a modified Wolman-style pebble count (Leopold 1970) was conducted on June 28–29, 2016, within mapped facies. Pebble counts were entered into a Microsoft Excel spreadsheet and the D_{50} and D_{84} particle sizes were computed (Table F-1). Pebble counts were not conducted within Facies 4 and 15 because they were mapped as sand and Facies 1 because it was mapped as bedrock. The D_{50} (median) values within each of the mapped facies were used to determine an initial Manning's *n* roughness value for use in the model (Table F-2). Manning's *n* values for each of the mapped facies were a result of an iterative process during model calibration (Section 5.3 of this appendix).

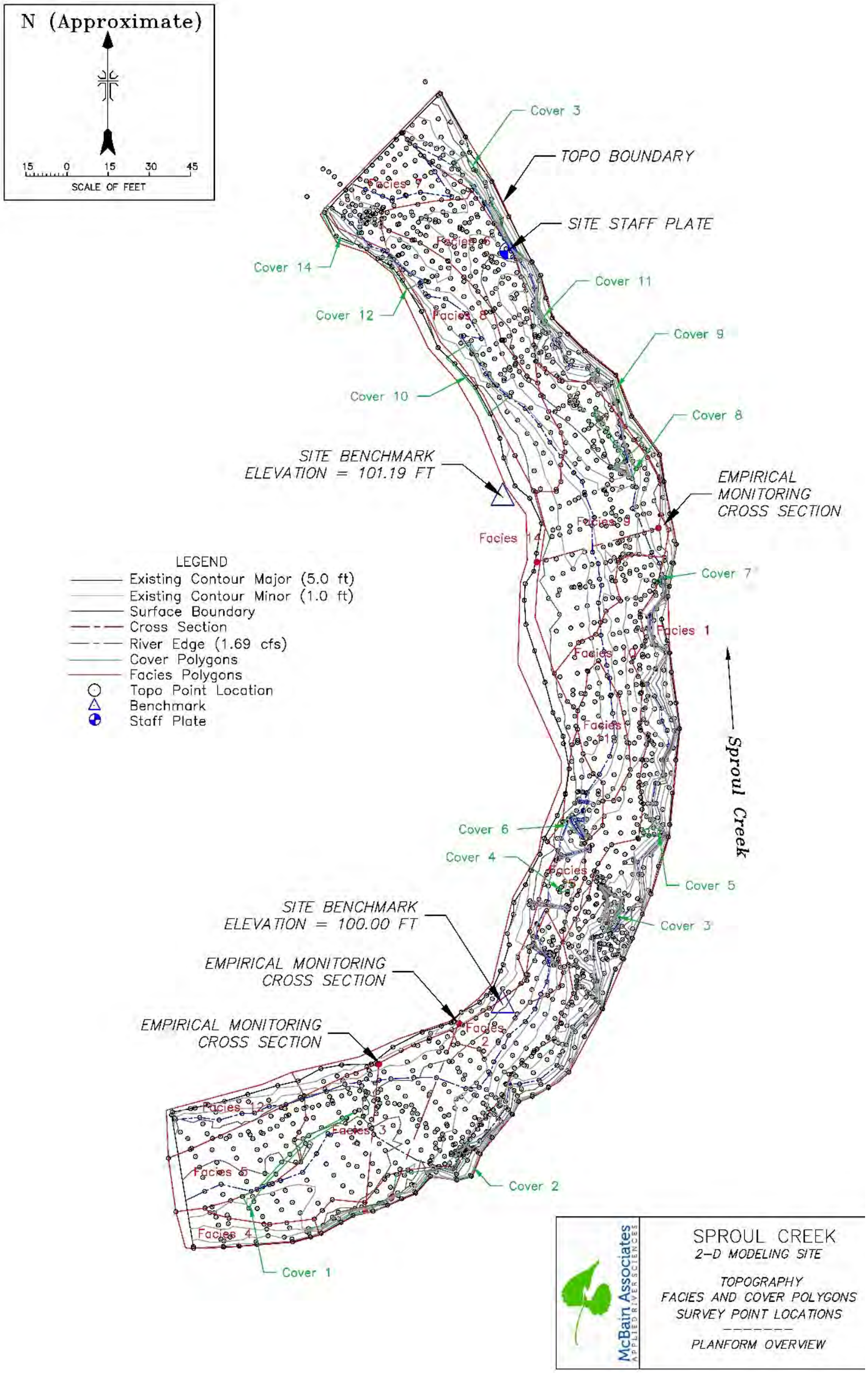

Figure F-3. Sproul Creek modeling site map, showing facies and cover boundaries, topographic survey points, and boundaries.

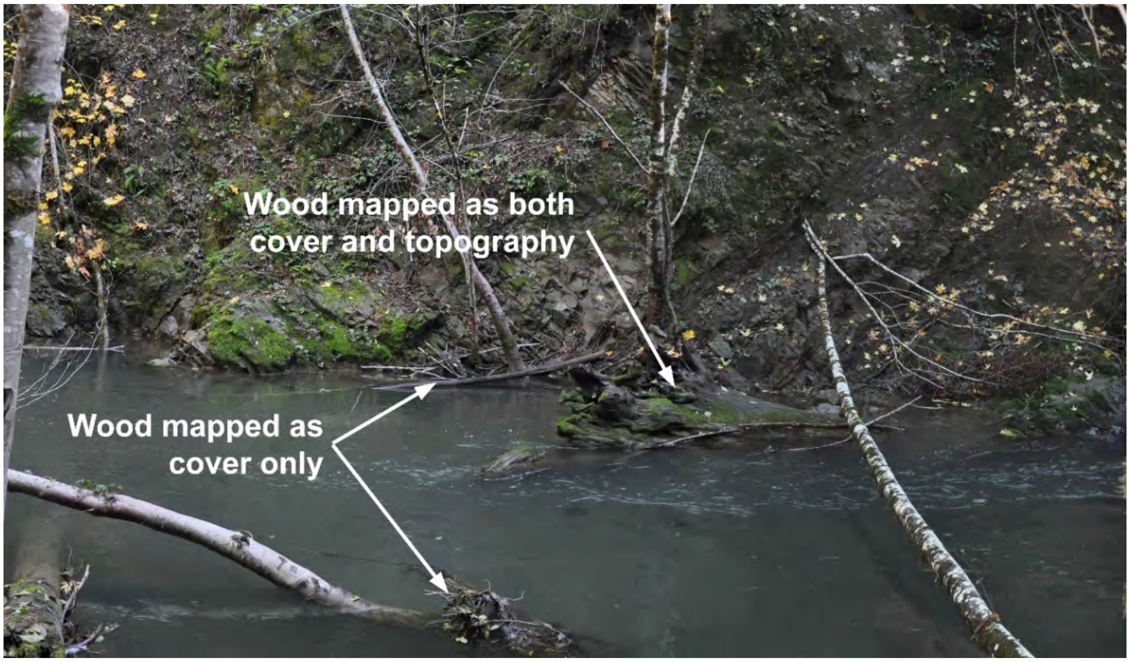

Figure F-4. Example 2-D hydraulic modeling site looking from left to right bank showing large wood mapped as cover only and as both topography and cover.

Table F-1.Results from pebble counts at modeling site facies for D_{50} and D_{84}.

	Facies													
	1⁺	**2**	**3**	**4**	**5**	**6**	**7**	**8**	**9**	**10**	**11**	**12**	**14**	**15**
D_{84} (mm)	200	36	99	< 2	59	43	98	36	155	49	20	152	152	< 2
D_{50} (mm)	200	12	57	< 2	26	24	51	12	101	25	< 2	< 2	< 2	< 2

+ Br = Bedrock.

Table F-2. Beginning Manning's n *values for channels from Phillips and Tadayon (2006), as well as final values used as a result of adjustments made to better fit observed depth and water surface data for each calibration flow.*

Channel Bed Type	**Median Size of Bed Material (mm)**	**Beginning *n* Value Phillips and Tadayon (2006)**	**Final *n* Value Used SToRM Calibration**
Sand	< 2	0.020–0.035	0.037–0.056
Gravel	2–64	0.028–0.035	0.040–0.071
Cobble	64–256	0.030–0.050	0.043–0.081
Boulder	> 256	0.040–0.070	0.055–0.094

3.3 Cover

As part of a topographic survey, large trees and wood accumulations were captured in the topography and mapped as hydraulic refuge (cover) polygons. In addition, constructed habitat features within the 2-D modeling site, including logs and boulders cabled into the channel bed and banks, were large enough to influence channel hydraulics in the 2-D modeling site, and were included as part of the surveyed topography (Figure F-3, Figure F-4). Large and small wood (including the log surveyed as topography), tree roots, and vegetation that fell within the surveyed topographic boundary were mapped on June 28–29, 2016, as potential hydraulic cover using a Total Station (Figure F-3). These cover polygons (when they interact with flow) not only provide hydraulic refuge for salmonids, but they also may increase Manning's *n* coefficients above those generated from mapped substrate facies. As with substrate (facies) polygons, cover polygons were post-processed in AutoCAD Civil 3D and exported as a *.shp file for use in SToRM.

3.4 Streamflow

The CalTrout Upper Mainstem Sproul Creek gage was located within the 2-D modeling site boundary approximately 300 ft upstream of the 2-D modeling site staff plate (Figure F-1). CalTrout's observed 2-D site staff plate readings were paired with real-time streamflow measurements at their gaging station within the 2-D modeling site boundary to established a stage–discharge relationship for the 2-D model's downstream boundary condition (Table F-3).

In addition, streamflow exceedance probabilities (the probability that a specific streamflow is exceeded at any given time) were calculated from Sproul Creek and Bull Creek watershed scaling and correlation of 2-years of CT Sproul Creek gaging and 49-years of USGS Bull Creek gaging (USGS Gage: 11-476600, WY 1968-2016). Streamflow exceedance probabilities of 20%, 50%, and 80% were used to provide calibration and validation data collection flow targets (Table F-3, Figure F-5). For a more detailed explanation of methods used to calculate streamflow exceedance probabilities for the Upper Mainstem Sproul Creek, refer to Appendix A.

3.4.1 Developing Rating Curve for 2-D Hydraulic Model

A stage–streamflow rating curve was developed by MA for the 2-D hydraulic modeling site using the Excel-based computer program Brian's Aid for Rating Creating (BARC), developed by Brian J. Loving of the USGS (Loving 2002). The software follows standard USGS techniques (i.e., Kennedy 1984) to plot and evaluate the stage–streamflow relationship based on data collected for individual streamflow measurements (Figure F-6, Figure F-7). A total of 15 stage and streamflow data points were collected, of which 13 were used to develop the 2-D modeling site rating curve. For each data point collected, staff plate observations at the downstream end of the 2-D hydraulic modeling site were paired with streamflow measurements collected along with the date and time. These data were used to determine the streamflow at the 2-D modeling site when the staff plate was read (Table F-3, Figure F-6, Table F-3, Figure F-7). The final rating curve provided downstream boundary conditions for streamflows not measured in the field (Table F-3).

Table F-3. All modeled streamflows and corresponding water surface elevations used for the upstream and downstream 2-D hydraulic model boundary conditions. For modeled flows that corresponded to streamflow measurements made by California Trout (CA) and used to generate the stage–discharge rating curve for the 2-D modeling site, are indicated by a "" or "+". In addition, percent streamflow exceedance was provided to reflect the probability that a modeled streamflow was exceeded.*

Streamflow at the 2-D Modeling Site Upstream Boundary (cfs)	Water Surface Elevation at the 2-D Modeling Site's Downstream Staff Plate (ft)	Streamflow Exceedance (%)	Notes
0.1+	97.08	96.8	CT Measurement 081016
0.5	97.16	88.0	From Rating Curve
1.0	97.22	81.6	From Rating Curve
1.9+	97.30	76.0	CT Measurement 062816
3.9*	97.42	64.5	CT Measurement 061016
7.1	97.55	55.1	CT Measurement 052516
12.0	97.66	48.1	From Rating Curve
12.7+	97.67	47.1	CT Measurement 050516
16.0	97.74	44.1	From Rating Curve
21.1*	97.75	39.6	CT Measurement 041316
30.0	97.94	33.8	From Rating Curve
40.0	98.07	29.4	From Rating Curve
50.4+	98.10	26.1	CT Measurement 110416
52.0	98.19	25.5	From Rating Curve
65.0	98.30	22.0	From Rating Curve
67.1+	98.25	21.5	CT Measurement 110316
80.4	98.39	18.9	CT Measurement 112216
90.0*	98.48	17.3	CT Measurement 110216
105.0	98.57	15.3	From Rating Curve
120.0	98.66	13.4	From Rating Curve
150.0	98.82	10.9	From Rating Curve
190.0	99.00	8.2	From Rating Curve

+Flow used in preparation of site streamflow rating curve but not modeled for habitat.

*Calibration and validation data collected on days when discharge measurements were made.

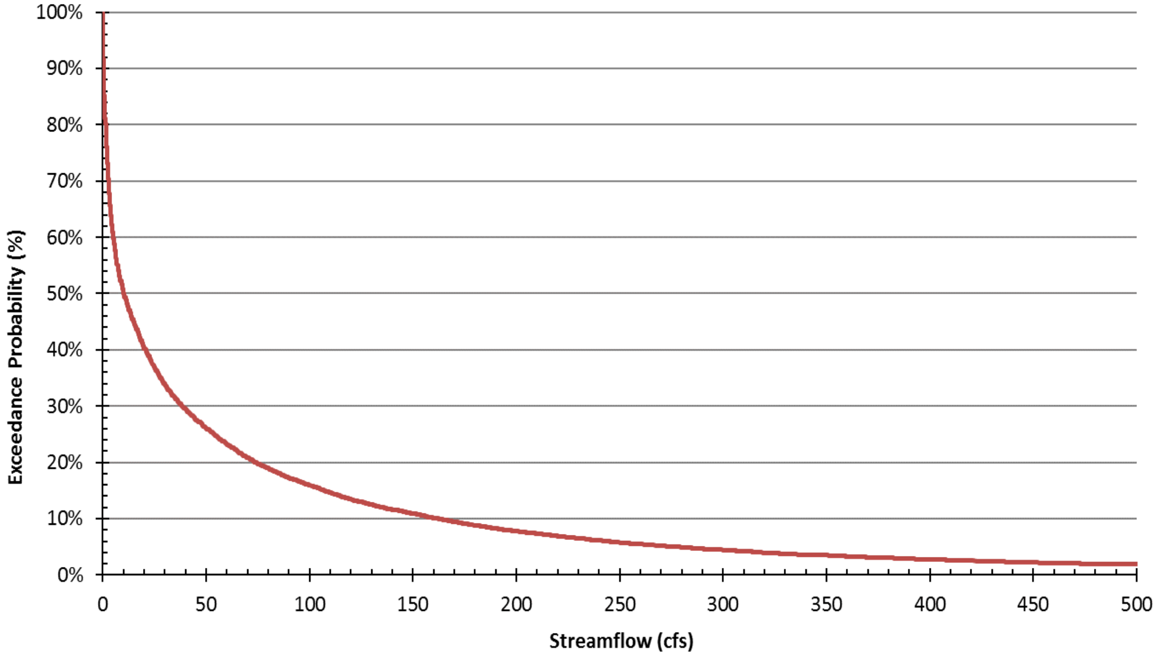

Figure F-5. Streamflow exceedance probability for the Mainstem Sproul Creek. For a complete explanation of flow exceedance probability calculation methods refer to Appendix A.

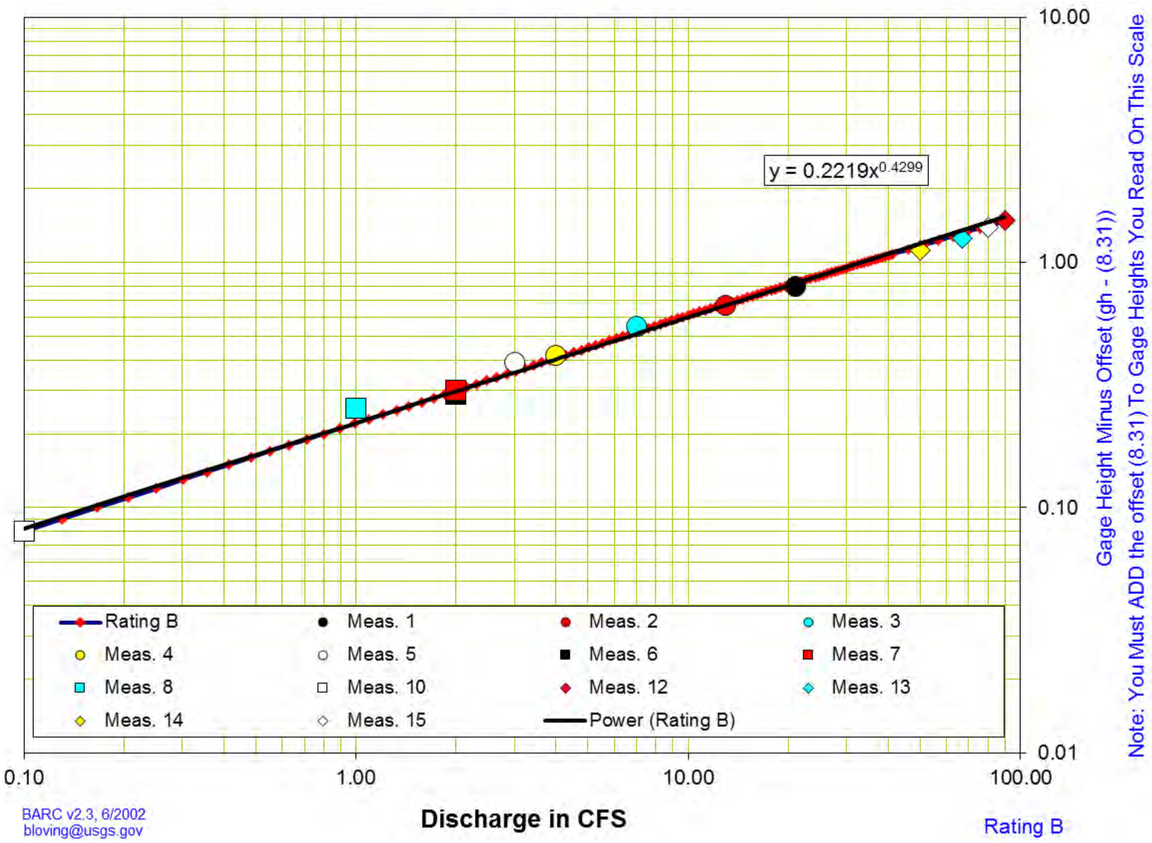

Figure F-6. Stage–streamflow rating curve developed for the 2-D hydraulic modeling site in the mainstem Sproul Creek study reach using BARC, developed by Brian J. Loving of the U.S. Geological Survey (Loving 2002).

BARC v2.3

Brian's Aid for Rating Creating
By Brian Loving, US Geological Survey

USGS science for a changing world

A new rating for Station: Upper Mainstem Sproul Creek
2D Modeling Site

Copy to Rating C

Single Offset/Breakpoint Ratings

	Regression	Rating A (Show)	Rating B (Show)	Rating C (Show)
Enter the Rating Offset	7.11	8.30	8.31	
Enter the Low Endpoint Gage Height	8.39	8.39	8.39	
Enter the Low Endpoint Discharge	0.41	0.1	0.1	
Enter a Breakpoint Gage Height (Optional)			8.92	
Enter a Breakpoint Discharge (Optional)			10	
Enter the High Endpoint Gage Height	9.79	9.79	9.79	
Enter the High Endpoint Discharge	151	90	90	

	Rating A	Rating B	Rating C
Sum of the Percent Differences	-15.59	-17.37	
Percent Difference Furthest From Zero	-24.09	-27.77	

Measurement Data

Use	Number	Gage Height	Discharge	Rated	Rating A % Diff.	Rating B % Diff.	Rating C % Diff.
☑	1	9.11	21		4.31	7.22	
☑	2	8.98	13		-0.85	3.02	
☑	3	8.86	7		-14.12	-11.48	
☑	4	8.73	4		-6.43	-6.78	
☑	5	8.7	3		-16.28	-17.30	
☑	6	8.6	2		12.38	7.92	
☑	7	8.61	2		3.78	-0.06	
☑	8	8.565	1		-24.09	-27.77	
☐	9	8.44	0.3				
☑	10	8.39	0.1		0.00	0.00	
☐	11	9.41	58				
☑	12	9.79	90		0.00	0.00	
☑	13	9.56	67		12.44	13.15	
☑	14	9.43	50		9.66	10.86	
☑	15	9.7	80		3.61	3.85	
☐							

Figure F-7. Screenshot from BARC (Loving 2002) spreadsheet showing measured stage and streamflow data used in the preparation of the rating curve.

3.5 Calibration and Validation Data

Calibration and validation data, consisting of water surface elevation, depth, and velocity measurements, were collected between April and November 2016 (Table F-3, Figure F-8). Empirical water surface elevations and velocities were measured at the 2-D modeling site between the downstream and upstream boundaries along with streamflow measured in the field.

Water surface elevations are required at the model's upstream and downstream boundaries. Ideally, to provide reasonable hydraulic predictions for modeled flows not measured in the field (e.g., no calibration or validation data collected), modeled flows should not exceed ± 50% of the range of measured streamflows. For example, a model calibrated and validated to a streamflow of 100 cfs flow may be used to predict modeled flows down to 50 cfs and up to 150 cfs, while a 300 cfs flow may be used to predict down to 150 cfs and up to 450 cfs. This may not always be possible, and some flexibility may be necessary due to time constraints, streamflows available to measure, and safety as flows get higher. For the upper mainstem Sproul Creek 2-D modeling site, the 90.0 cfs calibration and validation point was near the upper limit of our data collection capabilities due to water depths and velocities.

For the upper mainstem Sproul Creek 2-D modeling site, calibration and validation data were collected as follows:

- April 13, 2016, for a streamflow of 21.1 cfs (Table F-3); 64 water surface, depth, and velocity measurements were taken (Figure F-8).
- June 10, 2016, for a streamflow of 3.9 cfs (Table F-3); 66 water surface, depth, and velocity measurements were taken (Figure F-8).
- November 2, 2016, for a streamflow of 90.0 cfs (Table F-3); 55 water surface, depth, and velocity measurements were taken. However, 7 of the measurement locations were outside the modeling boundary, leaving 48 calibration/validation usable points (Figure F-8).

Measurements were made using a top set wading rod with a Marsh-McBirney flow meter to measure depth and velocity at each location. The wading rod had a prism attached to the top so that a Total Station, oriented to the site control, could shoot in the location (northing and easting) of each calibration and validation point, as well as the elevation of the bed and water surface (Table F-4, Figure F-8). Total Station data were downloaded to AutoCAD Civil 3D and exported to Microsoft Excel for post-processing. Field-measured depths and velocities for each corresponding point were added into the exported Microsoft Excel spreadsheet (Table F-4). Data within spreadsheets were then separated into easting, northing, and velocity/water surface elevation and exported as comma separated files (*.csv) for import into SToRM. Negative values reference streamflow that is oriented upstream.

In order to capture calibration and validation data for streamflow with a 20% exceedance probability (Table F-3), data collection spanned two water years between April 13, 2016 (WY 2016), to November 2, 2016 (WY 2017). Since no large rainfall events occurred between April 13, 2016, and November 2, 2016 (with the exception of the 90.0 cfs flow that was achieved on the November 2, 2016 sampling date), and that the topography was surveyed in June 2016, site topography was not expected to have changed prior to the November 2, 2016, data collection date.

During calibration and validation data collection periods, the staff plate at the downstream boundary was read at the beginning and end of each survey to ensure flows remained relatively steady. The maximum change in water surface elevation during calibration and validation data collection occurred during the November 2, 2016, collection date. The change in staff plate readings was 9.81 ft to 9.77 ft, or a drop of 0.04 ft, over the period of 2 hours. A streamflow measurement made at the same time took approximately 1 hr with a staff plate change of 9.80 ft to 9.79 ft, or a decrease of 0.01 ft. Therefore, no adjustment to the assigned streamflow (90.0 cfs) was made for the calibration and validation data collected on November 2, 2016.

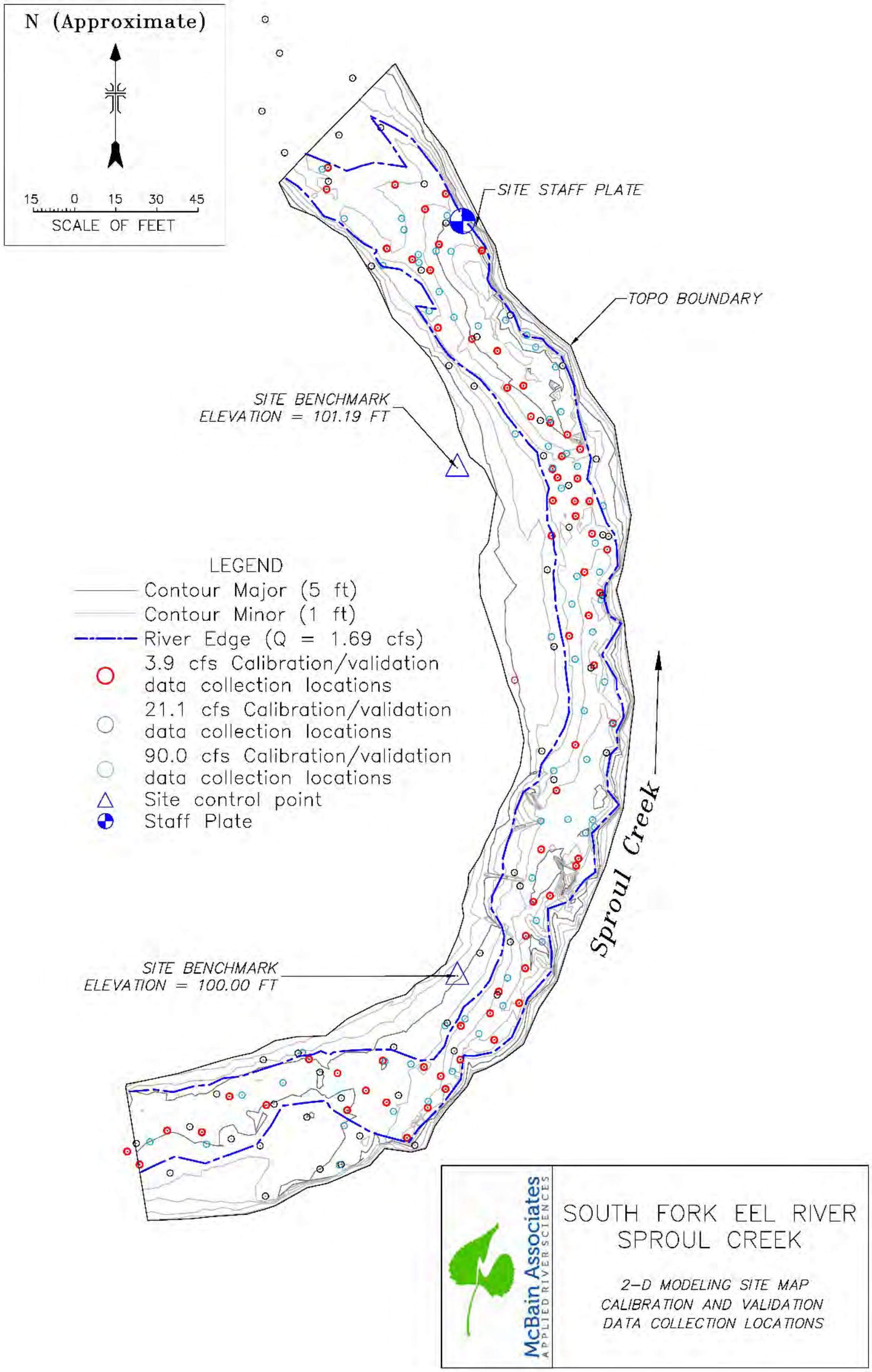

Figure F-8. Calibration (water surface elevation) and validation (velocity) measurement locations taken for all dates.

Table F-4. Example of calibration and validation data collected at 2-D modeling site at a streamflow of 90.0 cfs on November 2, 2016.

Point #	Easting (ft)	Northing (ft)	Water Surface Elevation (ft)	Depth (ft)	Velocity (ft/sec)
1005	9953.06	10289.56	98.45	1.01	1.03
1006	9956.91	10306.40	98.38	0.93	2.87
1007	9972.12	10309.08	98.52	1.32	1.54
1009	9987.97	10288.62	98.52	1.67	1.27
1010	9995.86	10274.35	98.51	3.40	0.38
1012	9986.88	10257.20	98.48	1.73	1.15
1013	10007.16	10232.94	98.42	3.72	−0.04
1014	10006.16	10214.95	98.40	0.00	0.00
1015	10030.31	10202.44	98.48	3.00	2.86
1017	10031.44	10189.58	98.44	0.96	1.89
1018	10040.59	10178.75	98.97	1.75	5.05
1019	10050.57	10188.36	98.59	0.00	0.00
1020	10055.13	10160.17	99.55	1.75	1.24
1021	10040.74	10163.50	99.44	1.68	3.75
1022	10032.80	10148.01	99.56	0.73	1.20
1023	10035.26	10119.98	99.63	0.80	1.26
1024	10048.74	10112.26	99.61	3.68	1.75
1025	10030.80	10081.97	99.71	0.93	0.48
1026	10054.33	10081.34	99.66	2.95	1.03
1027	10020.84	10037.76	99.68	2.65	0.39
1028	10035.20	10071.58	99.66	3.04	0.94
1029	10053.00	10138.67	99.58	3.15	1.01
1030	10053.07	10160.72	99.58	1.92	1.95
1031	10019.31	10240.80	98.40	1.84	0.09
1032	10038.42	10222.41	98.45	2.96	−0.89
1038	10022.88	10032.86	99.72	3.85	0.42
1039	10019.34	10012.45	99.65	2.76	0.64
1040	10008.23	10008.37	99.68	0.00	0.00
1041	10014.54	9993.11	99.71	2.48	2.66
1042	9996.36	9982.90	99.72	0.81	0.45
1043	9998.90	9972.76	99.73	2.75	2.40
1044	9976.84	9974.15	100.27	0.40	4.10
1045	9978.58	9956.61	100.21	0.95	2.72
1046	9984.52	9938.38	100.36	0.00	0.00
1047	9957.73	9955.60	100.79	0.90	3.12
1048	9964.49	9941.78	100.44	0.90	0.70
1049	9957.68	9931.37	100.55	1.37	−0.02
1050	9949.98	9929.69	100.54	0.30	0.99

Point #	Easting (ft)	Northing (ft)	Water Surface Elevation (ft)	Depth (ft)	Velocity (ft/sec)
1051	9945.23	9948.65	100.95	0.80	3.14
1053	9949.93	9965.04	101.09	1.25	3.32
1054	9941.98	9971.95	101.21	0.00	0.00
1055	9933.26	9953.37	101.34	1.55	2.23
1056	9928.17	9938.20	101.37	0.94	1.64
1057	9930.11	9919.85	101.11	0.72	0.00
1058	9917.63	9940.70	101.40	1.60	2.04
1059	9912.31	9957.08	101.32	1.30	2.62
1060	9902.53	9945.13	101.39	1.74	2.73
1061	9895.38	9928.26	101.45	0.97	1.03

4 MODEL QA/QC CRITERIA

Preparation of a 2-D hydraulic model requires quality checks along the way. These quality checks provide confidence that hydraulic parameters predicted by the model are reasonably accurate. At this time, there are no industry-established standard criteria for model setup, calibration, and validation. The best resource available for 2-D model setup, calibration, and validation criteria is found in the *Standards for Physical Habitat Simulation Studies*, prepared by the Sacramento Fish and Wildlife Office (USFWS 2011). Six criteria listed in the USFWS (2011) report are:

1. **Mesh Quality**: The quality of the fit between the final bed profile and the computational mesh, as measured by the Mesh Quality Index (QI) value, should be at least 0.2.
2. **Water Surface Elevation**: Calibration is considered to have been achieved when the water surface elevation levels (WSELs) predicted by the 2-D model at the upstream transect is within 0.1 ft of the WSEL predicted by PHABSIM for the highest simulated flow (or observed at the highest measured flow).
3. **Solution Change/Net Flow**: When the model is run to steady state at the highest flow simulated, the solution change should be less than 0.00001 and the net flow should be less than 1%.
4. **Froude Number**: For low gradient streams, the maximum Froude number should be less than 1 (i.e., subcritical flow).
5. **Velocity & Depth Validation**: The model is considered validated when the correlation between at least 50 spatially-distributed measured and simulated values is greater than 0.6 for velocity and 0.8 for depth.
6. **Biological Verification**: As biological verification, the Mann-Whitney U test should be used to determine whether the combined suitability predicted by the 2-D model was higher at locations where redds, fry, or juveniles were present versus locations where redds, fry, or juveniles were absent.

The 2-D model criteria listed above were established for the 2-D hydraulic model River2D. Therefore, some of the criteria listed above are River2D-specific and cannot be directly applied to other 2-D models. However, these criteria provide a reasonable starting point that can be modified to fit a broader range of hydraulic models. For application with SToRM and other 2-D models, recommended adjustments to the USFSW (2011) criteria listed above are discussed below in Sections 4.1 through 4.6. Final recommended criteria for 2-D model setup, calibration, and validation for use with SToRM are provided in Section 4.7.

4.1 Mesh Quality

The Mesh Quality Index (QI) value is an index of calculation mesh quality built into the River2D hydraulic model. The QI in River2D allows the user to evaluate triangle size and shape to ensure long irregular or thin triangles are not formed in the calculation mesh, which could result in an unstable model and poor calculation results. Many 2-D models use polygons with more than three sides, eliminating problems associated with long thin triangles. Other models, such as SToRM, allow the user to input minimum angles for triangles when building the calculation mesh, thus eliminating formation of long thin triangles. For these reasons, the following criteria are recommended to evaluate mesh quality: (1) calculation mesh angles should not be less than 30 degrees; and (2) when differencing a DTM generated from calculation mesh bed elevations with a DTM generated from surveyed topography, total area greater or less than the average D_{84} within the active channel should be less than 5%.

4.2 Water Surface Elevation

Calibration as defined above is considered to have been achieved when the water surface elevation predicted by the 2-D model at the upstream boundary transect is within 0.1 ft of the water surface elevation predicted by PHABSIM for the highest predicted flow (or observed at the highest measured flow). We do not recommend the use of one model to calibrate another model. Rather, calibration of 2-D models should use observed water surface elevations. Therefore, the model-predicted water surface elevation for a known streamflow should be within 0.1 ft of the corresponding observed water surface elevation at the upstream end of the modeled site. In addition, we recommend that a number of observed spatially-distributed water surface elevation points be collected. As described in Section 4.7 of this appendix, the minimum number of spatially-distributed points should be relative to the size/length of the site. For Sproul Creek, more than 50 water surface measurements were taken at spatially-distributed points within the mainstem Sproul Creek 2-D modeling site. The recommended criterion when comparing all observed water surface elevations to corresponding values predicted by the model is that the root mean squared error (RMSE) should be less than 0.1.

4.3 Solution Change/Net Flow

This criterion involves looking at the solution change for the highest flow. We suggest that a stable steady-state 2-D hydraulic model be evaluated for all calibration flows (not just the highest flow). In addition, we recommend that one or more of the following criteria, including modifications to USFWS (2011) should be used: (1) the relative change between iterations of the average water depth for all nodes within the modeling boundary should be less than 0.00001; (2) the depth-averaged root mean square (RMS) for all nodes within the modeling boundary should be less than 0.001; (3) the total change in mass of water within the computational domain between computational iterations should be zero; and (4) the net change between inflow and outflow at the final time step should be less than 1%.

4.4 Froude Number

For low gradient streams, the maximum Froude number should typically be less than 1.0 (i.e., subcritical flow). Flosi et al. (2010) describe a low gradient stream as having a slope less than 4% and few exposed boulders. There are exceptions where channels with gradients greater than 1% and a relatively large number of exposed boulders have locations where supercritical flow (i.e., Froude number greater than 1.0) is reached. Unsteady models, such as SToRM and RAS-2D, have the capacity to predict supercritical flow. Therefore, we propose the following adjustment to this criterion: (1) the maximum Froude number for the majority of sites should be less than 1.0, and (2) for those occasions when a Froude number exceeds 1.0, a reasonable explanation should be provided to explain the model's prediction of supercritical flow (i.e., riffle crest).

4.5 Velocity & Depth Validation

The criterion used to determine whether the model is validated is whether the correlation between at least 50 spatially-distributed observed and predicted velocities is greater than 0.6 and depths is greater than 0.8. The correlation targets of 0.6 for velocity and 0.8 for depth are reasonable. To calculate the correlation, we recommend the Pearson's *r* correlation coefficient equation as presented in Section 5.6 of this appendix. For all three validation flows, more than 50 velocity and depth measurements were taken at spatially-distributed points within the mainstem Sproul Creek 2-D modeling site.

4.6 Biological Verification

As biological verification, the Mann-Whitney U test should be used to determine whether the combined habitat suitability predicted by the 2-D model was higher at locations where targeted species and life stages (i.e., salmonid redds, young of the year (YOY), and juveniles) were present versus locations where redds, fry, or juveniles were absent. Biological verification is an important component to support habitat predicted by the 2-D model; however, this is more a verification of the habitat suitability criteria used than the hydraulic parameters predicted by the model. Therefore, we recommend that biological verification not be included as part of this hydraulic appendix. However, this type of biological verification could be used in conjunction with predicted suitable habitat calculated from 2-D model hydraulic output and habitat suitability indices.

4.7 Recommended QA/QC Criteria Modified from USFWS (2011)

The following QA/QC criteria were used in the setup, calibration, and validation of the 2-D model used in the mainstem Sproul Creek instream flow assessment report. Final recommended QA/QC criteria include:

1. **Mesh Quality**: Calculation mesh angles should not be less than 30 degrees. In addition, total area greater or less than the average D_{84} within the active channel, when differencing a DTM generated from calculation mesh bed elevations with a DTM generated from surveyed topography, should be less than 5%.
2. **Water Surface Elevation**: Predicted water surface elevations should be within 0.1 ft of measured water surface elevations at the upstream end of the modeled site for a specific flow, and a minimum number of measured spatially-distributed water surface elevation points should have a RMSE less than 0.1 when compared to corresponding water surface elevation values predicted by the model. The minimum number of spatially-distributed points should be relative to the size/length of the site. The target of 50 spatially-distributed points provides a reasonable minimum target.
3. **Solution Change/Net Flow**: Model stability for all calibration flows should meet two or more of the following criteria: (1) the relative change between iterations of the average water depth or the RMS of water depth for all nodes within the modeling boundary should be less than 0.00001 or 0.001, respectively; (2) the total change in mass of water within the computational domain between computational iterations should be zero; and (3) the net change between inflow and outflow at the final time step should be less than 1%.
4. **Froude Number**: For low gradient streams, the maximum Froude number should be less than 1.0 (i.e., subcritical flow). For those occasions when a Froude number exceeds 1.0, location of supercritical flow and rationale explaining why the model predicted supercritical flow should be provided.
5. **Velocity and Depth Validation**: Pearson's *r* correlation coefficient between spatially-distributed measured and simulated velocities is greater than 0.6 and depths is greater than 0.08. The target of 50 spatially-distributed points provides a reasonable minimum target.

5 SETTING UP, RUNNING, CALIBRATING, AND VALIDATING MODEL

Once the topographic, substrate, cover, streamflow, and calibration and validation data were collected and appropriately formatted for model input, the model was prepared. Model preparation may be started even if additional calibration and validation data are likely needed. Setting up and running the model prior to collecting all field data allows opportunities to identify and fill in information gaps, such as topography and substrate. In this case, the Sproul Creek model was set up, run, calibrated and validated for flows of 3.9 cfs, 21.1 cfs, and 90.0 cfs (Figure F-8). No additional calibration or validation data were needed to meet the instream flow study objectives for the upper mainstem Sproul Creek reach.

5.1 Creating the Calculation Mesh

The first and probably the most critical step in accurately depicting surveyed topography is development of a calculation mesh that is fine enough to capture the topographic detail surveyed. The calculation mesh needs to ultimately provide a reasonable estimate of existing micro-habitat, yet be coarse enough to keep model run times reasonably low. To determine if the calculation mesh adequately captures the surveyed topography, bed elevations associated with the calculation mesh were exported from the model to Auto CAD Civil 3D. A DTM from bed elevations was generated and then differenced from the DTM generated from the surveyed topography. The resulting difference map shows areas of cut and fill between the two surfaces. The preferred outcome is that the two surfaces are the same: zero cut and fill. When the existing topography includes nearly vertical walls (banks, boulders, and/or wood), the calculation mesh will likely not be able to capture these features exactly. For the model to accurately calculate flow, some calculation mesh polygon (typically 0.5 to 3 m^2) is required to capture surveyed topography, including near vertical banks and boulders. This typically results in areas that are lower or higher than the surveyed topography along these features.

Once the *.tpo file (generated from surveyed 2-D site topography) was imported into iRIC, a matrix of non-overlapping triangles (calculation mesh) was generated by SToRM and overlaid onto the imported topography. The calculation grid was created following these steps:

1. A mesh boundary encompassing the area to be modeled within the existing DTM was drawn (Figure F-9).
2. Breaklines were added along large wood features that created areas of mesh refinement (Figure F-9).
3. The calculation mesh (grid) was created such that the minimum angle for cell vertices was 30 degrees (eliminating long thin triangles) and the maximum area was 0.20 m^2 (approximately 2.15 ft^2; Figure F-10).
4. Elevations from the imported existing surveyed topography were assigned to each calculation mesh node.

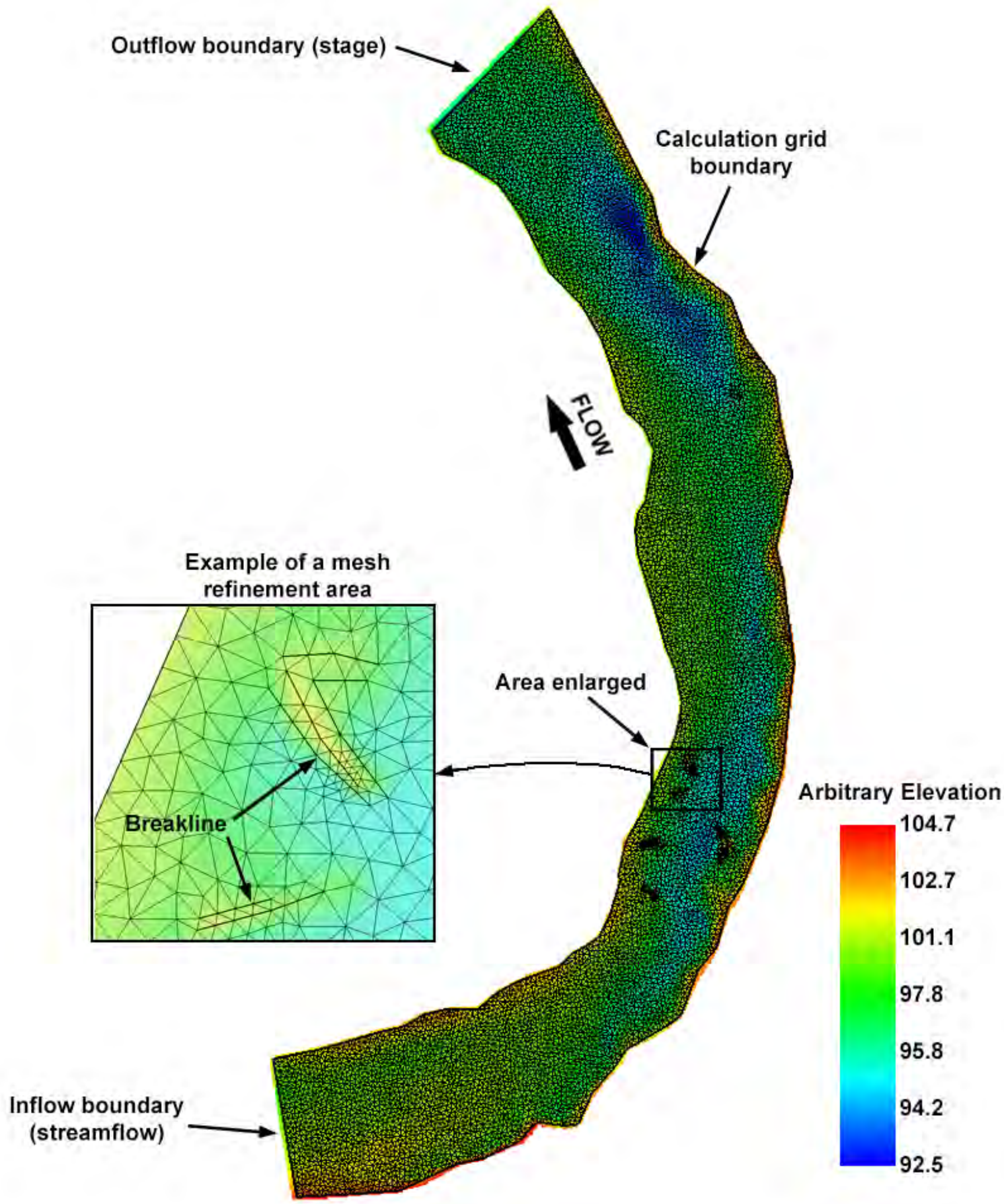

Figure F-9. Screen capture showing an overview of the Sproul Creek calculation mesh along with an area where break lines were added to refine the mesh.

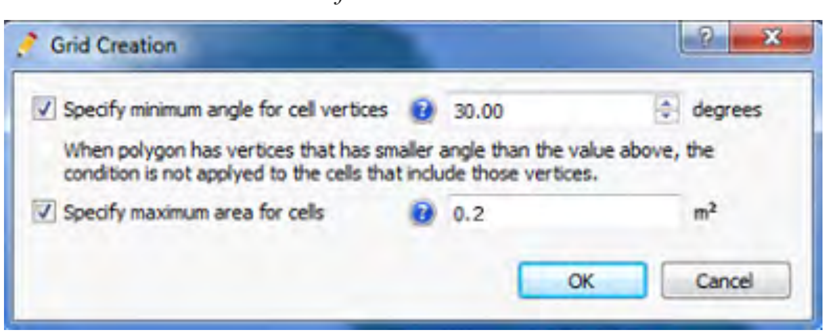

Figure F-10. SToRM grid creation window from Sproul Creek modeling site.

5.2 Calculation Mesh Quality (Recommended Criterion #1)

Calculation mesh quality is divided into two criteria:

Size and shape of mesh polygons. Because a minimum angle for cell vertices can be set as a parameter when generating the calculation mesh for internal angles (in this case 30 degrees), and maximum area for polygon cells is set to 0.20 m^2 (Figure F-10), no long thin or exceedingly large triangles are formed; therefore, calculation mesh polygon quality meets criteria established in Section 4.1.

How well the calculation mesh captures the existing ground DTM. Once the calculation mesh is built and existing surface elevations assigned to each mesh node, the calculation mesh with corresponding surface elevations is exported as a *.csv file for import into AutoCAD Civil 3D. The two-existing ground DTM's (from the original survey and calculation mesh) are differenced for comparison. The minimum elevation difference evaluated was 78.8 mm or 0.26 ft, which is less than the total weighted D_{84} particle size, by area, within the active channel of approximately 111 mm, or 0.36 ft (Table F-5). The area difference between DTM's was calculated by adding up the total area for each elevation difference bin and dividing it by the total calculation mesh area (Figure F-11). The percent total difference between DTM's is 2.6%, meeting established criteria of less than 5% (Table F-6, Figure F-11).

Table F-5. Average D_{84} particle size for the active channel within the 2-D modeling reach.

Facies #	Area (ft^2)	Percent Total Area	D_{84} (mm)	Weighted D_{84} (mm)
1	5,100	20.7%	200	41.4
2	605	2.5%	36	0.9
3	3,923	15.9%	99	15.7
4	488	2.0%	2	0.0
5	1,150	4.7%	59	2.8
6	1,225	5.0%	43	2.1
7	1,401	5.7%	98	5.6
8	1,879	7.6%	36	2.7
9	2,732	11.1%	155	17.2
10	1,567	6.4%	49	3.1
11	624	2.5%	20	0.5
12	662	2.7%	152	4.1
14	2,466	10.0%	152	15.2
15	845	3.4%	2	0.1
			Total Weighted D_{84} (mm)	**111.3**

Note: Number sequencing in field excluded Facies #13, which has been carried through reporting.

Table F-6. Statistical output from AutoCAD Civil 3D, based on differencing DTM's generated from surveyed topography and calculation mesh bed elevations.

General		
Base Surface	Sproul_Ck_Topo_062916	
Comparison Surface	Sproul 2-D Mesh Bed Elev Topo Final	
Number of points	42,272	
Area of surface comparison	23,030	Square ft
Surface area difference	3.76	%
Minimum X coordinate	9880.07	ft
Minimum Y coordinate	9911.56	ft
Maximum X coordinate	10064.25	ft
Maximum Y coordinate	10331.81	ft
Minimum elevation difference	−4.95	ft
Maximum elevation difference	2.95	ft
Mean elevation difference	0.006	ft
TIN		
Number of triangles	83,198	
Maximum triangle area	2.14	Square ft
Maximum triangle length	11.19	ft
Volume		
Cut Factor	1	Square ft
Fill Factor	1	Square ft
Cut volume between surfaces	5.64	Cubic yards
Fill volume between surfaces	5.18	Cubic yards
Net volume between surfaces	0.46	Cubic yards–cut

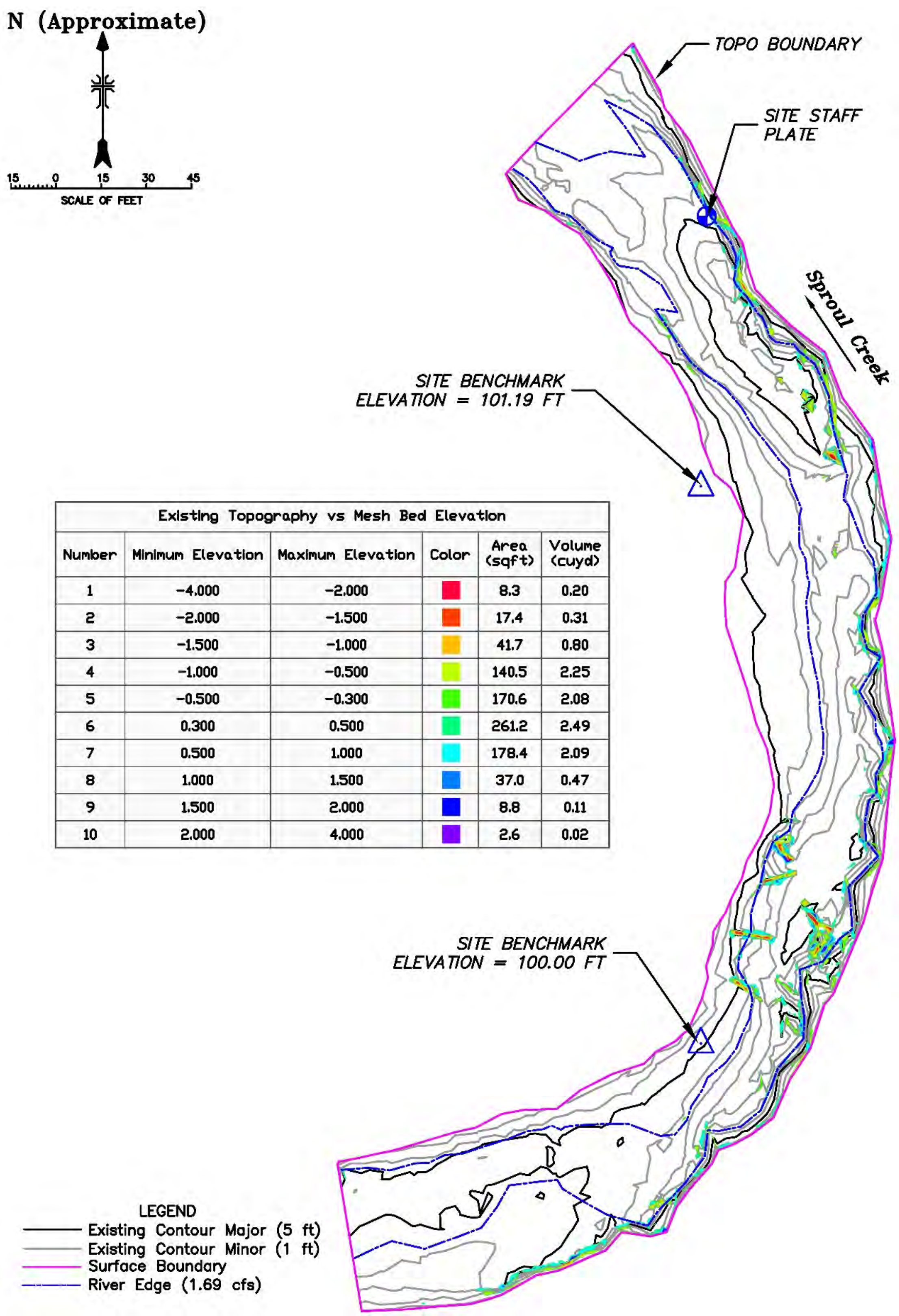

Existing Topography vs Mesh Bed Elevation

Number	Minimum Elevation	Maximum Elevation	Color	Area (sqft)	Volume (cuyd)
1	-4.000	-2.000		8.3	0.20
2	-2.000	-1.500		17.4	0.31
3	-1.500	-1.000		41.7	0.80
4	-1.000	-0.500		140.5	2.25
5	-0.500	-0.300		170.6	2.08
6	0.300	0.500		261.2	2.49
7	0.500	1.000		178.4	2.09
8	1.000	1.500		37.0	0.47
9	1.500	2.000		8.8	0.11
10	2.000	4.000		2.6	0.02

Figure F-11. Planform map showing topographic differencing of DTM's generated from surveyed topography and calculation mesh bed elevations.

5.3 Running the 2-D Model and Calibrating to Measured Water Surface Elevations (Recommended Criterion #2)

After the mesh quality met criteria and water surface calibration data were collected, initial Manning's *n* values for each facies/cover type, upstream flow boundary, and downstream water surface elevation boundary were set for each of the three calibration flows (Table F-7). The process to arrive at final Manning's *n* values was iterative until water surface calibration was achieved. Values for Manning's *n*, upstream flow boundary, and downstream water surface elevation boundary were then assigned to the corresponding calculation mesh nodes (Figure F-12). Calibrated Manning's *n* values were then plotted and a power function fit to each facies to develop a roughness–flow rating curve used to generate roughness values for each facies for each modeled flow (Figure F-13).

Initial starting conditions for the mainstem Sproul Creek modeling site were calculated for velocity direction and magnitude coefficients U and V, and water surface elevation Um (Equations 1, 2 and 3) and entered into the initial starting "coverage polygons" (Table F-8). These initial starting conditions are intended to fill model calculation mesh and provide an initial velocity direction and magnitude that expedite the time necessary for the model to reach a point of convergence. Initial starting coverage polygons, rather than uniform starting conditions, were used to better represent changes in flow direction within the mainstem Sproul Creek 2-D modeling site (Figure F-14). For either uniform initial starting condition or initial starting coverage polygons, velocity direction and magnitude coefficients (U and V, respectively), and water surface elevation (Um) are calculated (Equations 1, 2, and 3).

Uniform Starting Conditions or Starting Coverage Polygon Equations (Simões 2013):

$$U = Um*\cos(\Theta) \tag{1}$$
$$V = Um*\sin(\Theta) \tag{2}$$
$$Um = Q/A \tag{3}$$

Where:

U = Velocity direction coefficient
V = Velocity magnitude coefficient
Q = Streamflow
A = Averaged flow area within coverage polygon
Θ = Counterclockwise angle of flow path from north
Um = Averaged water surface elevation within the site or coverage polygon

Table F-7.Final Manning's n *roughness values and corresponding boundary conditions assigned for calibration flows.*

Upstream Boundary	**Downstream Boundary**	**Manning's *n* Roughness**													
Streamflow (cfs)	**WSE (ft)**	**1**	**2**	**3**	**4**	**5**	**6**	**7**	**8**	**9**	**10**	**11**	**12**	**14**	**15**
3.9	98.30	.050	.069	.081	.056	.071	.053	.073	.069	.094	.071	.056	.081	.081	.056
21.1	97.65	.040	.055	.065	.045	.057	.042	.058	.055	.075	.057	.045	.065	.065	.045
90.0	97.35	.037	.041	.059	.037	.052	.041	.055	.040	.063	.053	.038	.055	.055	.037

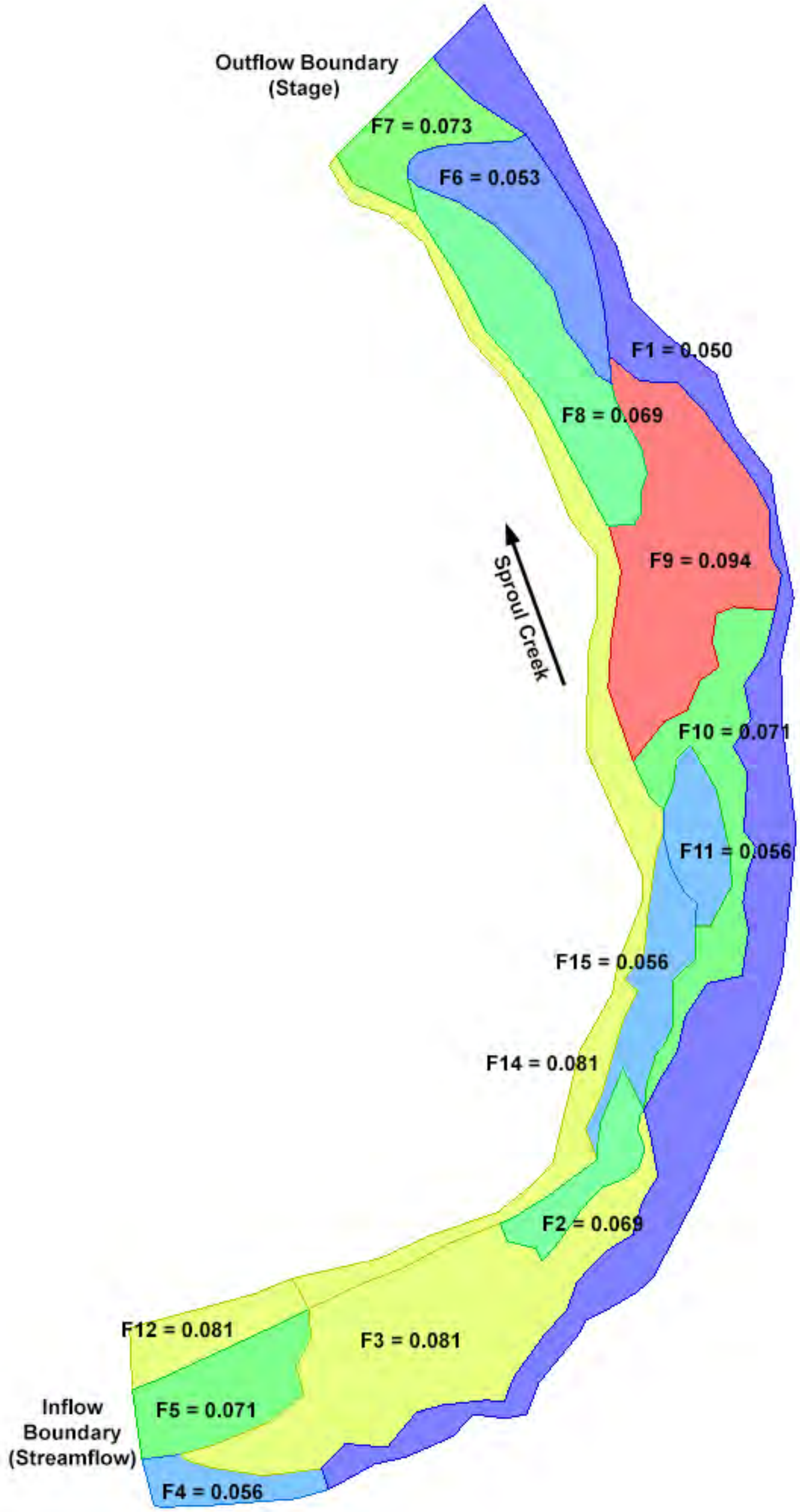

Figure F-12. Example of Manning's n *roughness values applied to Sproul Creek facies for a calibration flow of 3.9 cfs.*

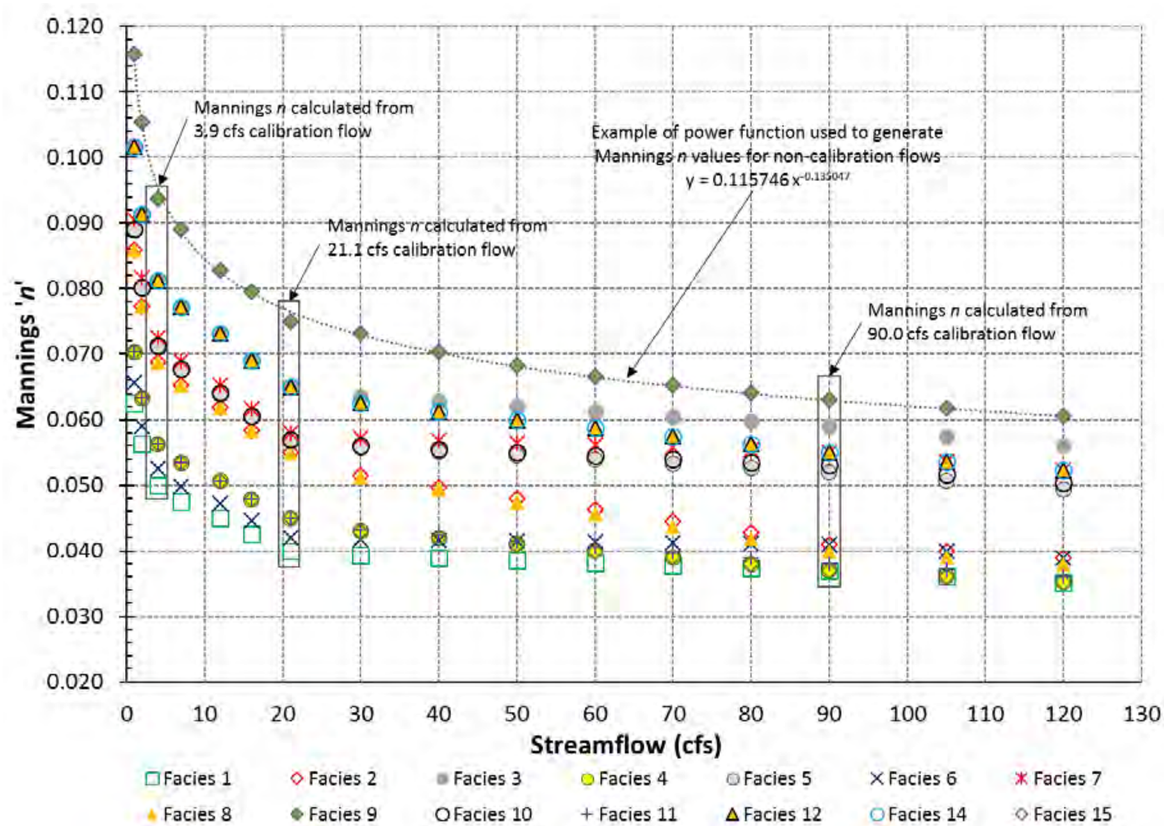

Figure F-13. Manning's n *roughness values generated from mainstem Sproul Creek calibration flows.*

Table F-8. Sproul Creek initial starting "coverage polygons" condition for all calibration flows entered into model setup under initial starting conditions.

Q (cfs)	Q (cms)	Average Wetted Width (m)	Average Depth (m)	Average Wetted Area (m^2)	Angle, θ (degrees)	Um = Q/A (m/s)	U=Um*cos(θ)	V= Um*sin(θ)	Stage (m)	Note
90.0	2.548	14.63	0.32	4.64	68	0.549	0.206	0.509	30.72	Upstream block
	2.548	10.06	0.69	6.93	8	0.368	0.364	0.051	30.38	Middle block
	2.548	8.84	0.91	8.08	324	0.315	0.255	−0.185	30.02	Downstream block
21.1	0.597	13.72	0.29	3.93	68	0.152	0.057	0.141	30.54	Upstream block
	0.597	8.23	0.46	3.81	8	0.156	0.155	0.022	30.13	Middle block
	0.597	8.53	0.46	3.90	324	0.153	0.124	−0.090	29.79	Downstream block
3.9	0.110	3.96	0.16	0.65	68	0.169	0.063	0.157	30.53	Upstream block
	0.110	5.18	0.29	1.52	8	0.073	0.072	0.010	29.91	Middle block
	0.110	7.92	0.37	2.90	324	0.038	0.031	−0.022	29.69	Downstream block

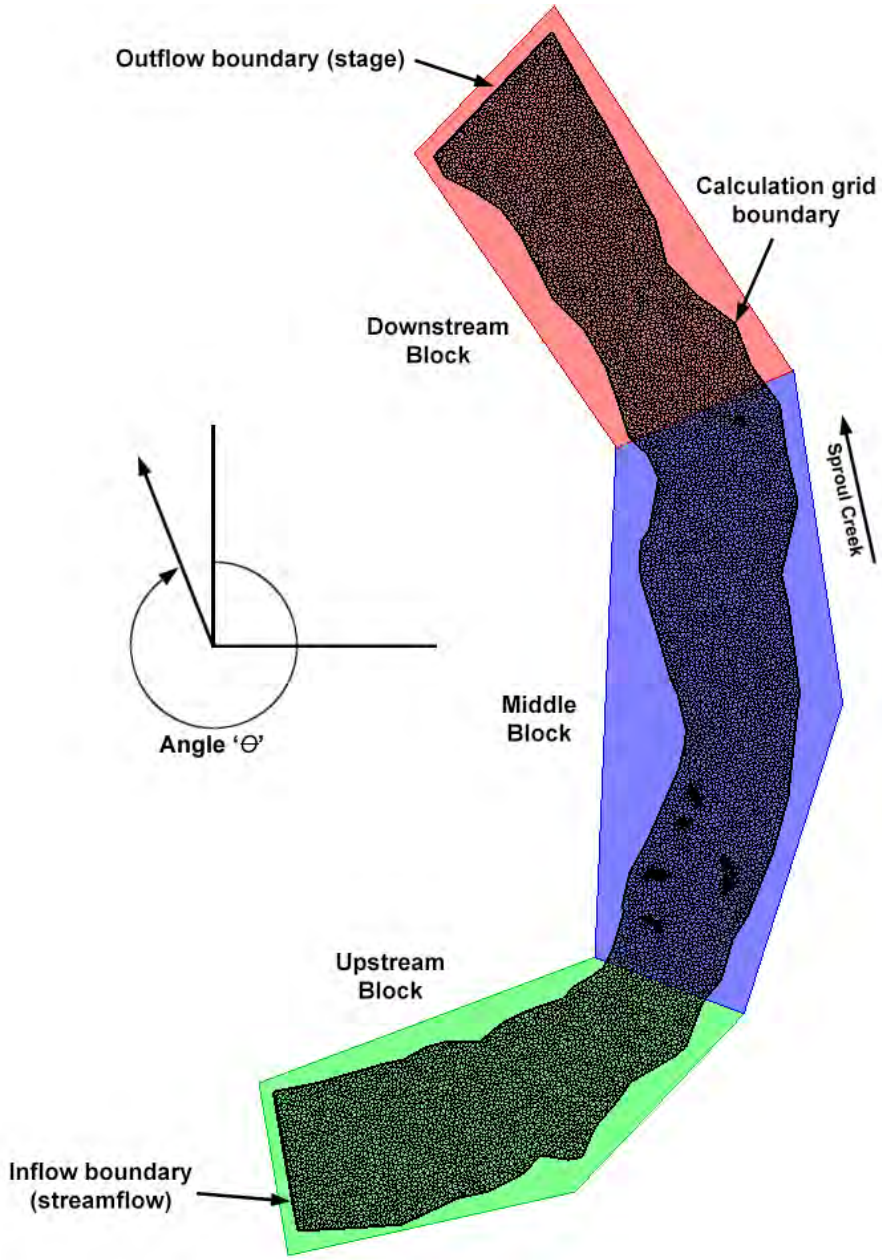

Figure F-14. Example of initial conditions coverage polygons for the mainstem Sproul Creek 2-D modeling site. Values for water velocity direction, magnitude, and average water surface elevation were added to each coverage polygon per Table F-8.

The 2-D model was run iteratively for each of the three calibration flows until the predicted water surface elevation was within 0.1 ft of observed water surface elevation at the upstream end of the modeled site (Table F-9). Observed spatially-distributed water surface elevation points were then compared to corresponding water surface elevation values predicted by the model (Figure F-15 through Figure F-18). Resulting RMSE for each flow was less than 0.1 (Table F-9). Therefore, the 2-D mainstem Sproul Creek hydraulic model met both calibration criteria associated with water surface elevation for all three calibration flows.

Table F-9. Calibration flows showing water surface difference between upstream-most measured and predicted water surface point, total number of measured points, and RMSE for all predicted and corresponding measured values.

Streamflow (cfs)	Upstream Most Predicted WSE (ft)	Upstream Most Observed WSE (ft)	Difference Predicted less Observed (ft)	Number of Observed WSE points	Root Mean Square Error	Average Difference for All Points (ft)	Maximum WSE Point Difference (ft)*	Number of Points Exceeding 0.10 ft WSE Difference
3.9	100.38	110.43	−0.05	66	0.026	0.01	0.15	5
21.1	100.81	100.77	0.04	64	0.023	0.02	0.16	4
90.0	101.48	101.45	0.03	48	0.035	0.01	0.27	7

* The maximum water surface difference provided is not recommended for use as calibration criteria. Factors such as waves in riffles, flow pulses, miss readings during flow measurements, and the fact that a 2-D model captures an average water surface can be cause for these differences. Overall, the number of points with a water surface difference exceeding 0.10 ft was less than 10 for each calibration flow.

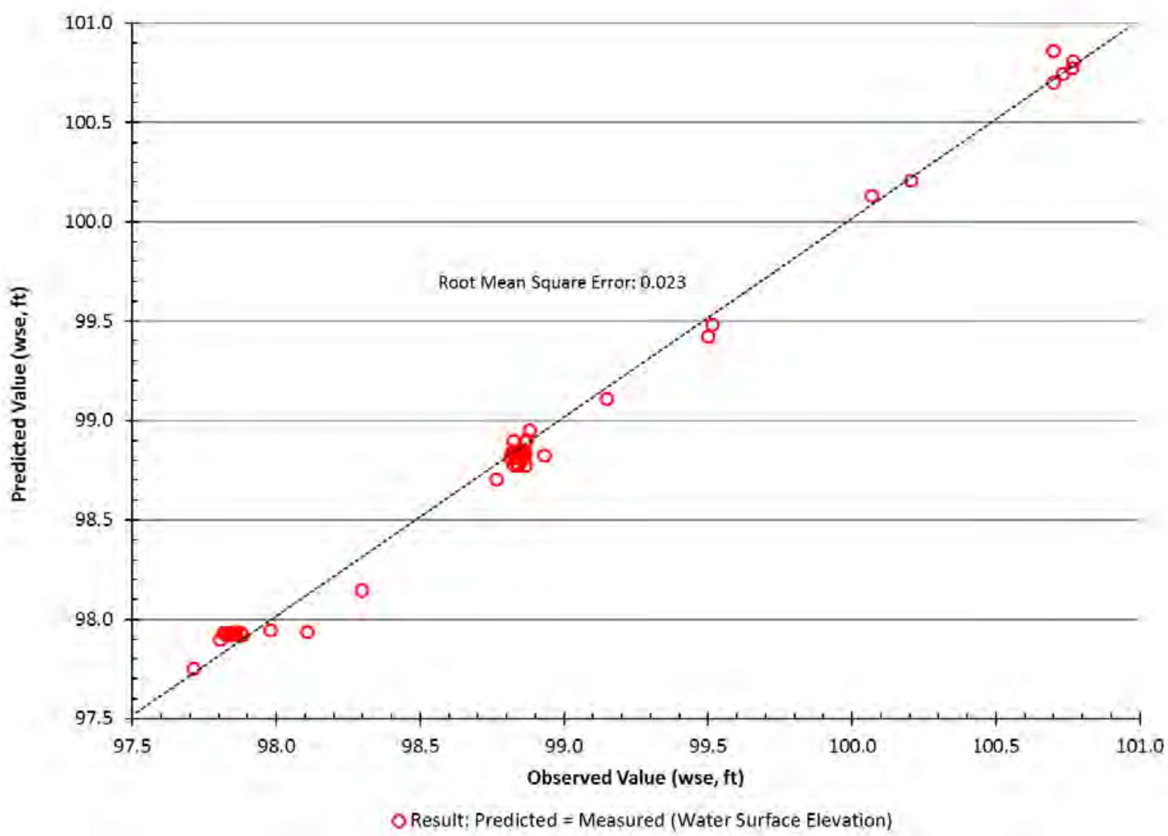

Figure F-15. Plot comparing predicted and observed water surface elevation for a streamflow of 21.1 cfs.

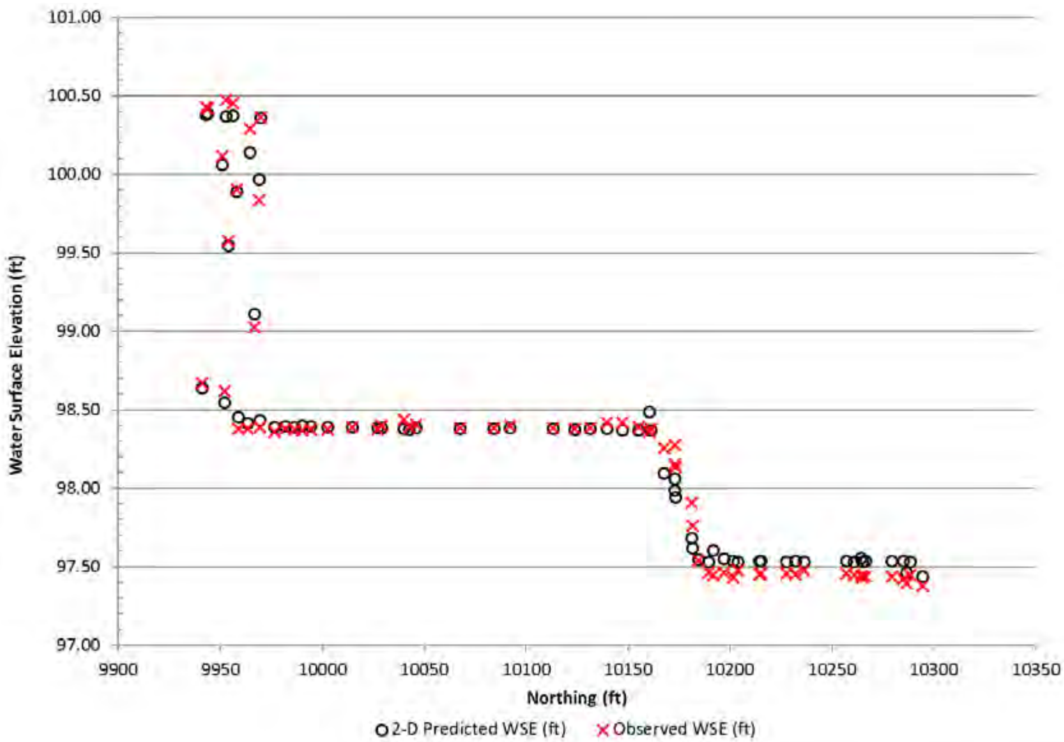

Figure F-16. Lateral distribution of points (based on northing) showing predicted and observed water surface elevations for a streamflow of 3.9 cfs.

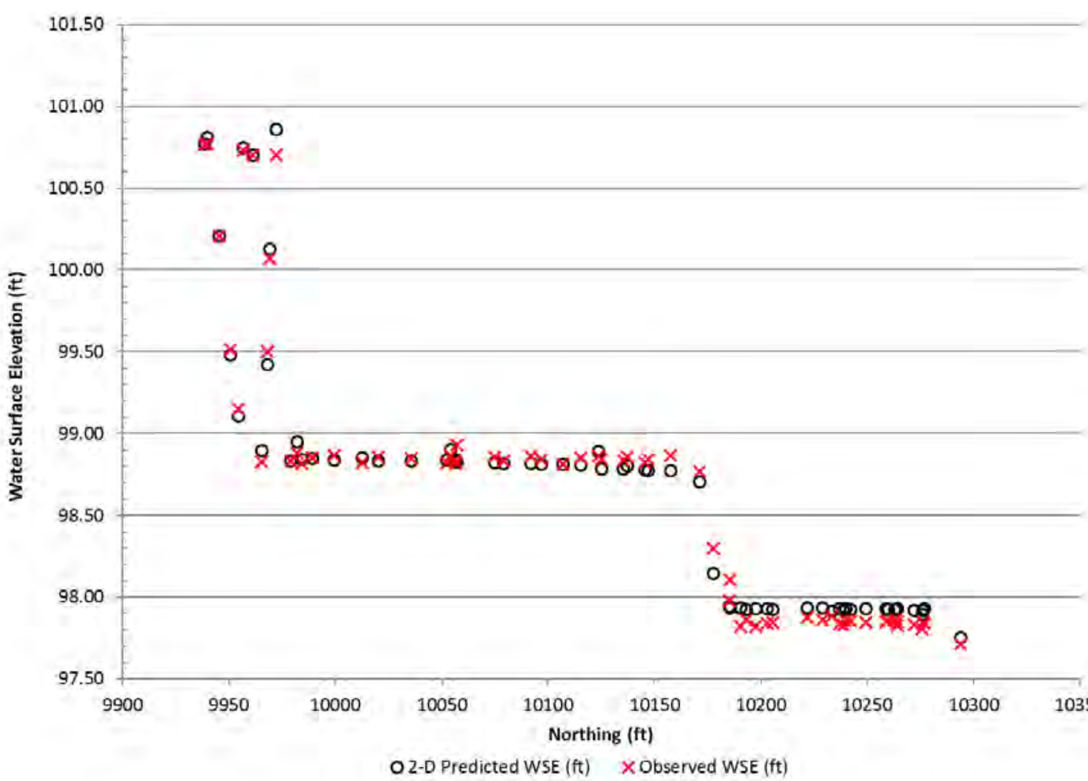

Figure F-17. Lateral distribution of points (based on northing) showing predicted and observed water surface elevations for a streamflow of 21.1 cfs.

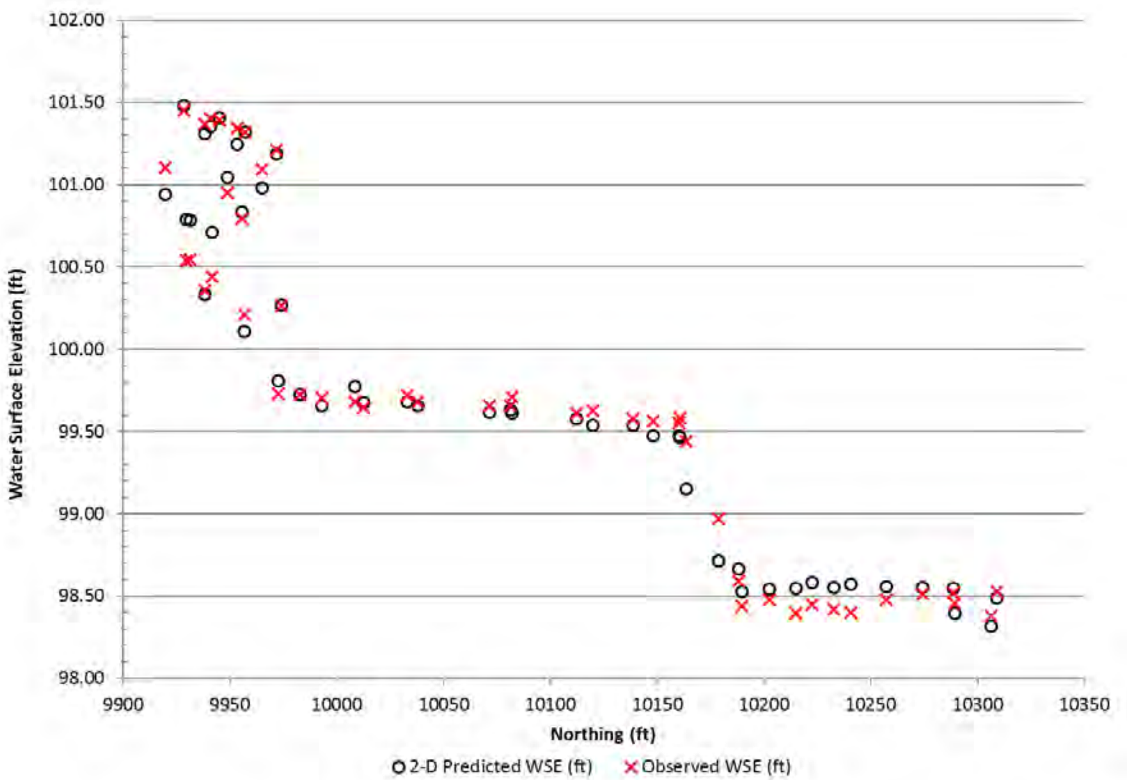

Figure F-18. Lateral distribution of points (based on northing) showing predicted and observed water surface elevations for a streamflow of 90.0 cfs.

5.4 Solution Change/Net Flow (Recommended Criterion #3)

Computational output from SToRM for all iterations (time steps) provides: (1) the relative change between model iterations of the RMS for water depth, (2) the total change in mass of water within the computational domain between iterations, and (3) the net change between inflow and outflow at the final time step. For all calibration flows, the RMS for relative change between time steps for water depth was less than 0.001, total water mass change between time steps within the modeling boundary was 0, and net change between inflow and outflow was less than 1% (Table F-10), thereby meeting model stability criteria. Model stability may be graphically shown by plotting inflow and outflow over time (Figure F-19). A plot of the 21.1 cfs inflow vs outflow showed the model reached stability at approximate time step 50,000 and remained stable for the remainder of the model run time (Figure F-19).

In addition to the criteria for model stability listed above, models with difficult solutions may be forcefully bound by setting the maximum velocity parameter (Figure F-20) to guarantee model survivability during the initial time steps (Simões 2013). However, the final solutions must always be computable without the use of this parameter (Simões pers. comm. 2016). Utilization of the bounding parameter was not necessary for the Sproul Creek 2-D modeling site, as solutions were relatively stable from the initial time step (Figure F-19).

Table F-10. Computational output from SToRM for the last two time steps for each calibration flow.

Streamflow (cfs)	Iteration Time Step	Within Modeling Boundary		Inflow (cfs)	Outflow (cfs)	Percent Change Inflow vs Outflow
		Root Mean Square of Water Depth	Total Mass of Water (lbs)			
3.9	999999	0.000164	919,724.5	3.885	3.876	0.23%
	1000000	0.000129	919,724.5	3.885	3.878	0.18%
	Percent Change between Iterations		**0**	**0.000%**	**0.052%**	
21.1	999999	0.000309	1,241,224.6	21.069	21.060	0.04%
	1000000	0.000282	1,241,224.6	21.069	21.060	0.04%
			0	**0.000%**	**0.000%**	
90.0	1999999	0.000276	1,885,349.17	89.971	90.035	0.07%
	2000000	0.000257	1,885,349.17	89.971	89.908	0.07%
	Percent Change between Iterations		**0**	**0.000%**	**0.141%**	

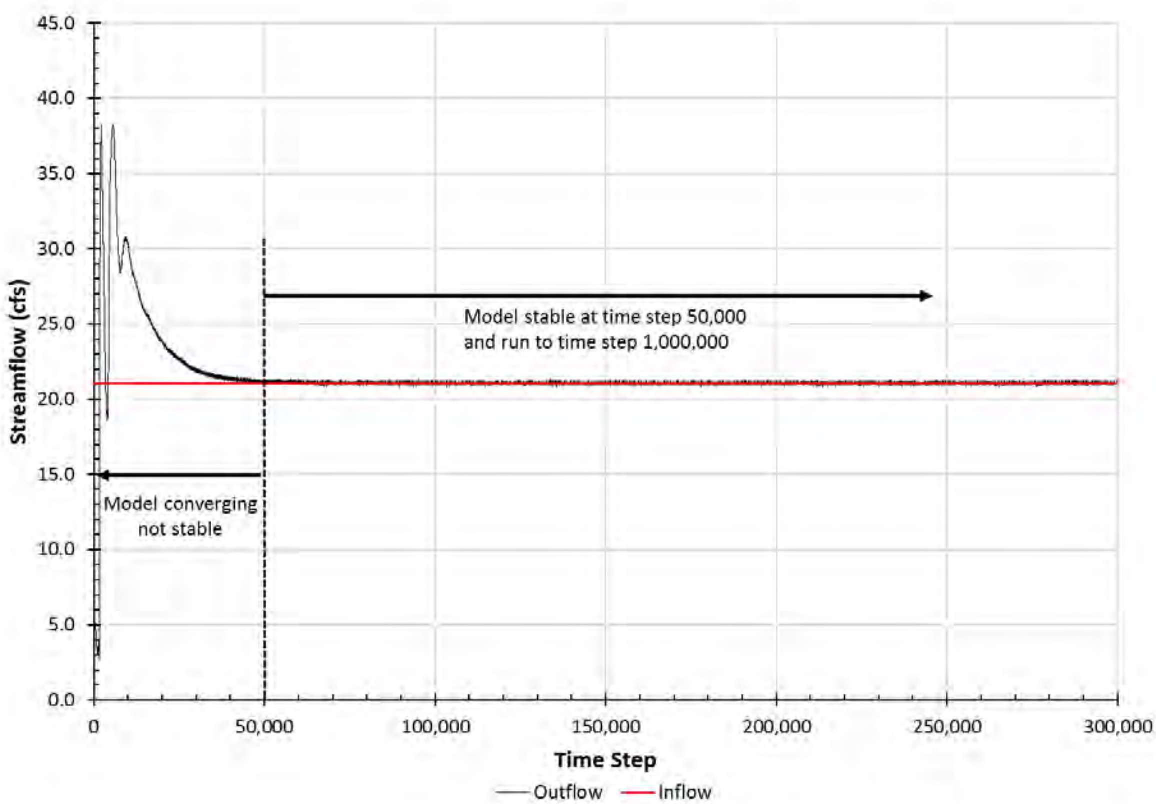

Figure F-19. Inflow and outflow plotted for each time step from 0 to 300,000 for the 21.1 cfs calibration flow.

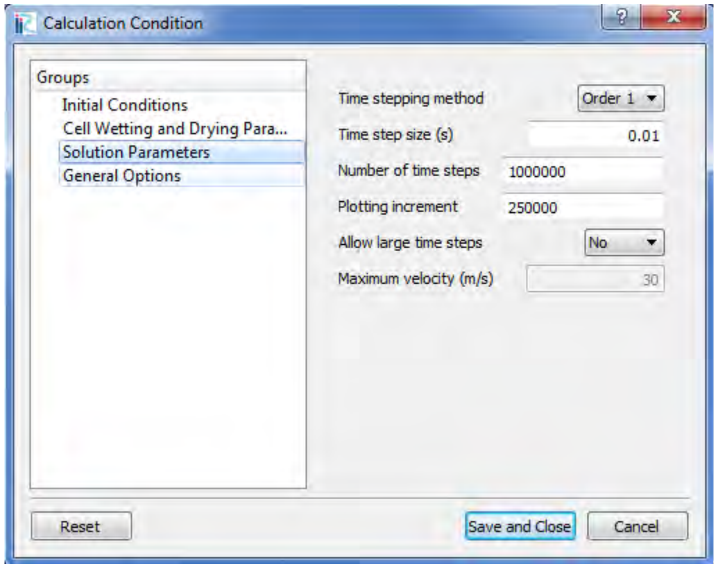

Figure F-20. Example from iRIC solution parameter window showing location to bound maximum velocity.

5.5 Froude Number (Recommended Criterion #4)

The mainstem Sproul Creek at the 2-D modeling site has a slope of 0.6% at 21.1 cfs, making this a low gradient stream. Although a Froude number for a low gradient stream is expected to be less than 1.0, shallow riffles and large exposed boulders may result in Froude numbers exceeding 1.0. Froude number was calculated for all three calibration flows using the depth and velocity at each node (Equation 4). For 3.9 cfs, the Froude number was less than 1.0 at all nodes, meeting recommended Criterion #4 (Table F-11). However, for 21.1 cfs and 90.0 cfs, the Froude number exceeded 1.0 at 9 and 20 nodes respectively (Table F-11, Figure F-21). There are large exposed boulders and one critical riffle within the Sproul Creek 2-D modeling site which resulted in very shallow flows and high velocities at a streamflow greater than 21.1 cfs. Given the hydraulic condition at this critical riffle and that all Froude numbers exceeding 1.0 were located within this critical riffle, these results are not considered out of the ordinary. Additionally, less than 0.4% of the modeled area was affected by Froude numbers greater than 1.0. Therefore, the model met this criterion.

$$F = V/\text{sqrt}(gh_m) \qquad (4)$$

Where:

F = Froude number at node
V = Mean column water velocity at node
g = Gravitational acceleration (32.174 ft/s^2)
h_m = Water depth at node

Table F-11. Summary of Froude number calculated for all nodes and the maximum value calculated provided for each calibration streamflow.

Streamflow (cfs)	Maximum Froude Number	Quantity of Froude Numbers Exceeding 1.0	Percent of 2-D Modeled Area Affected by Froude Number Greater than 1.0
3.9	0.805	0	0.00%
21.1	1.146	9	0.08%
90.0	1.455	20	0.19%

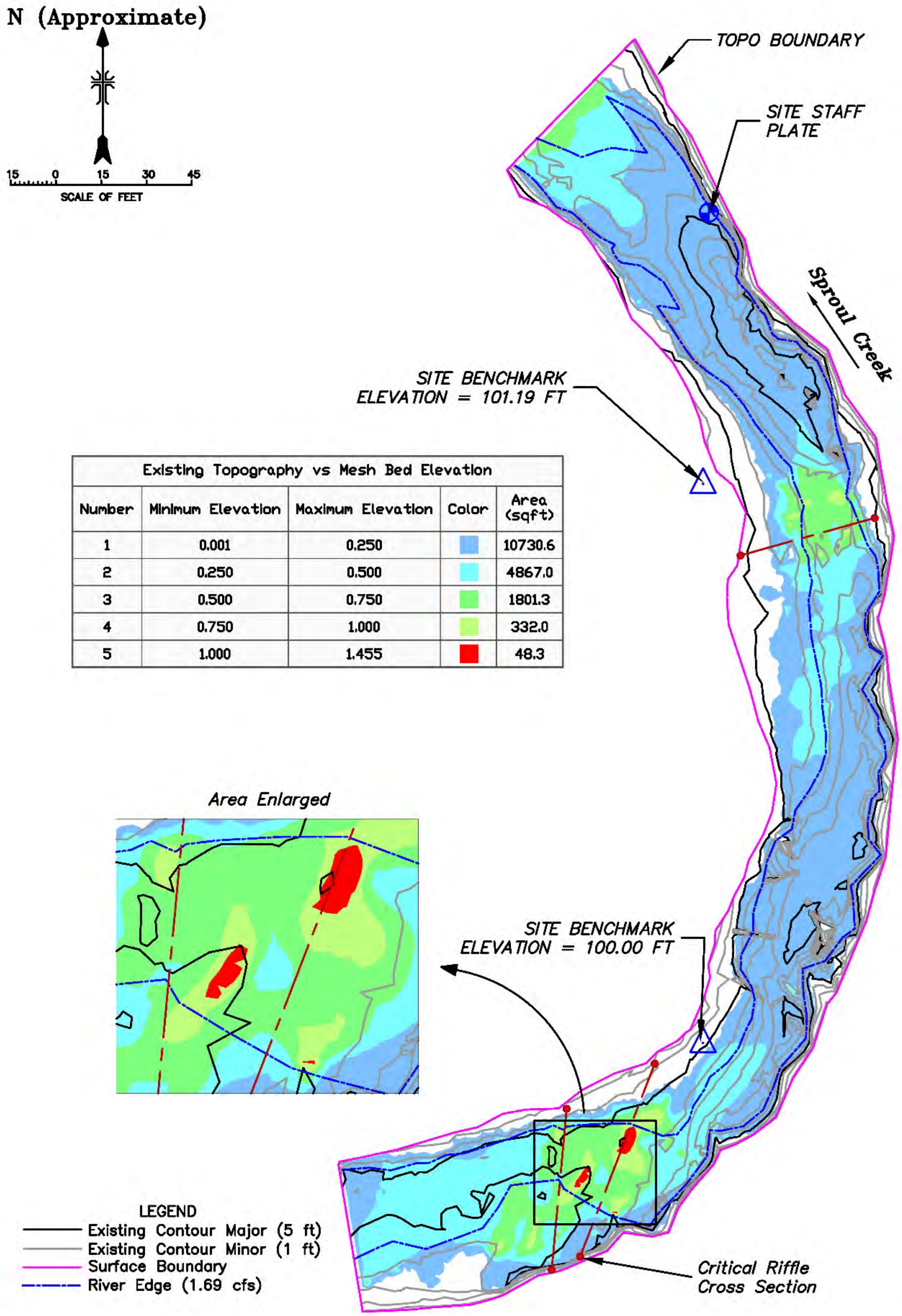

Existing Topography vs Mesh Bed Elevation				
Number	Minimum Elevation	Maximum Elevation	Color	Area (sqft)
1	0.001	0.250		10730.6
2	0.250	0.500		4867.0
3	0.500	0.750		1801.3
4	0.750	1.000		332.0
5	1.000	1.455		48.3

Figure F-21. Critical riffle cross section located within 2-D modeling site showing areas where the Froude number exceeded 1.0 (red polygons) at a streamflow of 90.0 cfs.

5.6 Velocity and Depth Validation (Recommended Criterion #5)

Velocity and depth validation points were collected at the same locations and streamflows that water surface elevation data were collected (Table F-4, Figure F-8). Table F-4 provides an example of velocity and depth validation data collected at the modeling site. Pearson's *r* correlation coefficient (Equation 5) between spatially-distributed observed and predicted velocities was calculated for all calibration flows, and was greater than 0.6 for velocity and 0.8 for depth for all calibration flows, thus meeting velocity and depth validation criteria (Table F-12, Table F-13). In addition to velocity and depth correlation, the maximum, minimum, and median differences between predicted and observed velocity and depth values were calculated (Table F-12, Table F-13). Lateral distribution of predicted and observed velocities (Figure F-22 through Figure F-24) and depths (Figure F-25 through Figure F-27) were compared for validation points (based on northing) at all calibration flows.

Pearson's *r* correlation coefficient:

$$r = \frac{N\sum xy - \sum(x)(y)}{\sqrt{[N\sum x^2 - \sum(x^2)][N\sum y^2 - \sum(y^2)]}} \qquad (5)$$

Where:

r = Pearson's correlation coefficient
N = number of values in each data set
$\sum xy$ = sum of the products of paired scores
$\sum x$ = sum of x (observed) scores
$\sum y$ = sum of y (predicted) scores
$\sum x^2$ = sum of squared x scores
$\sum y^2$ = sum of squared y scores

Table F-12. Calibration flows showing total number of observed points; maximum, minimum, and median difference from observed velocity values; and correlation between all predicted and corresponding observed velocity values.

Flow (cfs)	Number of Observed WSE points	Maximum Difference Predicted less Observed (ft/s)	Minimum Difference Predicted less Observed (ft/s)	Median Difference Predicted less Observed (ft/s)	Pearson's *r* Correlation Coefficient for All Predicted and Observed Velocities
3.9	66	−1.358	0.003	0.0263	0.823
21.1	64	1.287	0.001	0.122	0.869
90.0	48	1.523	0.002	0.062	0.898

Table F-13. Calibration flows showing total number of observed points, maximum, minimum, and median difference from observed depth values, and correlation between all predicted and corresponding observed depth values.

Flow (cfs)	Number of Observed WSE points	Maximum Difference Predicted less Observed (ft/s)	Minimum Difference Predicted less Observed (ft/s)	Median Difference Predicted less Observed (ft/s)	Pearson's *r* Correlation Coefficient for All Predicted and Observed Velocities
3.9	66	0.227	0.001	−0.013	0.965
21.1	64	1.119	0.001	0.017	0.957
90.0	48	1.201	0.005	−0.014	0.967

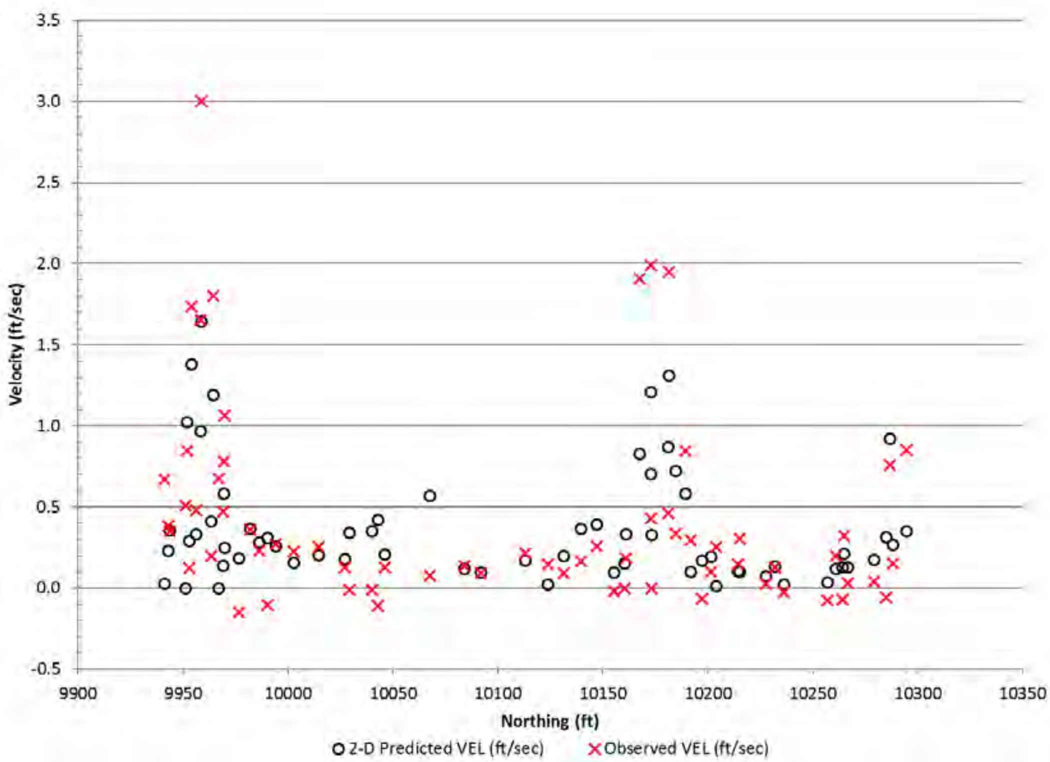

Figure F-22. Lateral distribution of points (based on northing) showing predicted and observed velocities for a streamflow of 3.9 cfs.

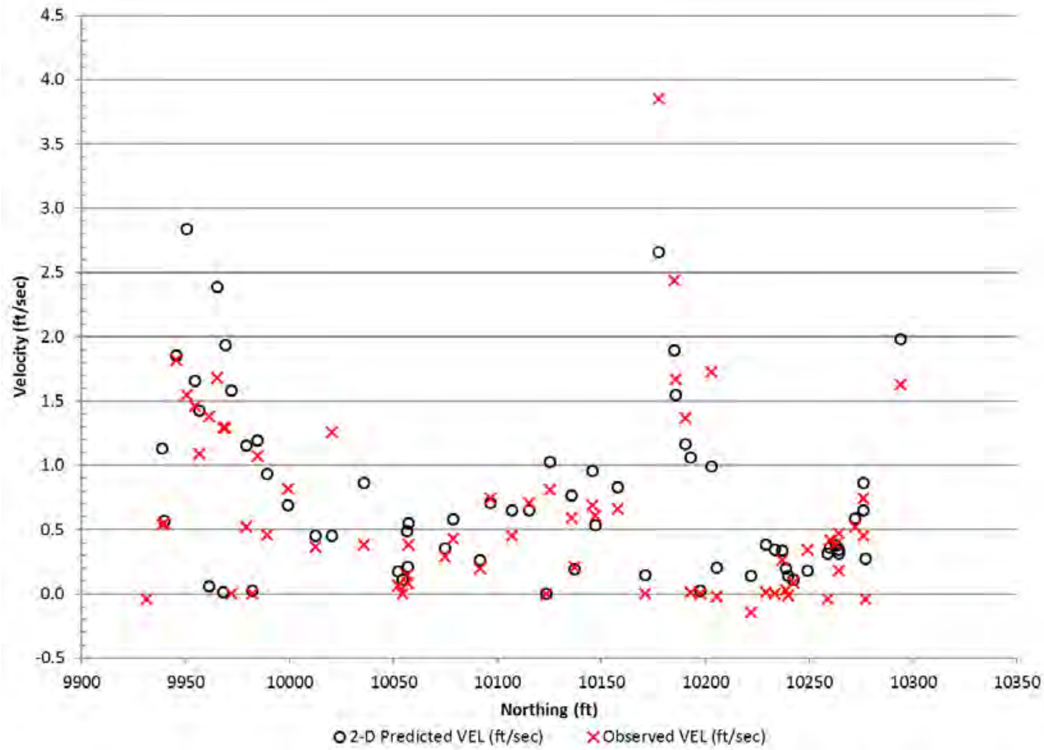

Figure F-23. Lateral distribution of points (based on northing) showing predicted and observed velocities for a streamflow of 21.1 cfs.

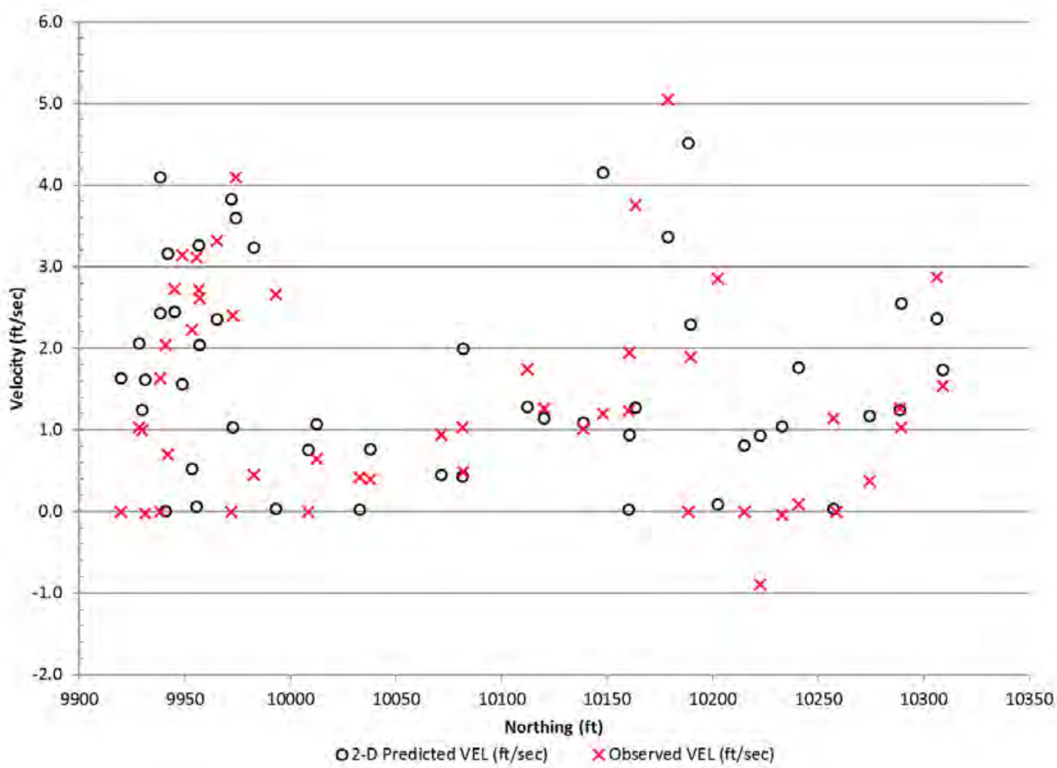

Figure F-24. Lateral distribution of points (based on northing) showing predicted and observed velocities for a streamflow of 90.0 cfs.

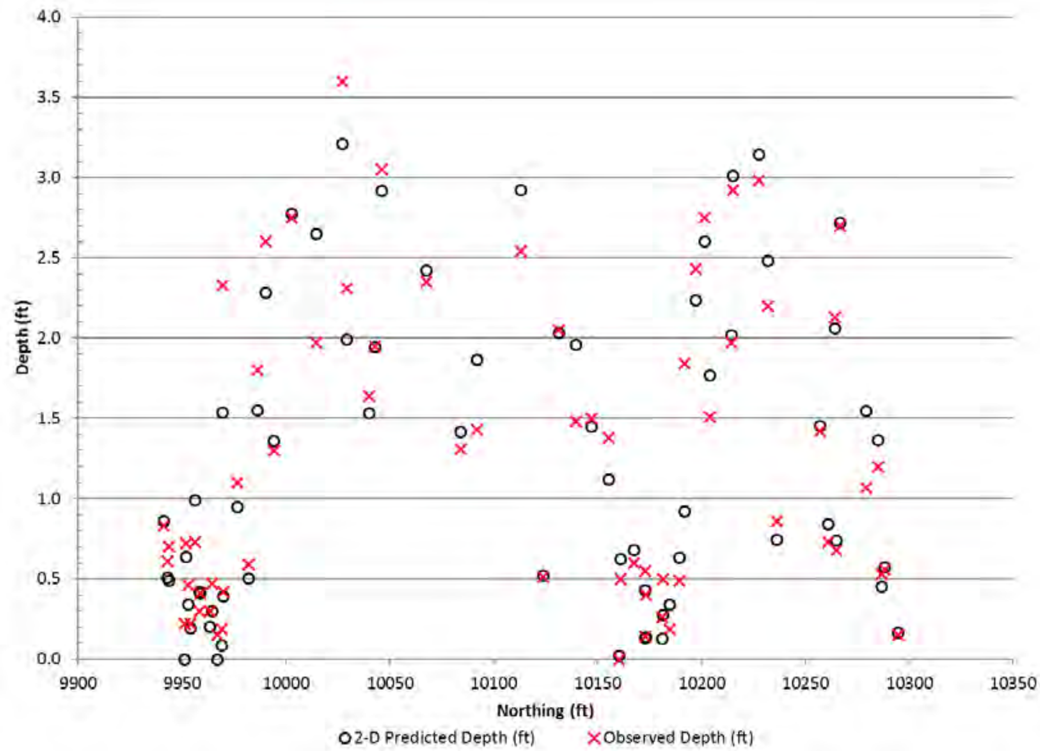

Figure F-25. Lateral distribution of points (based on northing) showing predicted and observed depths for a streamflow of 3.9 cfs.

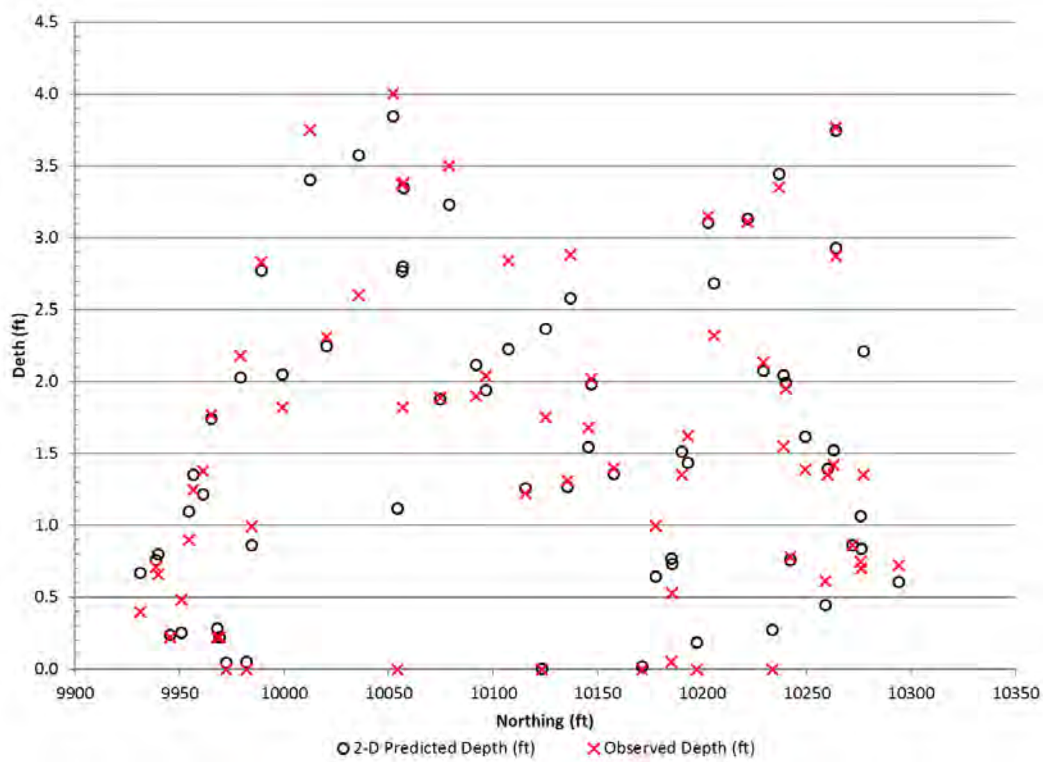

Figure F-26. Lateral distribution of points (based on northing) showing predicted and observed depths for a streamflow of 21.1 cfs.

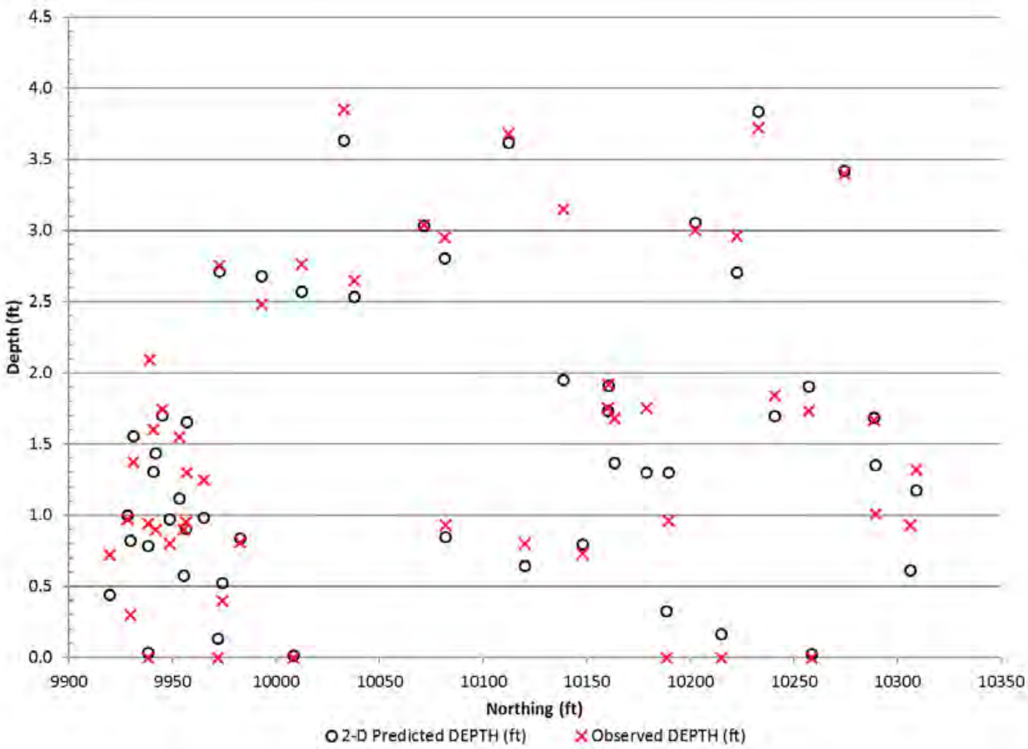

Figure F-27.Lateral distribution of points (based on northing) showing predicted and observed depths for a streamflow of 90.0 cfs.

5.7 Summary

The 2-D hydraulic model SToRM was successfully set up, run, calibrated, and validated for three streamflows. Model input parameters, such as stage, streamflow, downstream WSE boundary, upstream streamflow boundary, and Manning's *n* roughness were modified based on calibration streamflows (see roughness rating curve Figure F-13), while calculation mesh and run-time established for calibration streamflows were used to run the model for 15 additional flows. For example, the model input parameters established for the calibration flow of 21.1 cfs were modified, and mesh size and run-time were used to model streamflows of 12.0 cfs, 16.0 cfs, 30.0 cfs, 40.0 cfs, and 50.0 cfs. A total of 18 streamflows were run and 2-D hydraulic model results for each calculation node output to Microsoft Excel. Hydraulic output, including northing, easting, bed elevation, and water depth and velocity (Figure F-28 through Figure F-30) were used, along with field mapped substrate and cover (Figure F-3) and established habitat suitability criteria, to calculate weighted usable area for various targeted species and life stages (Section 6).

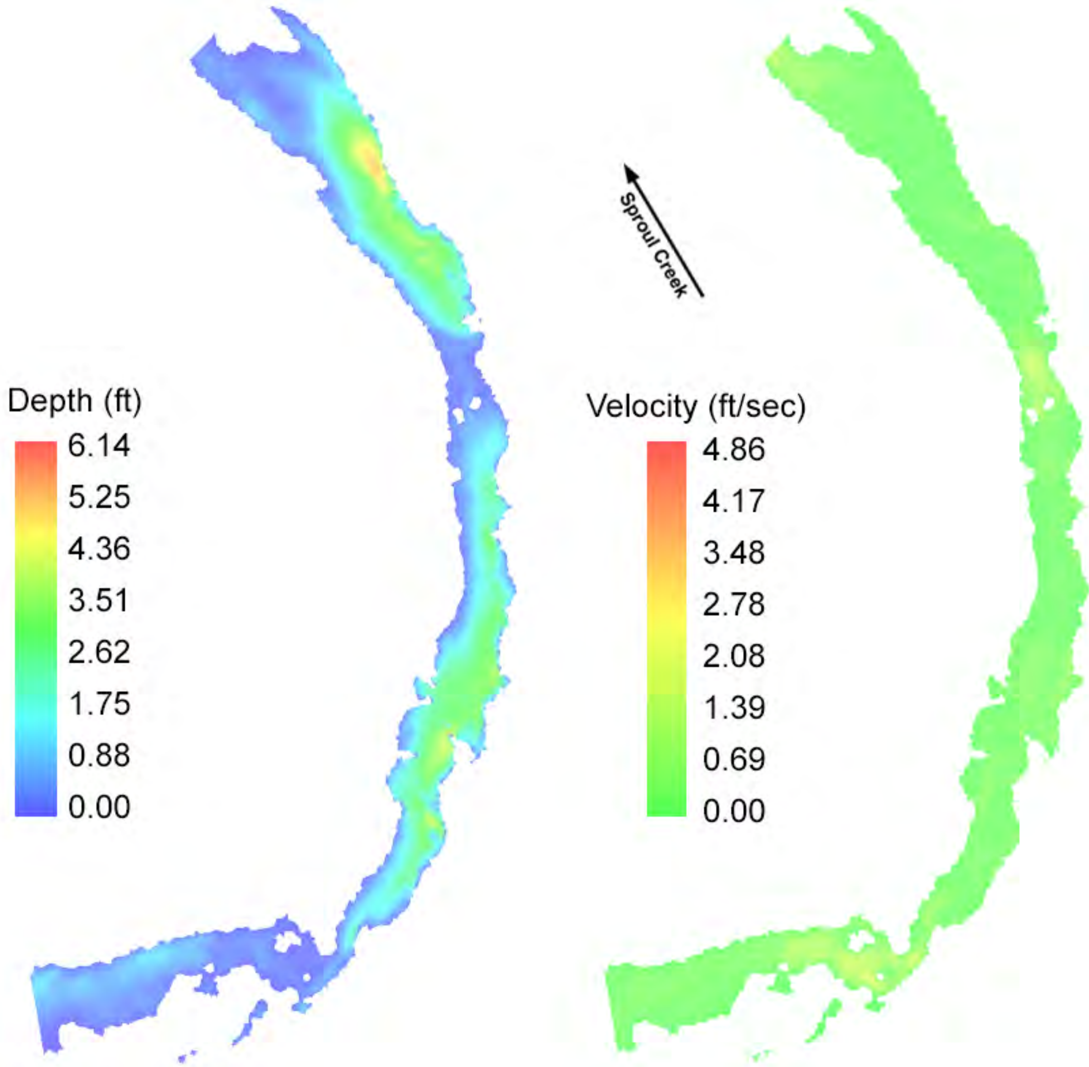

Figure F-28. Modeling result showing water depth and velocity for a streamflow of 3.9 cfs.

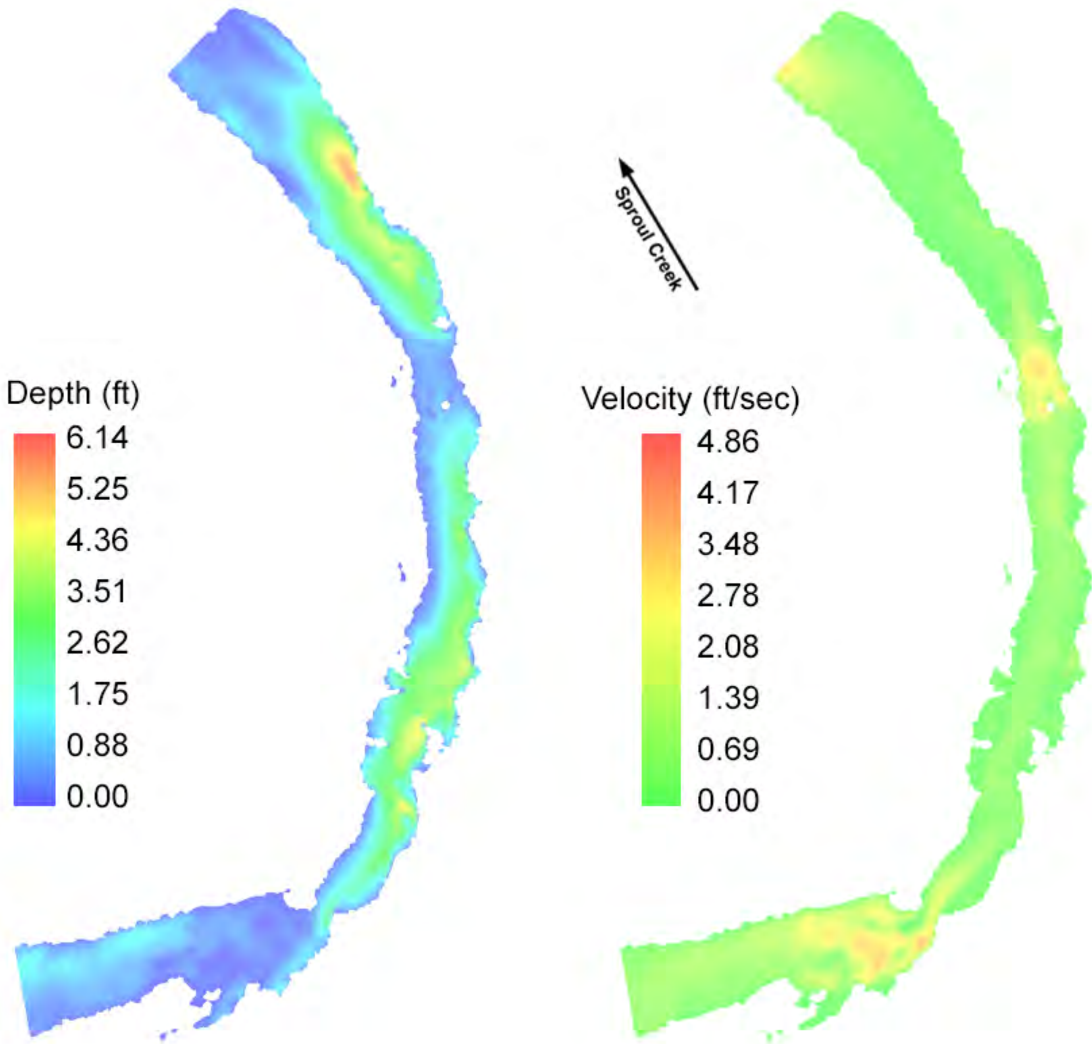

Figure F-29. Modeling result showing water depth and velocity for a streamflow of 21.1 cfs.

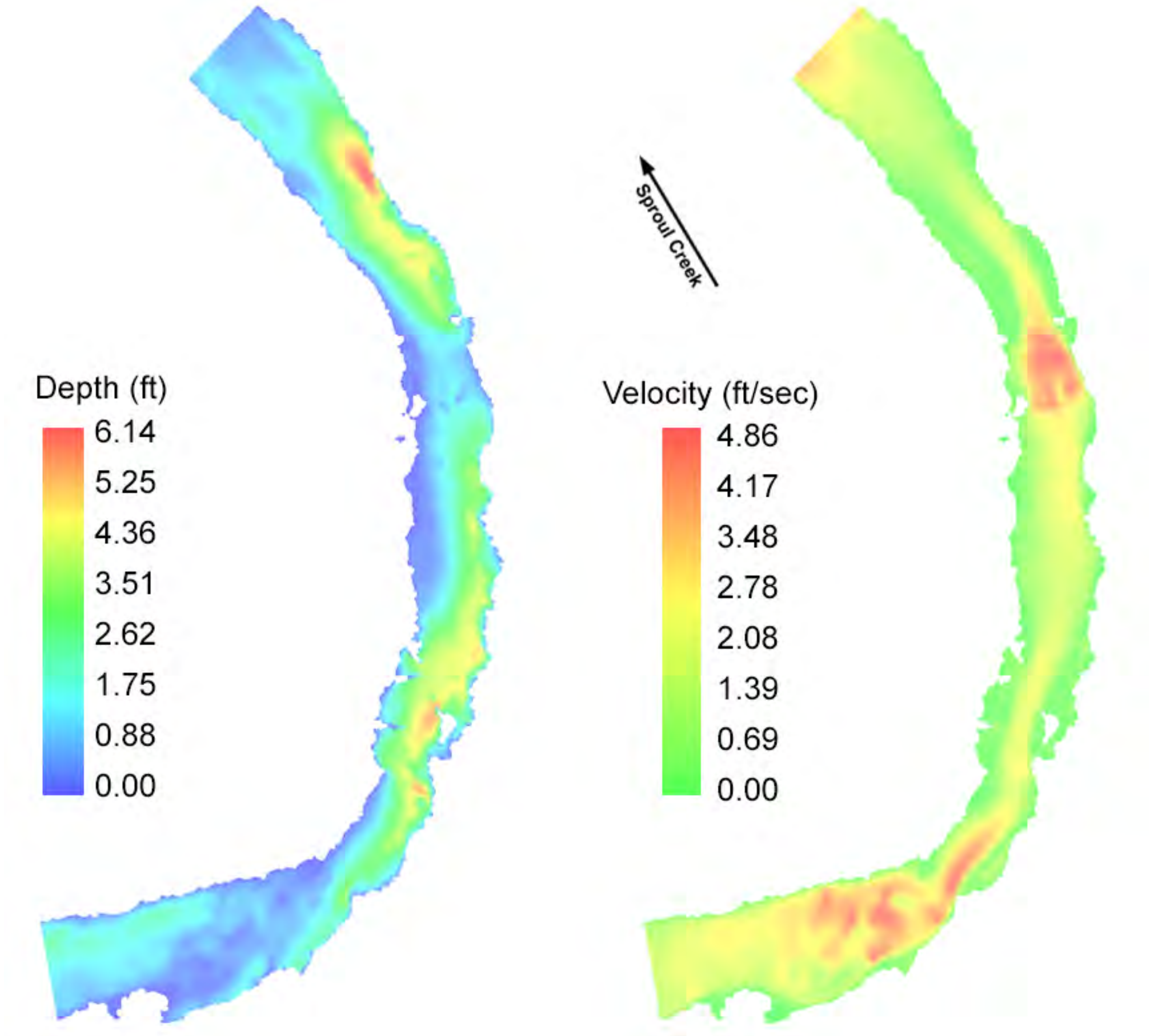

Figure F-30. Modeling result showing water depth and velocity for a streamflow of 90.0 cfs.

6 PREPARATION OF WEIGHTED USABLE AREA RATING CURVES

Weighted usable area (WUA) curves depict the quantity and quality of available habitat for targeted species and life stages in a section of a river at different flows. WUA curves are developed from selected habitat suitability indices (HSI) for targeted species and life stages, depth and velocity output from a 2-D hydraulic model run over a range of streamflows, and cover and substrate mapped in the field at the 2-D modeling site (Figure F-3). For the purpose of the Sproul Creek study, WUA curves were used in concert with empirical instream flow methods to identify flow thresholds for the four primary life history needs of Coho Salmon (*Oncorhynchus kisutch)* and steelhead (*O. mykiss;* Figure F-31).

6.1 Targeted Species and Life Stages

Coho Salmon, Chinook Salmon, and steelhead were selected as target species because they utilize the South Fork Sproul Creek at all freshwater life stages throughout the year (Figure F-31). While juvenile Chinook Salmon may occasionally over-summer, most migrate to the Pacific Ocean by mid to late spring, thus only spawning habitat was modeled for adult Chinook Salmon. The freshwater life stages of Chinook Salmond, Coho Salmon and steelhead are intimately linked to the hydraulic characteristics and morphology of small gravel and cobble bed streams – particularly the hydraulics of the riffle–pool sequence that provides spawning habitat for adult salmonids, as well as food production and rearing habitat for juveniles. Water diversions can affect each stage of freshwater life history for Chinook Salmond, Coho Salmon, and steelhead.

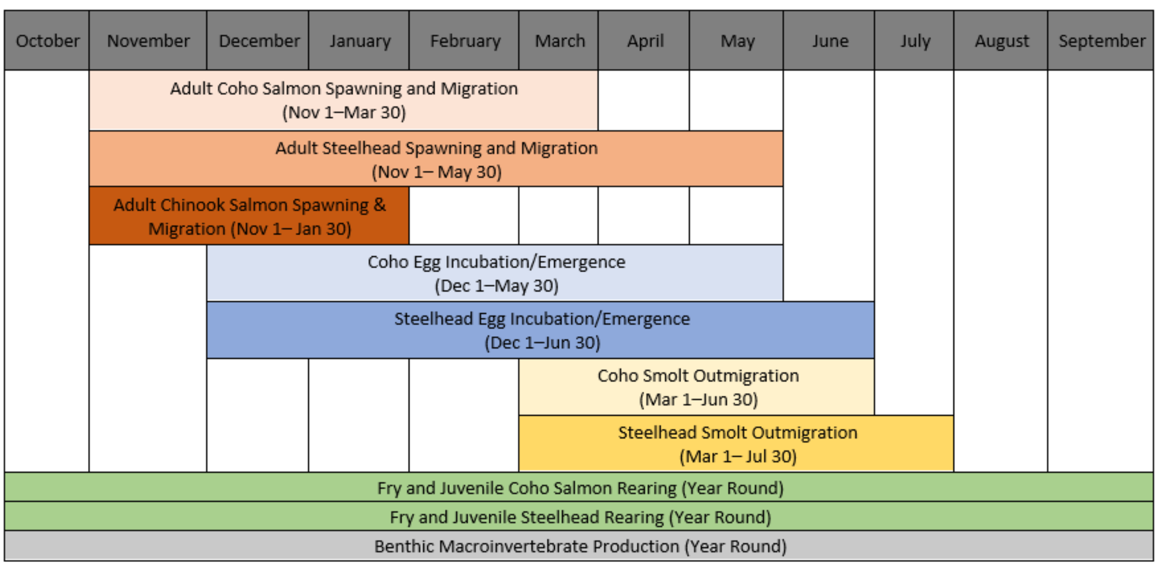

Figure F-31. Timing and duration of target species and life stages in the South Fork Eel River watershed.

For the purpose of developing WUA curves, target species and life stages most affected by freshwater habitat availability (vs. connectivity for passage) and their associated habitat needs were identified (Table F-14). The species-specific life stages were later used to determine the HSI used to calculate the WUA curves (Section 6.2). A more complete discussion of the periodicity of Coho Salmon, Chinook Salmon and steelhead in the South Fork Eel River is provided in the main report.

Table F-14. Targeted species and life stages in the South Fork Eel River watershed and their associated habitat needs.

Target Species and Life Stages	Habitat Needs
Adult Coho Salmon spawning	Depth, velocity, substrate availability
Young of the year (YOY) Coho Salmon rearing	Depth, velocity, cover availability
Juvenile Coho Salmon rearing	Depth, velocity, cover availability
Adult Chinook Salmon spawning	Depth, velocity, substrate availability
Adult steelhead spawning	Depth, velocity, substrate availability
YOY steelhead rearing	Depth, velocity, cover availability
Juvenile steelhead rearing (small (1+) and large (2+))	Depth, velocity, cover availability
Benthic macroinvertebrate (BMI) production	Depth, velocity, substrate availability

6.2 Habitat Suitability Indices

Habitat suitability indices are used to describe the relative appropriateness of habitat attributes for focal species and life stages (Bovee 1986, Normandeau Associates 2014). They are used in calculating WUA curves by weighting the suitability of modeled depth and velocity results, and observed cover and substrate values, in the 2-D model site at a specific flow. HSI were determined for each targeted species and life stage based on a review of relevant literature, including several Technical Review Teams for North Coast instream flow studies, recommendations from California Department of Fish and Wildlife (CDFW), and our professional experience (Table F-15). HSI depth, velocity, substrate, and cover curves for the target species and life stages were taken from Holmes et al. (2014), Hampton et al. (1997), Gore et al. (2001) and Dettman and Kelley (1986; Figure F-32 through Figure F-52).

Table F-15. Source of depth, velocity, substrate, and cover HSI curves used for calculating Coho Salmon and steelhead spawning, YOY and juvenile rearing habitat, and productive BMI riffle WUA curves from 2-D model outputs.

Species	Life Stage	Hydraulic (Depth and Velocity)	Cover	Substrate
Coho Salmon	Spawning	Hampton et al. (1997) Figure F-32 & Figure F-33	N/A	Dettman and Kelley (1986) Figure F-51
	YOY Rearing	Hampton et al. (1997) Figure F-34 & Figure F-35	Holmes et al. (2014) Figure F-48	N/A
	Juvenile Rearing	Hampton et al. (1997) Figure F-36 & Figure F-37	Holmes et al. (2014) Figure F-48	N/A
Steelhead	Spawning	Hampton et al. (1997) Figure F-38 & Figure F-39	N/A	Dettman and Kelley (1986) Figure F-51
	YOY Rearing	Holmes et al. (2014) Figure F-40 & Figure F-41	Holmes et al. (2014) Figure F-48	N/A
	Small Juvenile (1+) Rearing	Holmes et al. (2014) Figure F-42 & Figure F-43	Holmes et al. (2014) Figure F-48	N/A
	Large Juvenile (2+) Rearing	Holmes et al. (2014) Figure F-44 & Figure F-45	Holmes et al. (2014) Figure F-48	N/A
Chinook Salmon	Spawning	Hampton et al. (1997) Figure F-49 and Figure F-50	N/A	Dettman and Kelley (1986) Figure F-51
BMI	Ephemeroptera	Gore et al. (2001) Figure F-46 and Figure F-47	N/A	Gore et al. (2001) Figure F-52

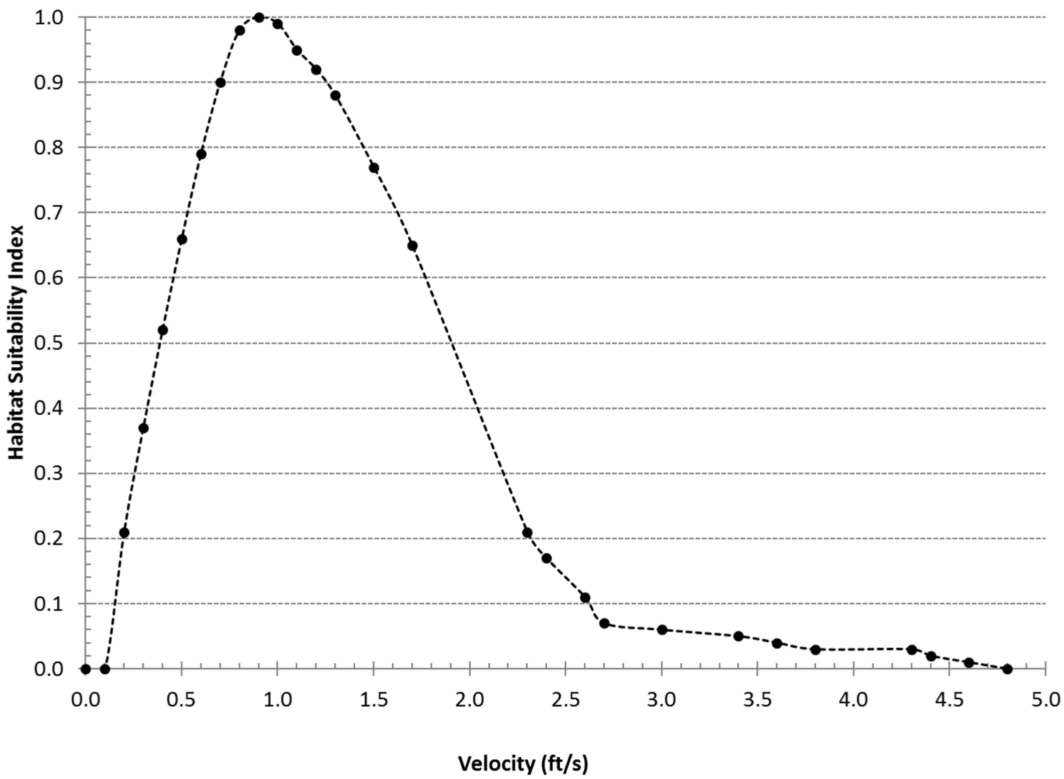

Figure F-32. Velocity HSI for Coho Salmon spawning habitat. Adapted from Hampton et al. (1997).

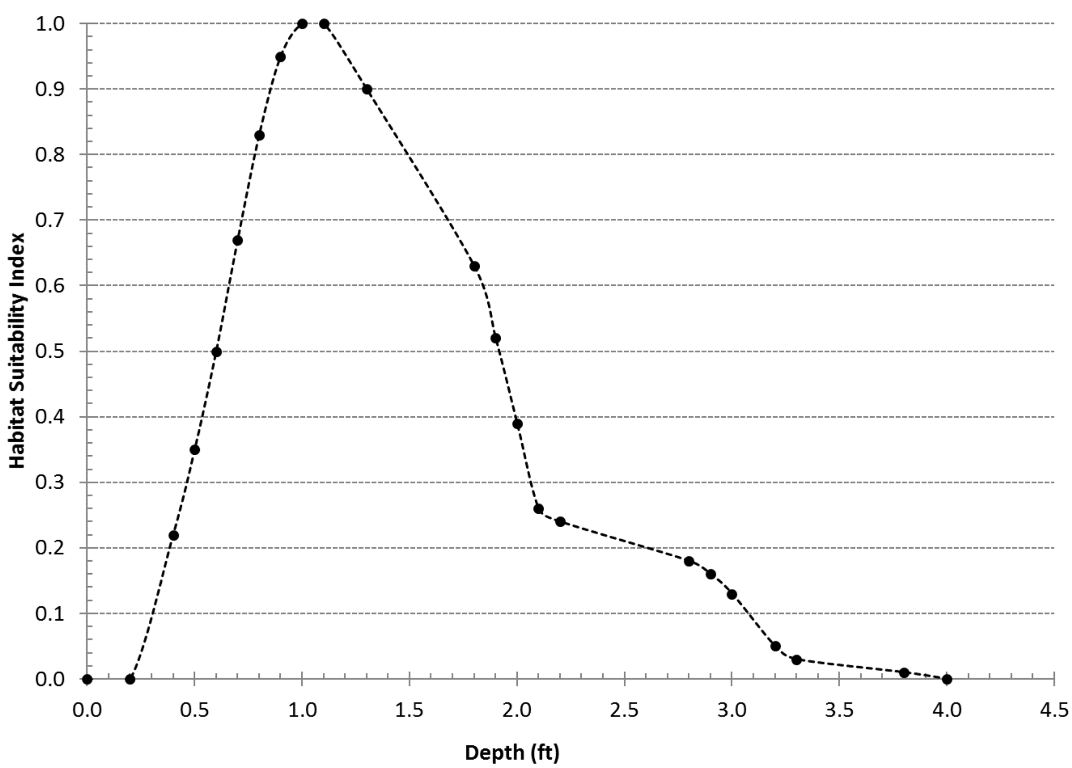

Figure F-33. Depth HSI for Coho Salmon spawning habitat. Adapted from Hampton et al. (1997).

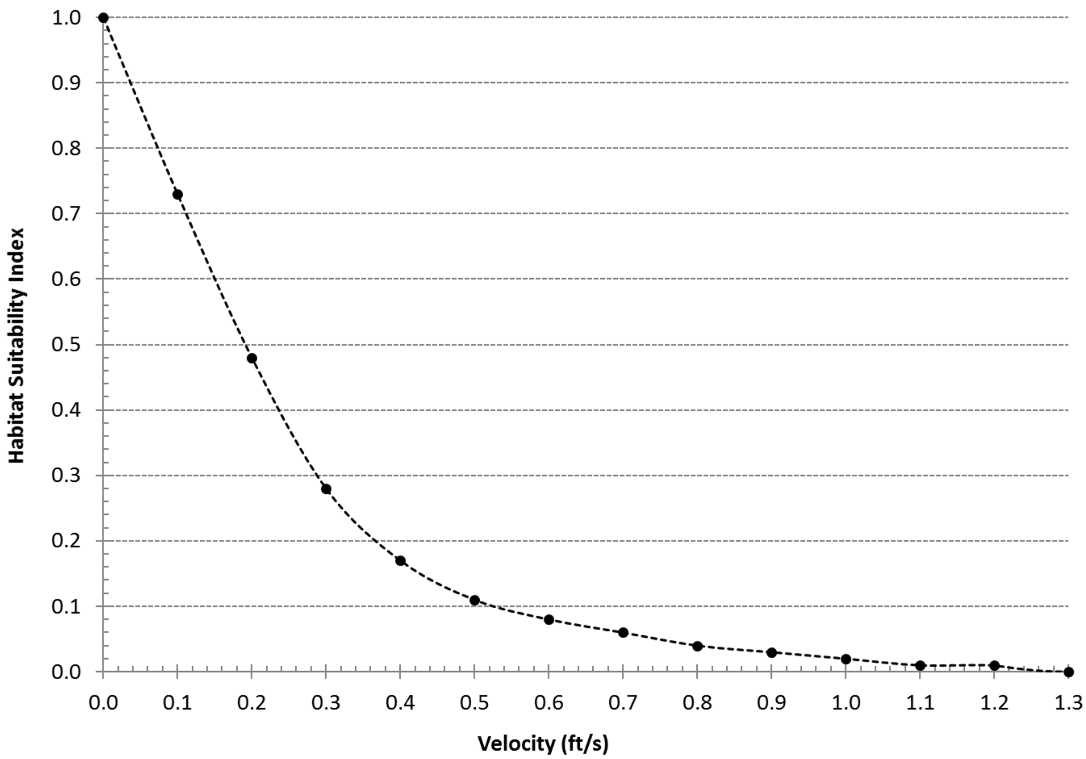

Figure F-34. Velocity HSI for Coho Salmon YOY rearing habitat. Adapted from Hampton et al. (1997).

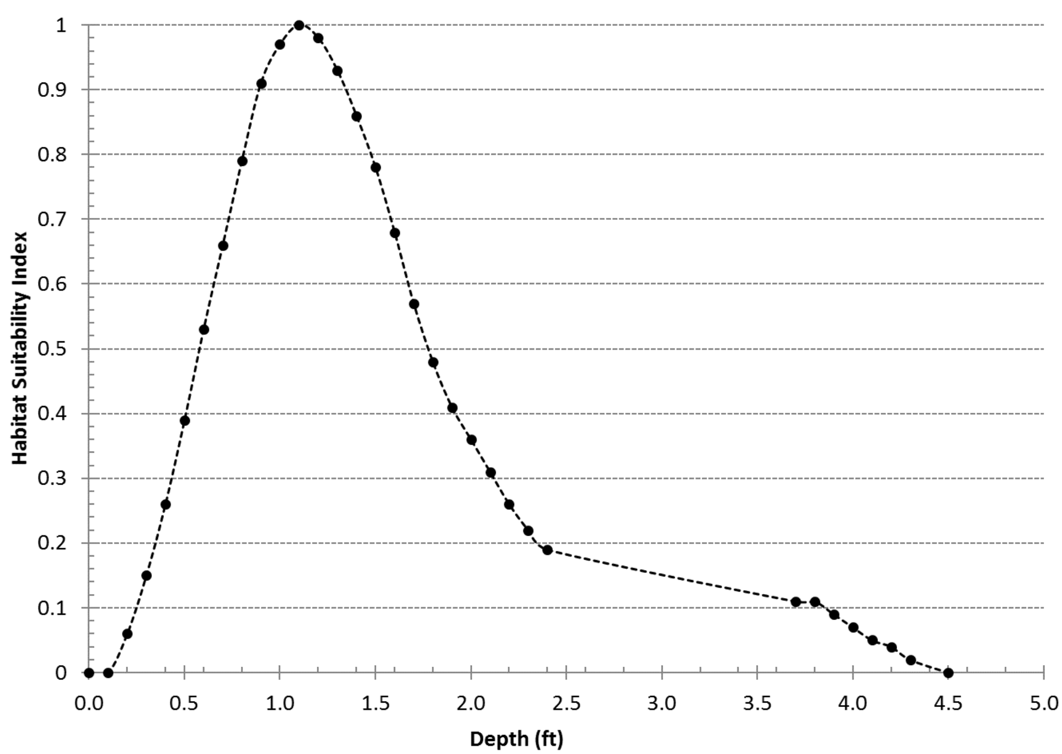

Figure F-35. Depth HSI for Coho Salmon YOY rearing habitat. Adapted from Hampton et al. (1997).

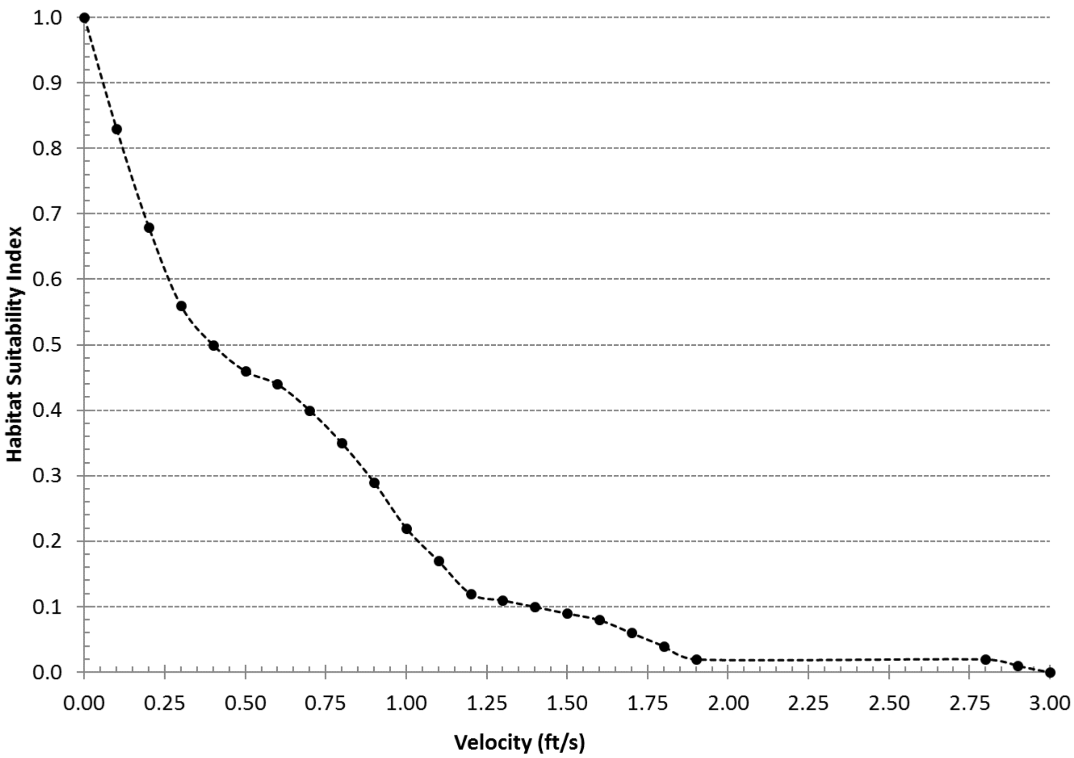

Figure F-36. Velocity HSI for Coho Salmon juvenile rearing habitat. Adapted from Hampton et al. (1997).

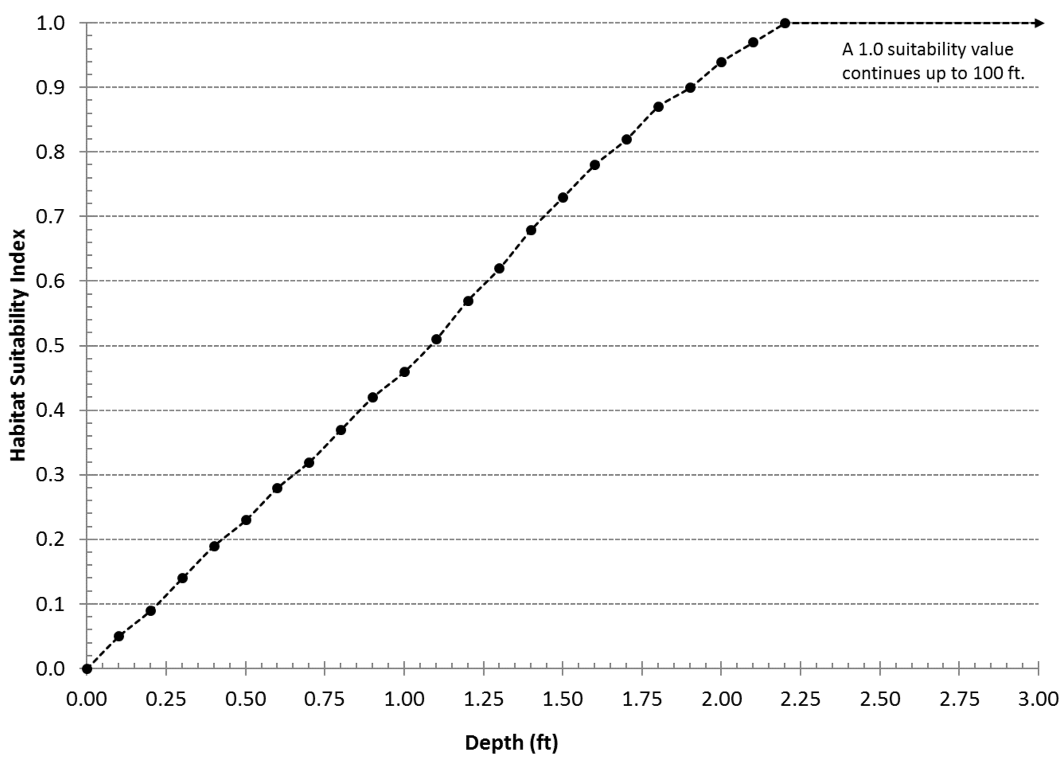

Figure F-37. Depth HSI for Coho Salmon juvenile rearing habitat. Adapted from Hampton et al. (1997).

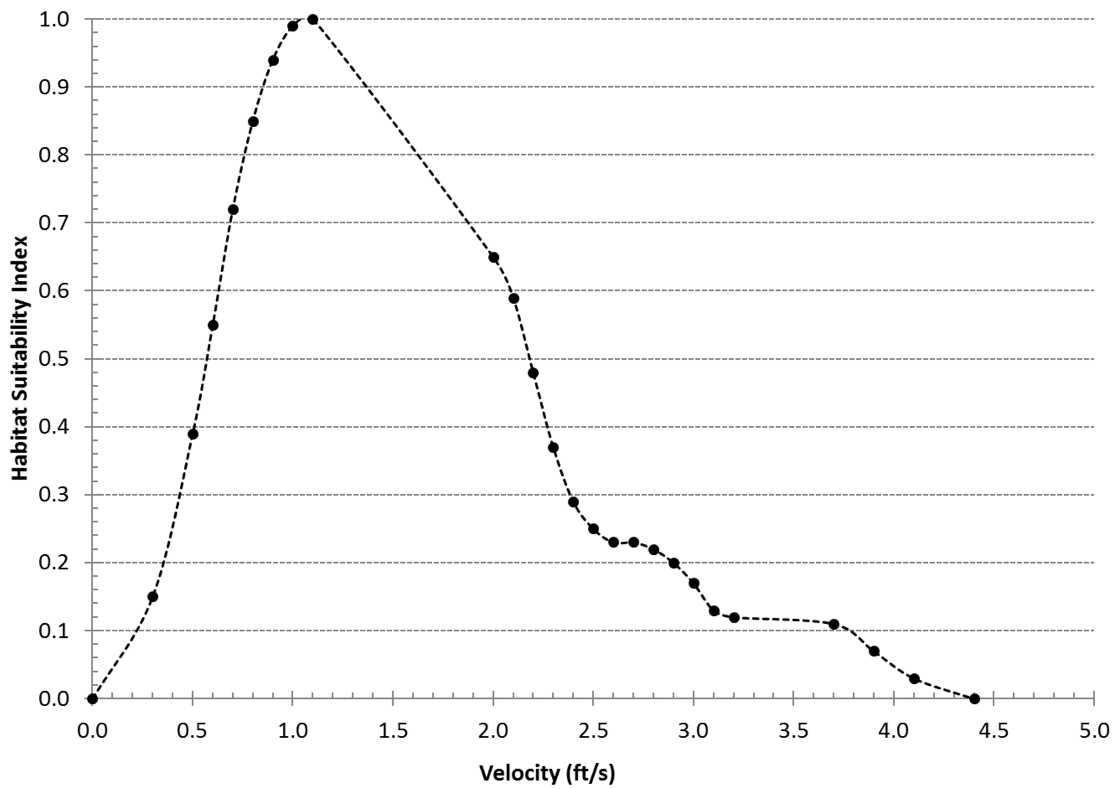

Figure F-38. Velocity HSI for steelhead spawning habitat. Adapted from Hampton et al. (1997).

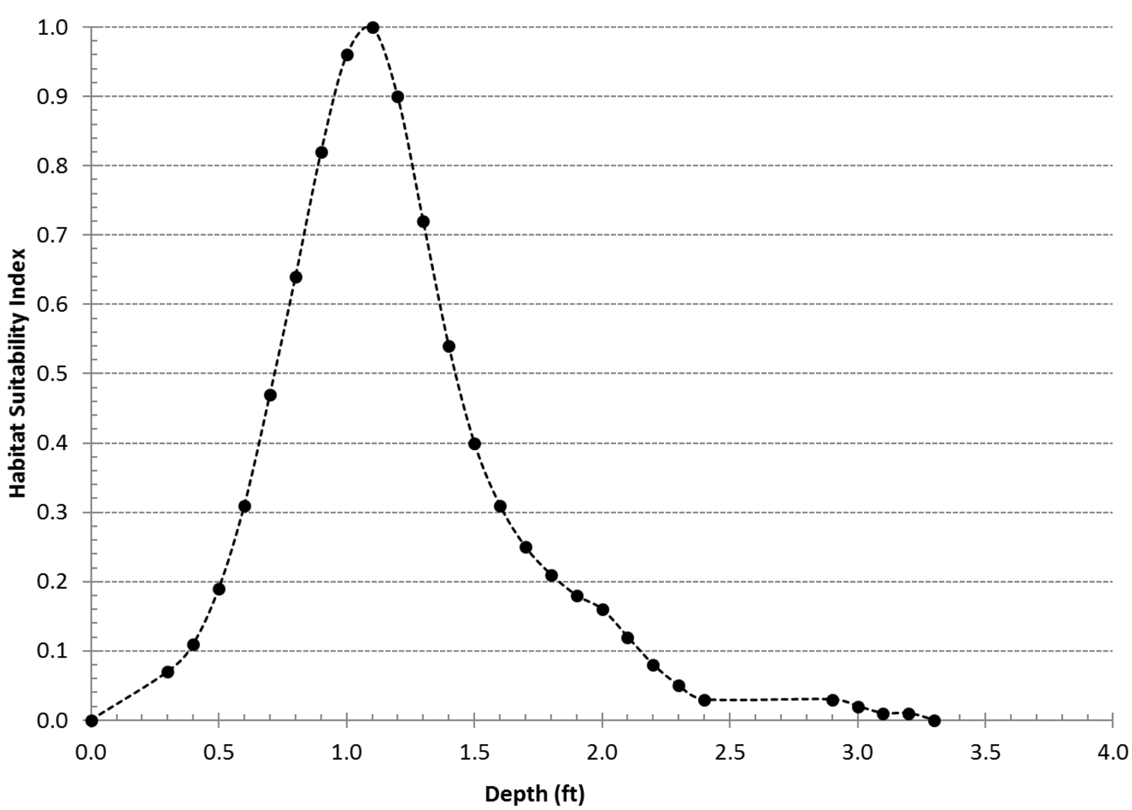

Figure F-39. Depth HSI for steelhead spawning habitat. Adapted from Hampton et al. (1997).

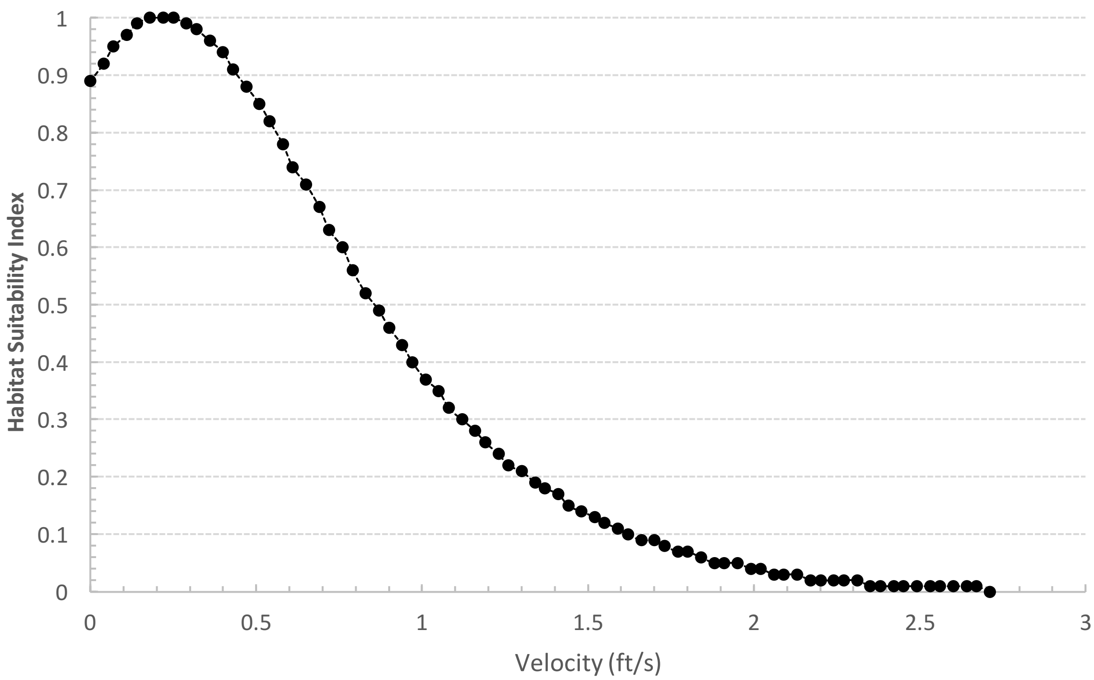

Figure F-40. Velocity HSI for steelhead YOY rearing habitat. Adapted from Holmes et al. (2014).

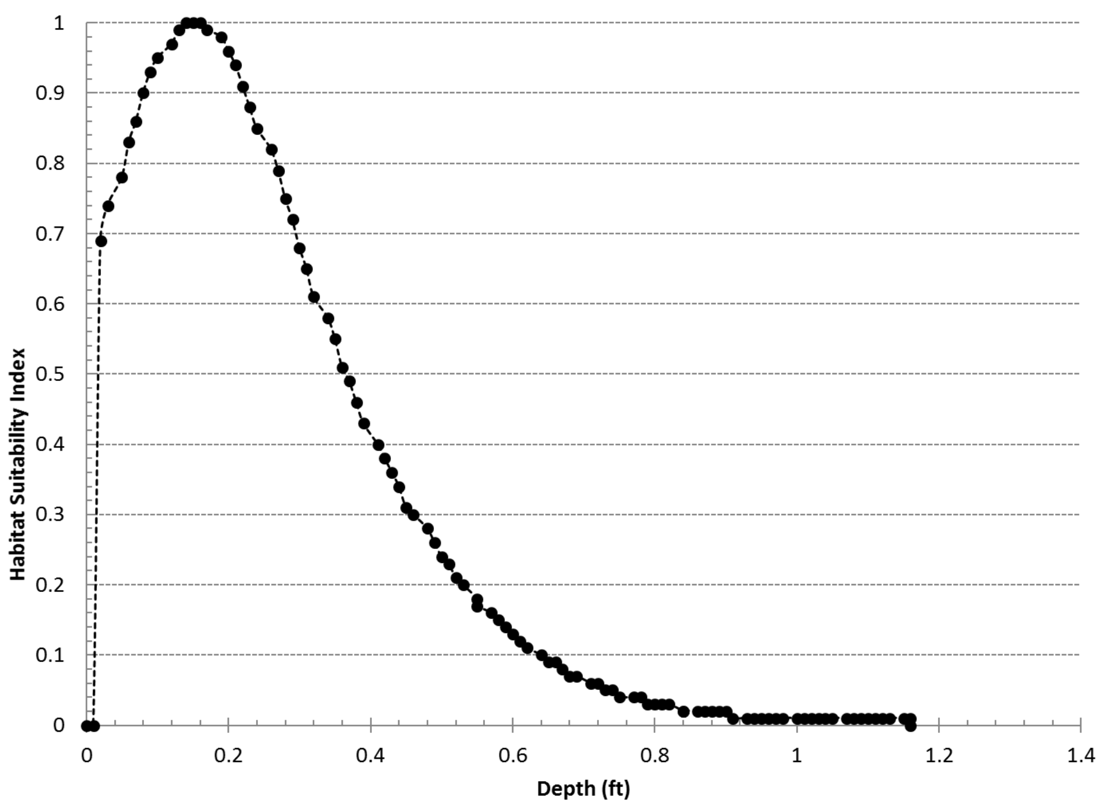

Figure F-41. Depth HSI for steelhead YOY rearing habitat. Adapted from Holmes et al. (2014).

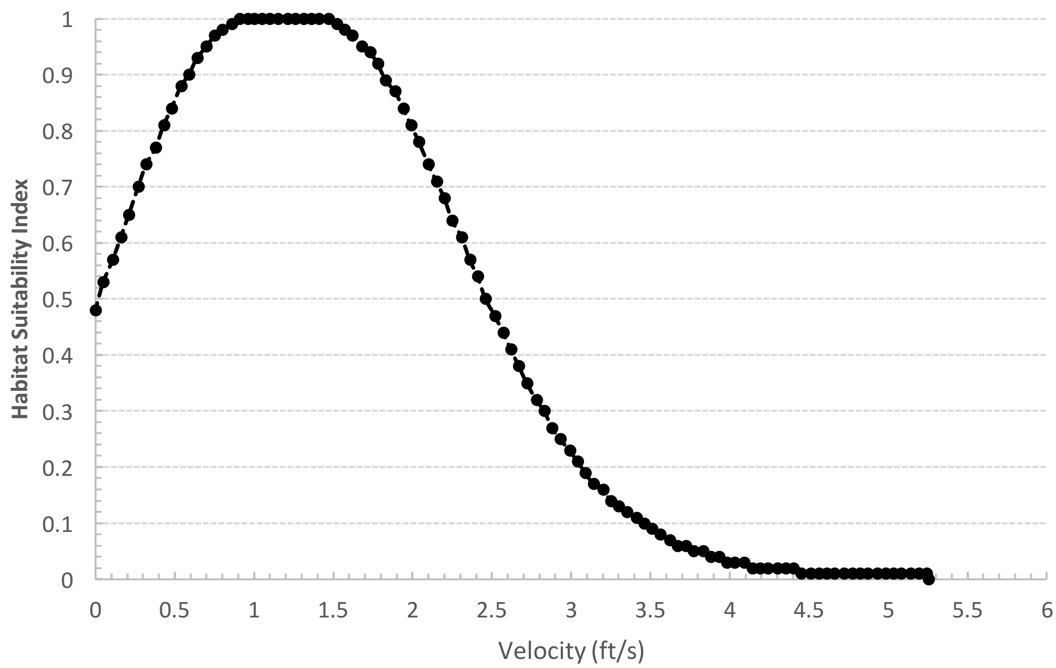

Figure F-42. Velocity HSI for small (1+) juvenile steelhead rearing habitat. Adapted from Holmes et al. (2014).

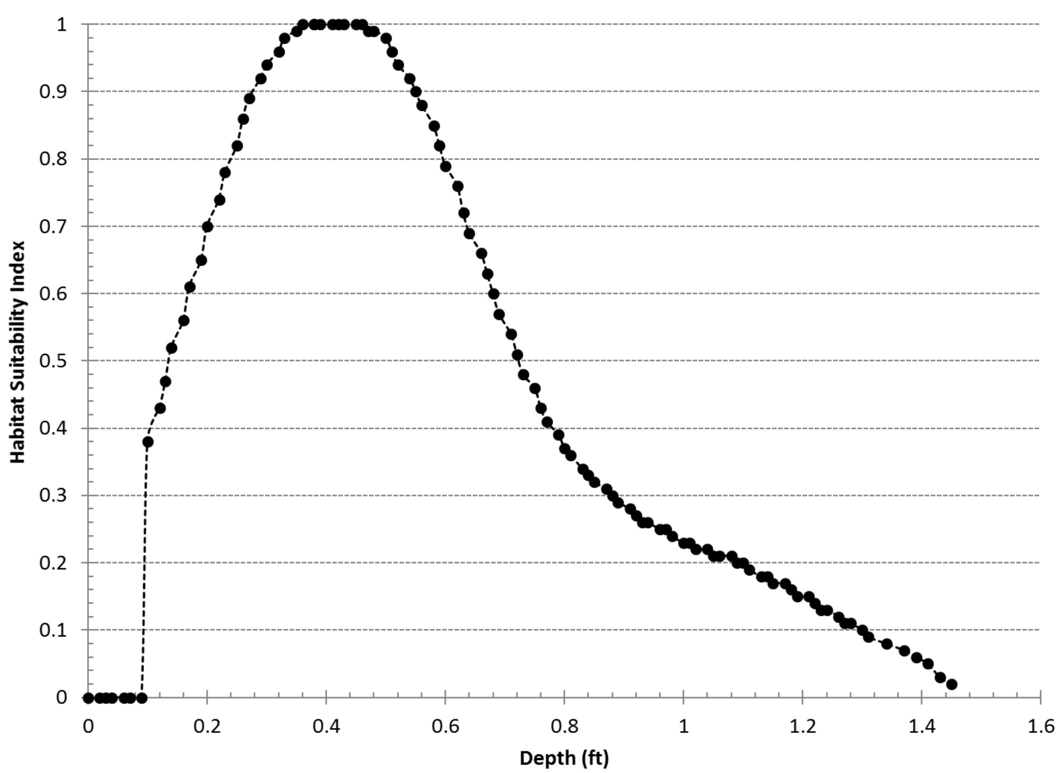

Figure F-43. Depth HSI for small (1+) juvenile steelhead rearing habitat. Adapted from Holmes et al. (2014).

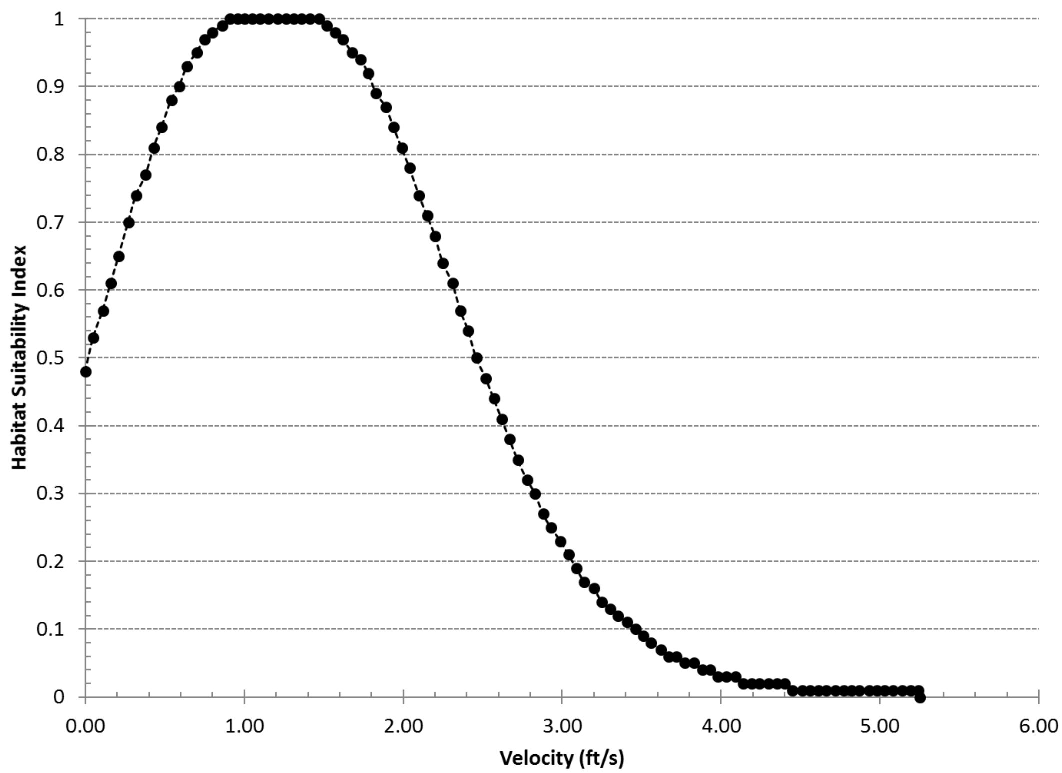

Figure F-44. Velocity HSI for large (2+) juvenile steelhead rearing habitat. Adapted from Holmes et al. (2014).

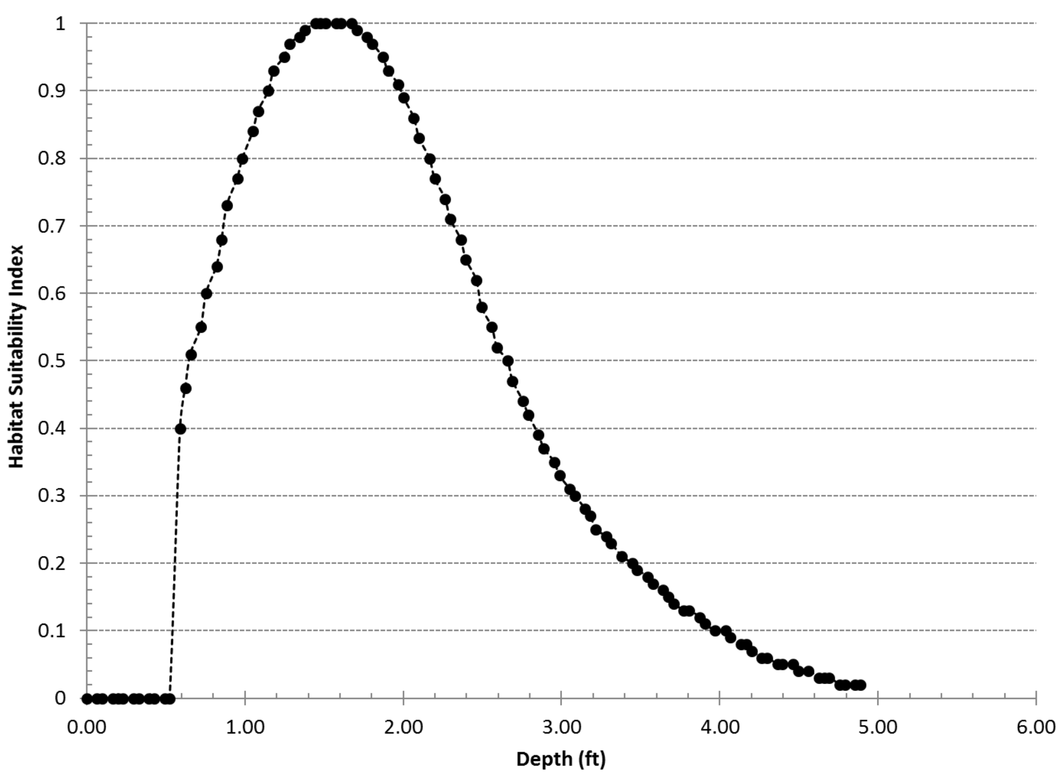

Figure F-45. Depth suitability for large (2+) juvenile steelhead rearing habitat. Adapted from Holmes et al. (2014).

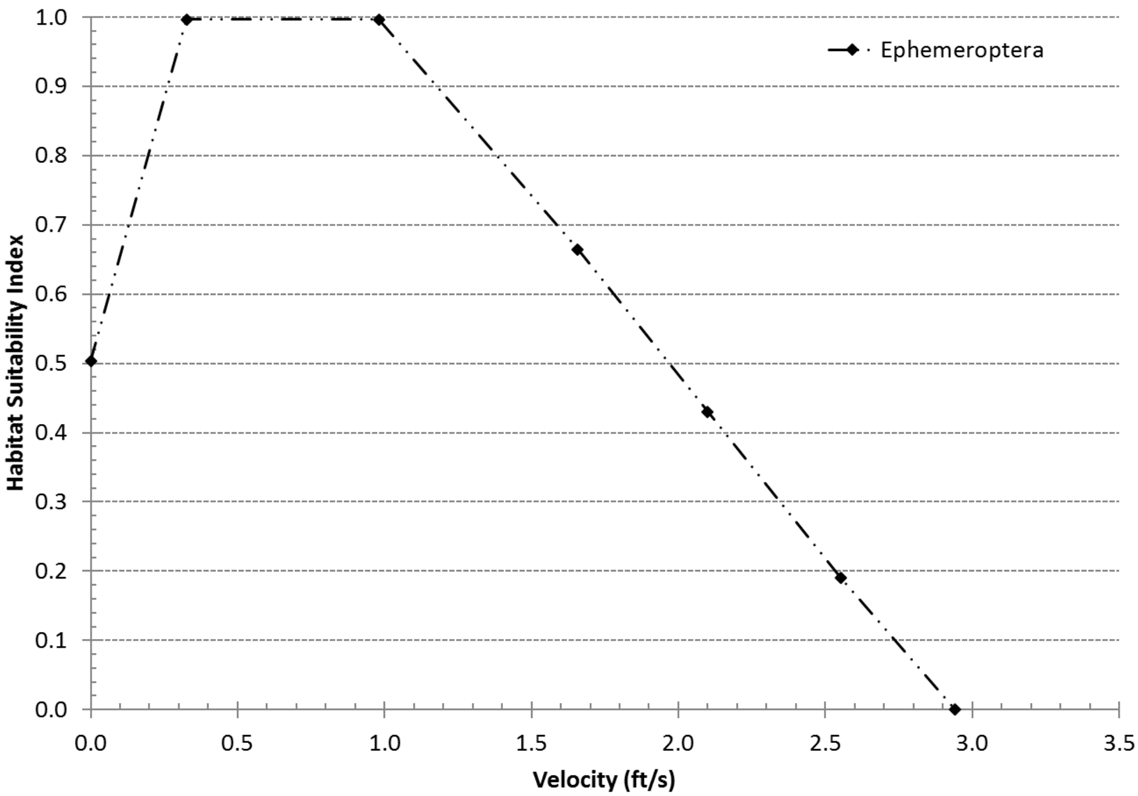

Figure F-46. Velocity HSI for productive Ephemeroptera (BMI) habitat based on 1,200 samples. Adapted from Gore et al. (2001).

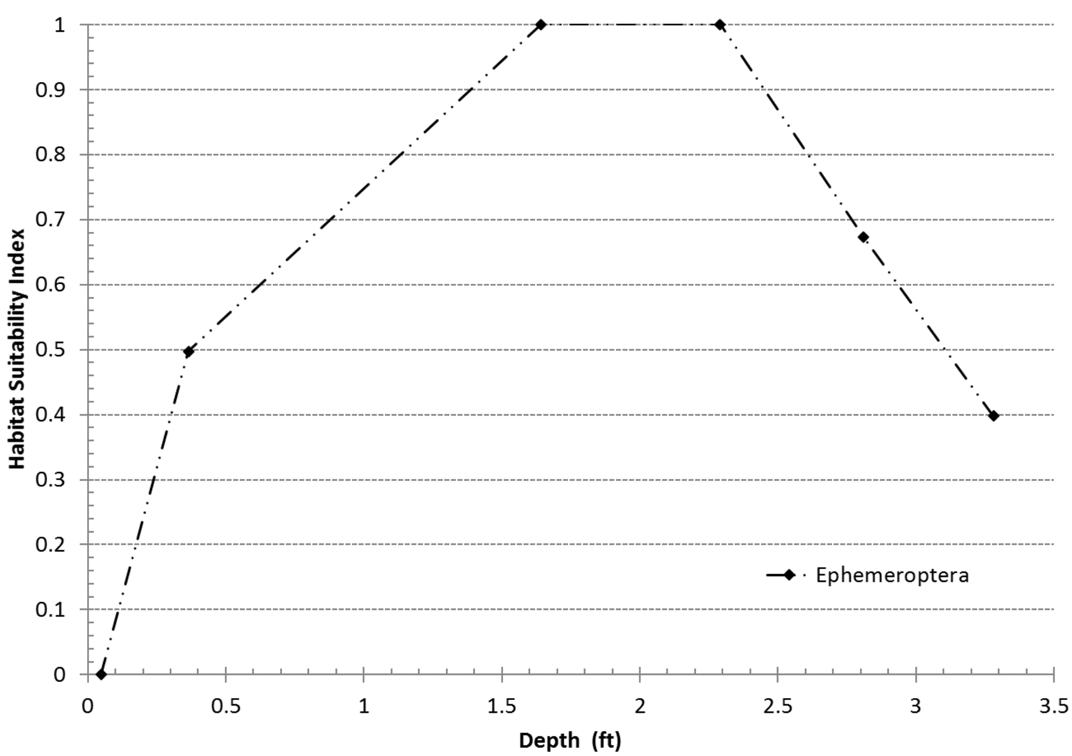

Figure F-47. Depth HSI for productive Ephemeroptera (BMI) habitat based on 1,200 samples. Adapted from Gore et al. (2001).

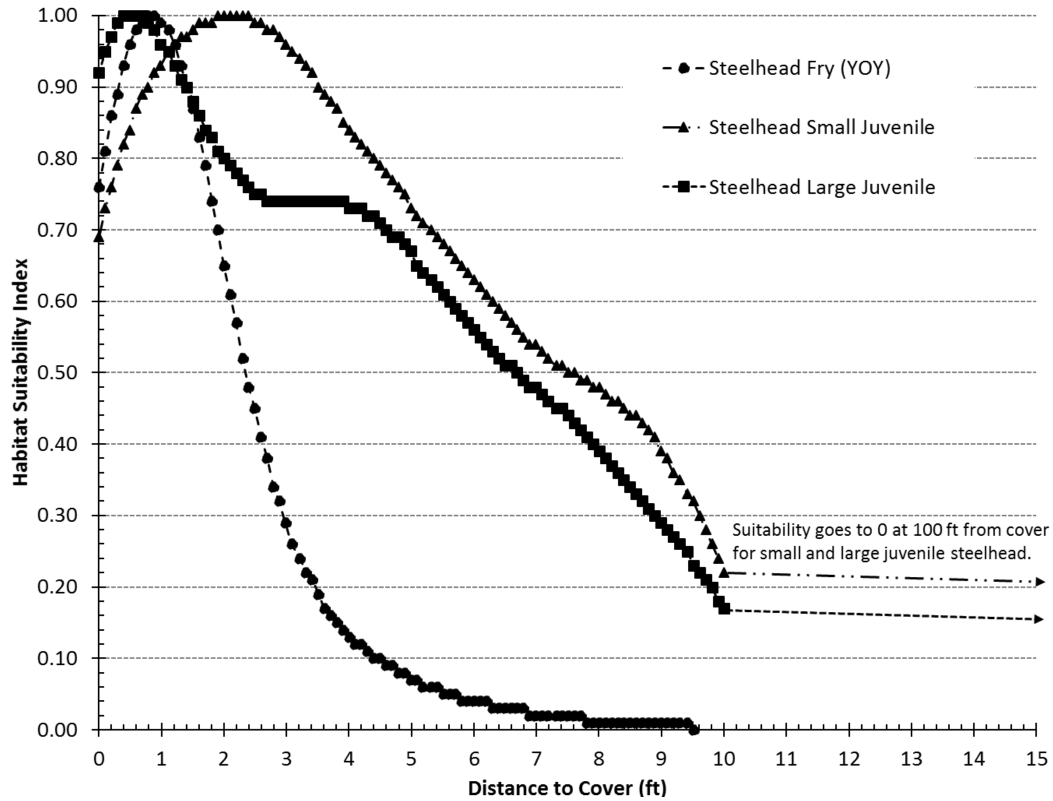

Figure F-48. Distance to cover HSI for steelhead YOY and small (1+) and large (2+) juvenile steelhead. Adapted from Holmes et al. (2014). Distance to cover HSI for steelhead was also used for YOY and juvenile Coho Salmon.

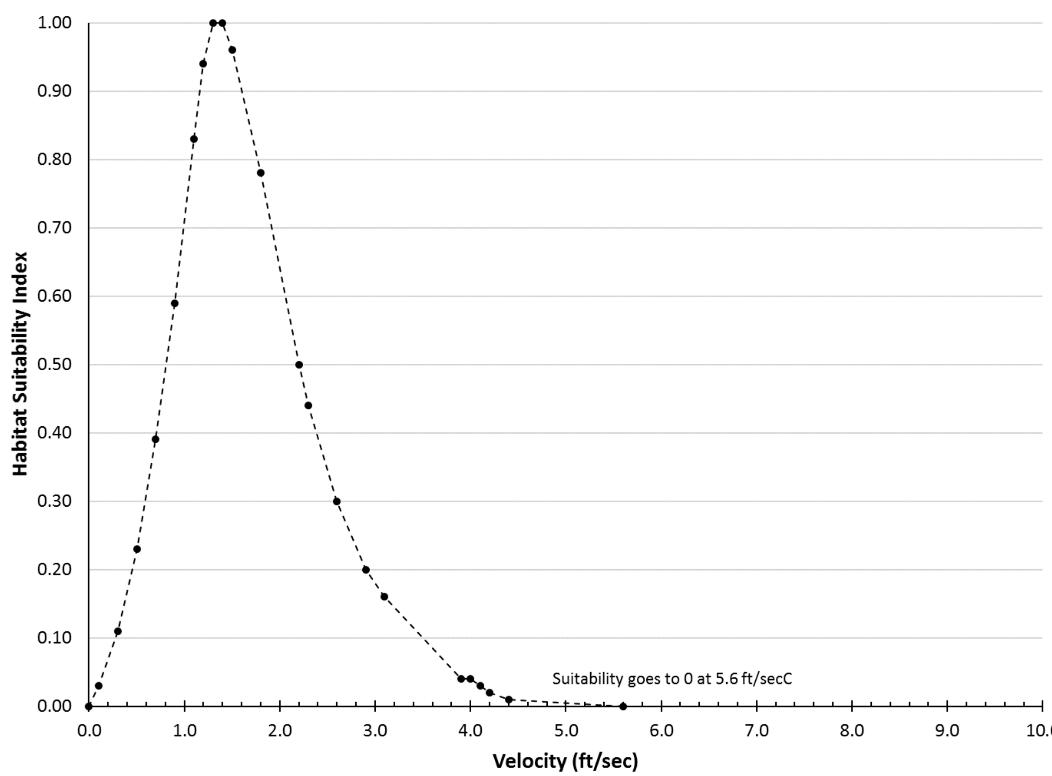

Figure F-49.Velocity HSI for Chinook Salmon spawning. Adapted from Hampton et al. (1997).

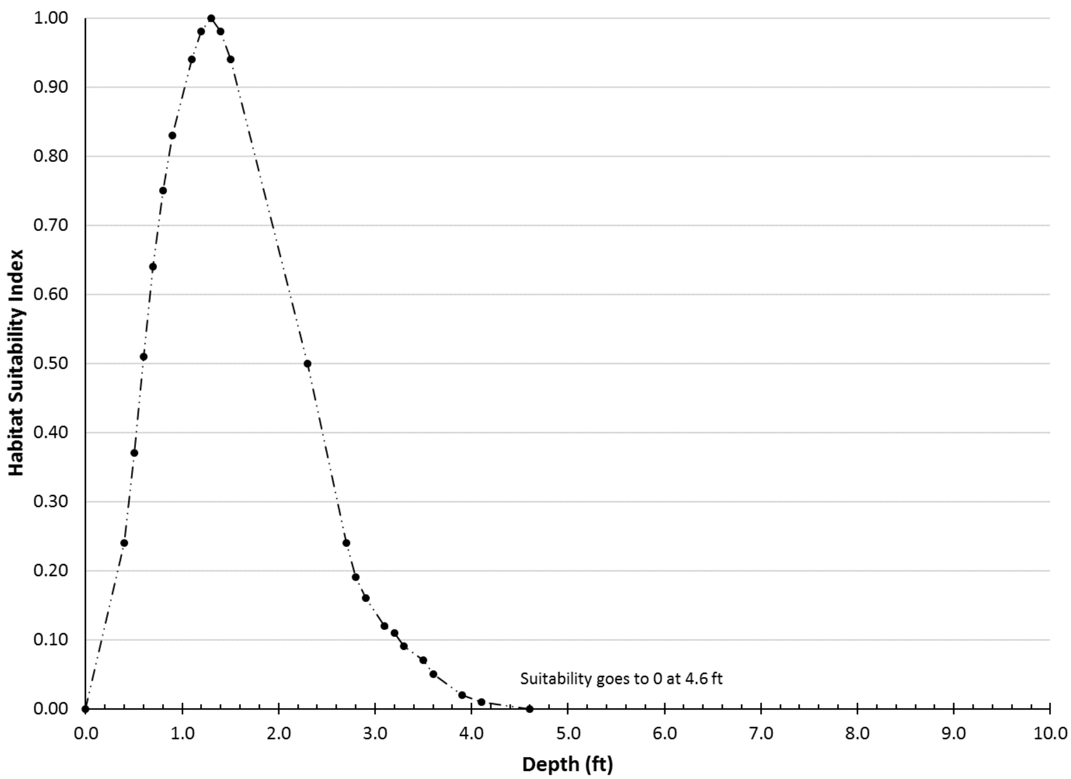

Figure F-50.Depth HSI for Chinook Salmon spawning. Adapted from Hampton et al. (1997).

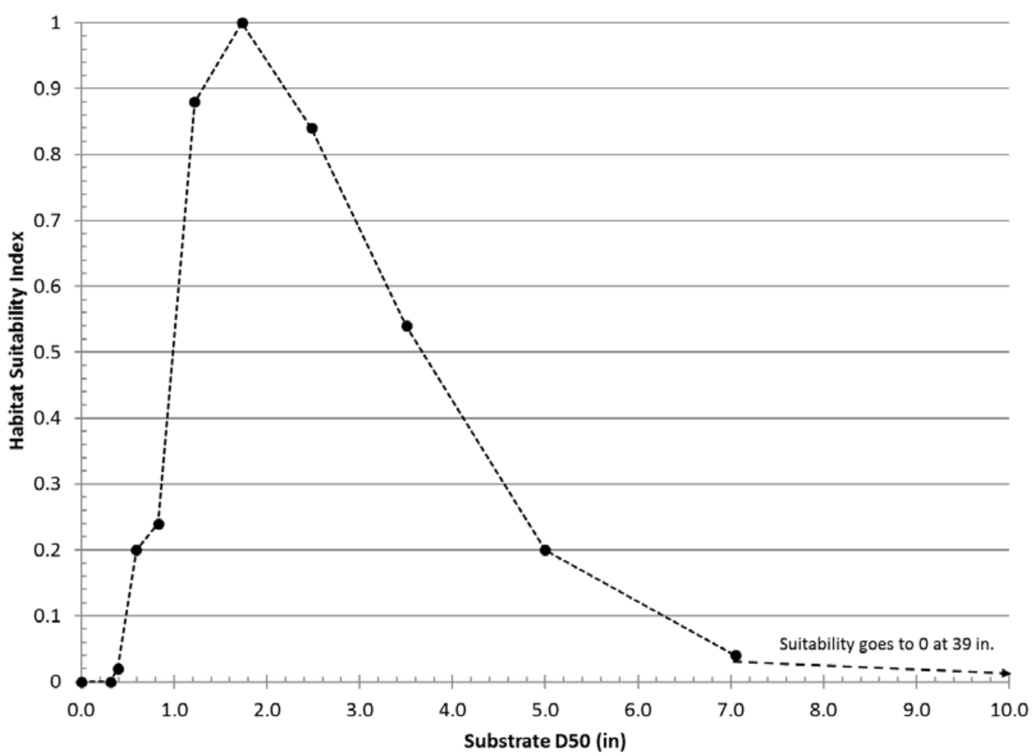

Figure F-51. Substrate HSI for Coho and Chinook Salmon and steelhead spawning. Adapted from Dettman and Kelley (1986).

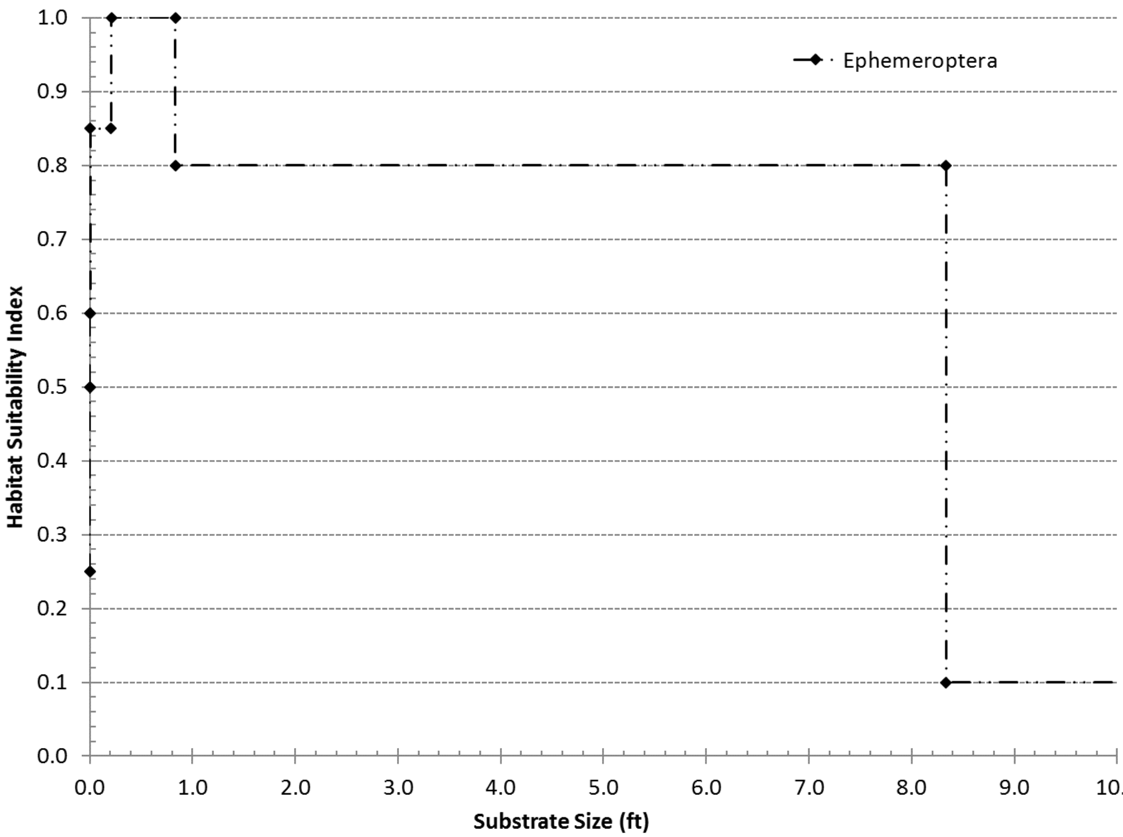

Figure F-52. Substrate HSI for Ephemeroptera (BMI) production. Adapted from Gore et al. (2001).

6.3 Calculating WUA

Data collected for 2-D model setup and calibration were also used for WUA calculations. The cover and substrate polygons mapped during topographic surveys (Figure F-3) were digitized in GIS, providing distance to cover and particle size (D_{50}) values for each mesh node (point). Since a mesh grid of points is typically irregular in spatial distribution, Thiessen polygons are developed around each mesh point and an area (ft^2) is calculated and assigned to each point (Figure F-53). Values assigned to each point for distance to cover, D_{50}, and area were exported to Excel from GIS and combined with a modeled flow's depth and velocity data to calculate WUA habitat curves (Table F-16).

Depth, velocity, distance to cover, and substrate values for each mesh point were converted to HSI values from the HSI curves for each species and life stage described in Section 6.1. Weighted HSI for each mesh point (HSI_i) were calculated using the product method (Equation 6), in which all HSI values for each mesh point are multiplied together (Figure F-54):

$$HSI_i = HSI_1 \times HSI_2 \ldots \times HSI_n \qquad (6)$$

HSI_i values were then multiplied by the corresponding mesh point area (ft^2) to calculate a WUA value (Equation 7) for each mesh point (Figure F-54, Table F-17):

$$WUA = \sum_{i=1}^{n} A_i HSI_i \qquad (7)$$

Where:

A_i is the area of the mesh point

The WUA values for each mesh point are summed to return a single WUA value for each modeled flow (Table F-18, Table F-19) and plotted as habitat rating curves (Figure F-55). In addition, planform maps of HSI at specific streamflows can show where the areas with the highest WUA occur (Figure F-57).

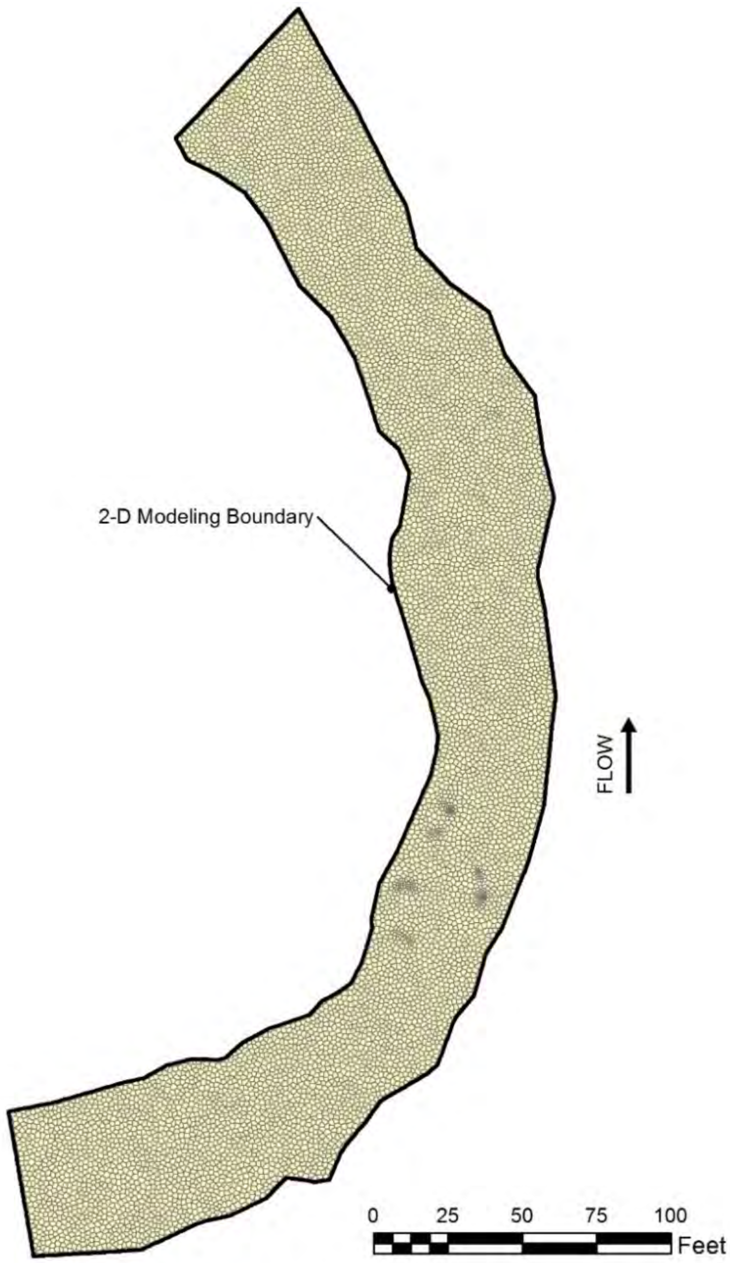

Figure F-53. Planform view of Thiessen polygons developed around each calculation mesh point.

Table F-16. Example of GIS output results for four sample mesh points after field data were digitized and applied to the mesh grid. GIS outputs were used in calculating WUA curves.

Point ID	Easting (ft)	Northing (ft)	Area (ft^2)	Depth (ft)	Velocity (ft/sec)	Distance to Cover (ft)	Particle Size (mm)
289	9880.066	9960.315	1.30	0.68	0.29	1.60	0.11
290	9888.534	9911.557	1.41	0.77	0.35	78.70	< 0.02
291	9911.666	9912.797	1.28	0.70	0.31	1.40	0.11
292	9925.09	9913.829	1.51	0.12	0.06	80.00	< 0.02

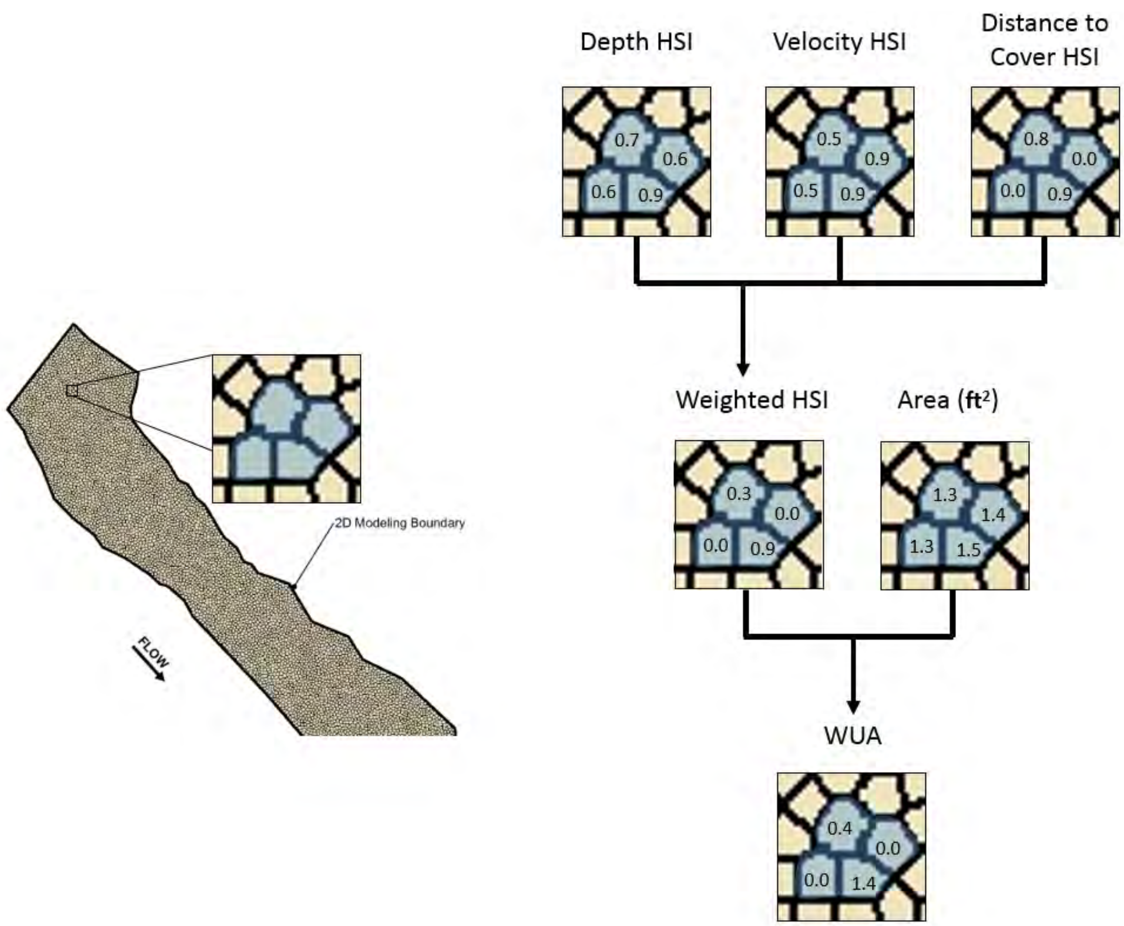

Figure F-54. Schematic showing how HSI values assigned to habitat variables associated with a mesh point are weighted using the product method and converted into WUA for each mesh point polygon.

Table F-17. Assigned HSI values for depth, velocity, distance to cover, and substrate, and total WUA values for four sample mesh points for a streamflow of 21.1 cfs

Point ID	Assigned Depth HSI	Assigned Velocity HSI	Assigned Distance to Cover HSI	Area (ft^2)	WUA Depth & Velocity No Cover	WUA Depth, Velocity, & Cover
289	0.72	0.51	0.85	1.30	0.47	0.40
290	0.60	0.95	0.00	1.41	0.81	0.00
291	0.70	0.52	0.91	1.28	0.47	0.42
292	0.97	0.99	0.00	1.51	1.46	0.00
Total WUA (for these four points)					**3.21**	**0.82**

Table F-18. WUA for the Sproul Creek 2-D model site for targeted species and juvenile life stages derived from HSI for modeled depth and velocity results, and either substrate (*) or distance to cover (+) data. Values were plotted to create WUA curves (Figure F-55).

Streamflow (cfs)	Streamflow Exceedance (%)	Steelhead			Coho Salnon		Productive BMI Habitat*
		YOY Rearing +	Small Juvenile Rearing+	Large Juvenile Rearing+	YOY Rearing+	Juvenile Rearing+	
0.5	88.0	701	1,211	910	897	1,442	3,740
1.0	81.6	741	1,274	943	898	1,473	3,949
2.0	76.0	772	1,403	1,011	867	1,485	4,340
4.0	64.5	796	1,643	1,137	804	1,507	4,924
7.0	55.1	801	1,932	1,313	777	1,548	5,494
12.0	48.1	765	2,226	1,571	740	1,566	5,990
16.0	44.1	733	2,412	1,739	698	1,541	6,233
21.1	39.6	680	2,572	1,888	632	1,460	6,351
30.0	33.8	631	2,827	2,124	554	1,413	6,525
40.0	29.4	566	2,978	2,288	470	1,326	6,482
52.0	25.5	498	3,030	2,382	417	1,250	6,263
65.0	22.0	450	3,019	2,427	383	1,160	5,969
80.0	18.9	410	2,923	2,401	346	1,092	5,618
90.0	17.3	398	2,831	2,343	334	1,070	5,365
105.0	15.3	374	2,675	2,241	315	1,033	4,991
120.0	13.4	360	2,500	2,119	317	1,003	4,649
150.0	10.9	326	2,189	1,886	284	957	4,027
190.0	8.2	283	1,939	1,676	226	889	3,570

Table F-19. WUA for the Sproul Creek 2-D model site for targeted species and adult life stages derived from HSI for modeled depth and velocity results, and substrate (*) data. Values were plotted to create WUA curves (Figure F-55).

Streamflow (cfs)	Streamflow Exceedance (%)	Steelhead Adult Spawning*	Coho Salmon Adult Spawning*	Chinook Salmon Adult Spawning*
0.5	88.0	73	158	99
1.0	81.6	94	201	122
2.0	76.0	140	332	179
4.0	64.5	271	622	327
7.0	55.1	509	1,014	574
12.0	48.1	855	1,424	945
16.0	44.1	1,068	1,653	1223
21.1	39.6	1,220	1,793	1478
30.0	33.8	1,459	2,031	1891
40.0	29.4	1,560	2,058	2134
52.0	25.5	1,578	1,974	2265
65.0	22.0	1,494	1,795	2248
80.0	18.9	1,344	1,561	2105
90.0	17.3	1,232	1,402	1970
105.0	15.3	1,062	1,179	1768
120.0	13.4	908	995	1570
150.0	10.9	675	747	1222
190.0	8.2	558	658	1003

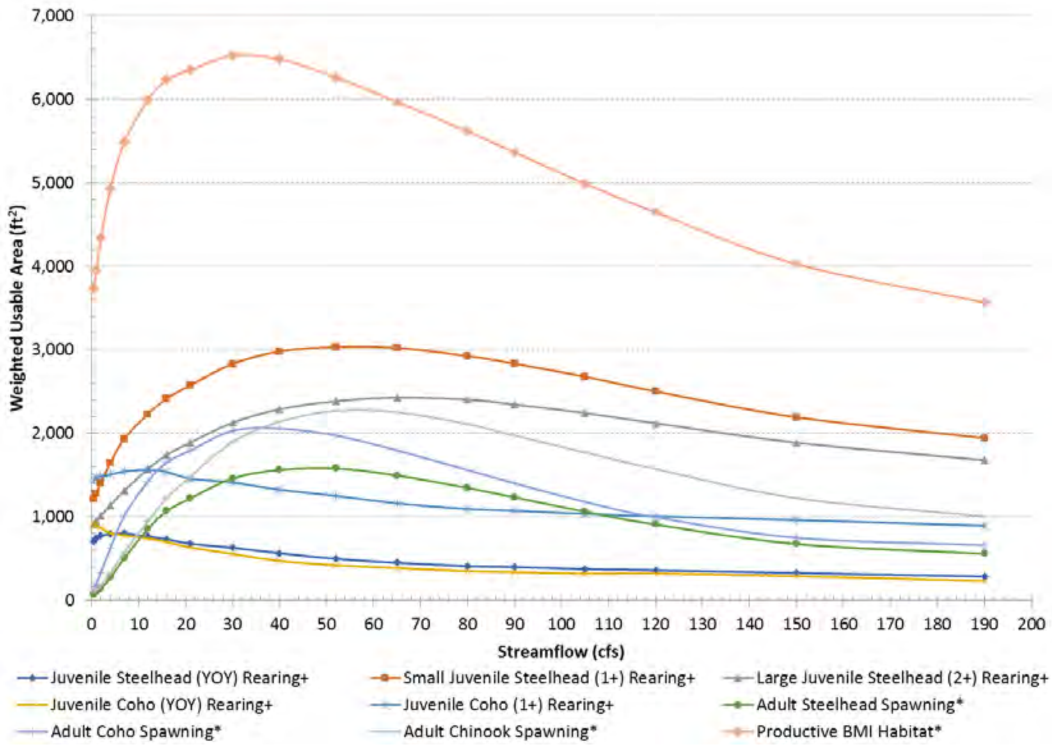

Figure F-55. WUA for the Sproul Creek 2-D modeling site for targeted species and life stages derived from HSI for modeled depth and velocity results and either substrate (*) or distance to cover data (+).

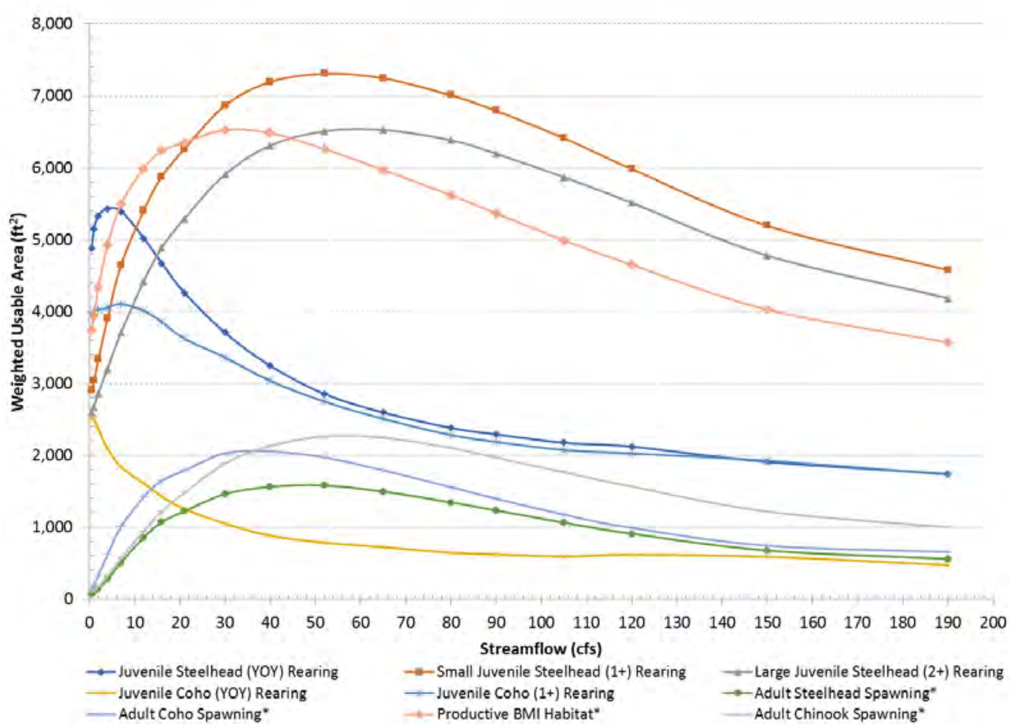

Figure F-56.WUA for the Sproul Creek 2-D modeling site for targeted species and life stages derived from HSI for modeled depth and velocity results and no cover. Substrate HSI was included for productive BMI habitat and spawning (*).

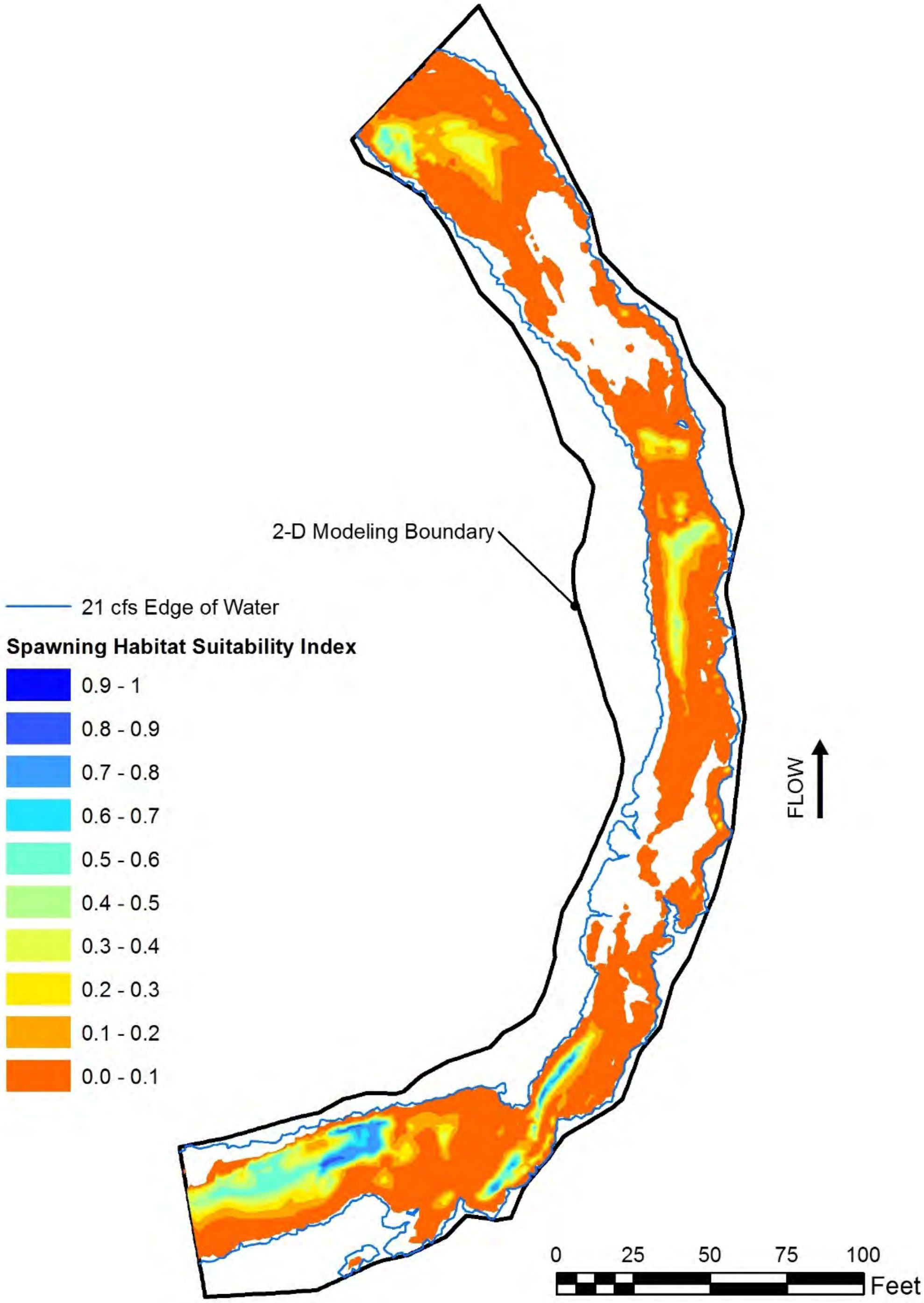

Figure F-57. Example of HSI output for steelhead spawning habitat displayed for a streamflow of 21.1 cfs.

6.4 Summary

Upper Mainstem Sproul Creek resulting 2-D hydraulic modeling site WUA curves (Figure F-55 and Figure F-56) for targeted species and life stages, were exported from Microsoft Excel for use in the time-series analysis (Appendix G). Time-series methods and resulting streamflows were calculated for targeted species and life stages, and water year type for each month. A complete description of time-series methods and resulting streamflows is provided in Appendix G.

7 REFERENCES

Bovee, K. D. 1986. *Development and evaluation of habitat suitability criteria for use in the instream flow incremental methodology*. No. FWS/OBS-86/7. USDI Fish and Wildlife Service.

Dettman, D. H., and D. W. Kelley. 1986. Assessment of the Carmel River steelhead resource, Volume 1. *Biological investigations*. Monterey Peninsula Water Management District, Monterey, CA.

Flosi, G., S. Downie, J. Hopelain, M. Bird, R. Coey, and B. Collins. 2010. *California Salmonid Stream Habitat Restoration Manual, Fourth Edition*. California Department of Fish and Game.

Gore J.A, J.B. Layzer, and J. Mead. 2001. Macroinvertebrate Instream flow Studies After 20 Years: A Role in Stream Management and Restoration. *Regulated Rivers: Research & Management*. Vol. 17. Pages 527–542.

Hampton, M., T. R. Payne, and J. A. Thomas. 1997. *Microhabitat Suitability Criteria for Anadromous Salmonids of the Trinity River.* US Fish & Wildlife Service, Arcata, CA.

Holmes, R.W., M.A. Allen, and S. Bros-Seeman. 2014. Habitat Suitability Criteria Juvenile Steelhead in the Big Sur River, Monterey County. *California Department of Fish and Wildlife, Water Branch Instream Flow Program Technical Report 14-1.*

International River Interface Cooperative (iRIC). 2014. iRIC Software, Changing River Science, User's Manual. River Center of Hokkaido, Japan.

Kennedy, E.J. 1984, *Discharge ratings at gaging stations: U.S. Geological Survey Techniques of Water-Resources Investigations*, book 3, chap. A10, 59 p. (Also available at http://pubs.usgs.gov/twri/twri3-a10/.)

Leopold, L.B. 1970. *An Improved Method for Size Distribution of Streambed Gravel*. Water Resources Research 6(5):1357-1366.

Loving, B. 2002. BARC (Brian's Aid for Rating Creating), V2.3, July 2002.

Normandeau Associates Inc. 2014. *Scott River Mesohabitat Delineation*. Scott and Shasta River Instream Flow Study Plan Development. October 27, 2014.

Phillips, J.V., and Tadayon, S. 2006. Selection of Manning's roughness coefficient for natural and constructed vegetated and non-vegetated channels, and vegetation maintenance plan guidelines for vegetated channels in central Arizona: U.S. Geological Survey Scientific Investigations Report 2006–5108, 41 p.

Simões, Francisco J.M. 2013. Using SToRM – A Short Primer. U.S. Geological Survey Geomorphology and Sediment Transport Laboratory: Golden, CO.

Simões, Francisco J.M. 2016. Response to CDFW's comments on the use of maximum velocity bounding parameter to achieve a stable solution through the smallest triangles. Personal communications, September 19, 2016.

U.S. Fish and Wildlife Service (USFWS). 2011. Sacramento Fish and Wildlife Office Standards for Physical Habitat Simulation Studies. Prepared by the Restoration and Monitoring Program, Sacramento, CA.